

Project Summary

Millimeter-wave systems, phased-array antennas and high performance components all require wideband circulators (and isolators) to perform diplexing and switching, to improve isolation and VSWR, and to construct IMPATT diode reflection amplifiers. Presently, most of the millimeter-wave circulators and isolators are available in the configurations of waveguide or stripline, both of which suffer from the shortcomings of bulky size/weight, narrow bandwidth, and poor compatibility with monolithic millimeter-wave integrated circuits (MMIC). MMW microstrip circulators/isolators can eliminate or improve these shortcomings. During the phase II R & D, E-Tek developed stub-tuned microstrip circulator configuration utilizing the electromagnetic fields perturbation technique, overcame the adhesion problems of microstrip metallization on new ferrite substrate, improved the fabrication, assembly, packaging techniques, and then successfully designed, fabricated a Ka band circulator which has isolation and return loss of greater than 16dB, insertion loss less than 0.7dB. To assess the steady and reliable performance of the circulator, a temperature cycling test was done over the range of -20°C to $+50^{\circ}\text{C}$ for 3 continuous cycles and found no significant impact or variation of circulator performance.

MMW circulators/isolators are the key components for MMW communication, radar, and phased array systems, and the key components for reflection amplifier, 50 ohm impedance matching, circuit isolation, switch, diplexer, etc.

Table of Contents

<u>Section</u>	<u>Page</u>
1.0	Introduction.....1
1.1	The Need for a Millimeter-wave Microstrip Circulator.....1
1.2	Technical Tasks in Phase II R & D.....6
1.2.1	Improve Millimeter-wave Microstripe Circulator Fabrication Process.....7
1.2.1.1	Dielectric Constant Measurement of Ferrite Substrate.....8
1.2.1.2	Coaxial-to-Microstrip Launcher Evaluation.....8
1.2.2	Millimeter-wave Microstrip Circulator Performance Improvement.....8
1.2.2.1	Design, Fabricate, and Test a Drop-in Circulator.....8
1.2.2.2	High Performance Circulator Test Fixture.....9
1.2.2.3	Loss Tangent of Ferrite Substrate.....10
1.2.3	Design, Fabricate, and Evaluate Circulator Package.....
1.2.4	Temperature Test of Millimeter-wave Microstrip Circulator.....11
1.3	Accomplishments of Phase II R & D.....11
2.0	Fabrication Considerations of High Performance Millimeter-wave Microstrip Circulation.....23

Table of Contents
(Continued)

<u>Section</u>	<u>Page</u>
2.1	Wide Operation Frequency and Bandwidth.....23
2.2	Low Insertion Loss.....24
2.3	High Isolation among Parts.....26
2.4	Low VSWR.....28
2.5	Minimum Temperature Impact.....28
2.6	Power Handling Capability.....30
2.7	Performance Uniformity and High Yield Rate.....33
3.0	Material Selection.....34
3.1	Ferrite Substrate Selection Guide.....34
3.1.1	Microwave and Millimeter Wave Ferrite Materials.....34
3.1.2	New Commercially Available Ferrite Substrates for Millimeter-wave Circulators.....36
3.2	Magnets.....36
3.3	RF Launcher Selections.....41
4.0	Fabrication Assembly Process Improvement Evaluation and Optimization.....44
4.1	Ferrite Substrate Metallization.....44
4.2	Substrate Preparation and Inspection.....51

Table of Contents

(Continued)

<u>Section</u>	<u>Page</u>
4.2.1	Ferrite Substrate Dielectric Constant & Loss Tangent.....52
4.2.2	Ferrite Substrate Size and Thickness Deviation.....52
4.2.3	Ferrite Substrate Surface Finish.....55
4.2.4	Ferrite Substrate Cleaning Procedure.....55
4.3	Optimized Photolithograph Process57
4.4	Permanent Magnets.....59
4.5	Coaxial to Microstrip Launcher Performance Evaluation.....64
5.0	Millimeter-wave Microstrip Circulator Experimental Results.....71
5.1	Mask Design Generation and Drop in Circulator Fabrication.....71
5.2	Drop-in Circulator Test Fixture Design and Fabrication.....75
5.3	Circulator Performance Evaluation and Test Results.....76
5.3.1	Performance Test Setup.....79
5.3.2	Experimental Results of 36 - 40 GHz Circulator.....79

Table of Contents
(Continued)

<u>Section</u>	<u>Page</u>
5.3.2	Experimental Results of 36 - 40 GHz Circulator.....79
5.3.3	Experimental Results of 31 - 37 GHz Circulator.....91
6.0	Design, Fabrication and Evaluation of Ruggedized Circulator Package.....96
6.1	Design of Ruggedized Circulator Package96
6.2	Fabrication of Circulator Package.....97
6.3	Temperature Cycling Test.....99
7.0	Conclusion and Recommendation.....111
7.1	Summary and Conclusion.....111
7.2	Recommendation.....113
	Appendix A.....116
	Appendix B.....131

List of Figures

<u>Figures</u>	<u>Page</u>
1.1	Beam Forming Network Employing Variable Power Dividers, Phase Shifters and Switching Circulators.....3
1.2	Schematic Diagram of Transmit/Receive Module.....4
1.3	Dual-Channel Phased-Array Module Using a Circulators...5
1.4	Schematic Diagram of a Magnetic Field Redistribution Broadband Circulator.....18
1.5	Experimental Model of a Stub Tuned Stripline Circulator.....19
1.6	Schematics of Some Configurations to be Studied by E-Tek.....19
1.7 (a)	Four-port Switchable Circulator.....20
1.7 (b)	Layout of 7-17 GHz Lange Coupler on a GaAs Substrate.....20
2.1	Resonant Loss Curve vs Applied Static Force.....27
2.2	Saturation Magnetization ($4\pi M_s$) as a Function of Temperature of Trans-Tech TT 86-6000 Ferrite.....29
2.3	Demagnetizing Curve at Different Temperatures.....31
3.1	Characteristics of Three High Performance Ferrite Substrates for Microwave Circulators.....37
3.2	Comparison of Saturation Magnetization vs Temperature Of Ferrites.....38

List of Figures

(Continued)

<u>Figures</u>	<u>Page</u>
3.3 (a) Typical Return Loss of 2.4 mm Launchers Joined by Microstrip Transmission Line	43
3.3 (b) Typical Return Loss of K Connector Launcher Joined by Microstrip Transmission Line.....	43
4.1 Gold Plating Jig.....	49
4.2 Setup for Gold Plating on Brass Block.....	50
4.3 Substrate Preparation and Inspection Procedure.....	53
4.4 Setup for Ferrite Substrate Dielectric Constant Measurement.....	54
4.5 Ferrite Process.....	56
4.6. Photolithograph Process.....	61
4.7 Magnetic Flux Density of Different Magnetic Materials (without ferrite) vs Temperature.....	62
4.8 Magnetic Flux Density of Different Magnetic Materials (with ferrite vs.temperature).....	63
4.9 Magnetic Flux Density of Various Magnets with Ferrite (10 mil.) vs. Distance.....	65
4.10 Magnet Flux Density Measurement vs. Bias Conditions...	66
4.11 Performance of K Connector Test Setup with Two K Connector Launchers and 0.3" 50 Ohm Transmission Line.....	67

List of Figures

(Continued)

<u>Figures</u>	<u>Page</u>
4.12	Performance of APC 2.4 Connector Test Setup with Two K to APC 2.4 Adapter, Two APC 2.4 Connector Launchers and 0.5" 50 Ohm Transmission Line.....68
4.13	Performance of K Connector Test Setup with Two K Connector Launchers and 0.4" Ferrite Substrate 50 Ohm Transmission Line.....70
5.1	Mask Layout of MMW Circulator.....72
5.2	Mask layout of MMW Circulator with Stubtuned Configurations..... 73
5.3	36-40 GHz Drop-In Circulator Unit..... 74
5.4	Drop-In Circulator/Isolator Test Fixture.....77
5.5	Assembled Circulator Drop-In Unit with Test Fixture...78
5.6	Circulator Insertion Loss/Isolation Testing Setup.....80
5.7	Circulator Return Loss Test Setup.....81
5.8	Performance Parameters of Microstrip Circulator at Port # 1 (W/O Tuning).....82
5.9	Performance Parameters of Microstrip Circulator at Port # 2 (W/O Tuning).....83
5.10	Performance Parameters of Microstrip Circulator at Port # 3 (W/O Tuning).....84

List of Figures

(Continued)

<u>Figures</u>	<u>Page</u>
5.11	Performance Parameters of Microstrip Circulators at Port # 1 (Tuning Using Metal Chips).....85
5.12	Performance Parameters of Microstrip Circulator at Port # 2 (Tuning Using Metal Chips).....86
5.13	Performance parameters of Microstrip Circulator at Port # 3 (Tuning Using Metal Chips).....87
5.14	Performance Parameters of Microstrip Circulator at Port # 1 (After Tuning by Using Absorbing Material).....88
5.15	Performance Parameters of Microstrip Circulator at Port # 2 (After Tuning by Using Absorbing Material).....89
5.16	Performance Parameters of Microstrip Circulator at Port # 3 (After Tuning by Using Absorbing Material).....90
5.17	Performance of 31 to 40 GHz Broadband Microstrip Circulator at Port #1.....93
5.18	Performance of 31 to 37 GHz Microstrip Circulator at Port #2.....94
5.19	Performance of 31 to 37 GHz Broadband Microstrip Circulator at Port #3.....95

List of Figures

(Continued)

<u>Figures</u>	<u>Page</u>
6.1 Ruggedized Millimeter-Wave Microstrip Circulator Package.....	98
6.2 Connector Launcher Housing Dimensions.....	100
6.3 Fully Assembled 36-40 GHz Circulator Package.....	101
6.4 Circulator Temperature Testing Setup.....	102
6.5 Circulator Temperature Testing Setup.....	103
6.6 (a) Insertion Loss Test of Circulator with ND-FE-B Magnet at 30°c (operation frequency 30-40GHz).....	105
6.6 (b) Insertion Loss Test of Circulator with ND-FE-B Magnet at 40°c (operation frequency 30-40 GHz).....	106
6.7 (a) Insertion Loss Test of Circulator with SM_2CO_{17} Cobalt Magnet at -20°c (operation frequency 30-40GHz).....	107
6.7 (b) Insertion Loss Test of Circulator with SM_2CO_{17} Cobalt Magnet at 50° c (operation frequency 30-40 GHz).....	108
6.8 (a) Return Loss Test of Circulator with SM_2CO_{17} Cobalt Magnet at -20° c (operation frequency 30-40 GHz).....	109
6.8 (b) Return Loss/Test of Circulator with SM_2CO_{17} Cobalt Magnet at 50°c (operation frequency 30-40 GHz).....	110

List of Figures
(Continued)

<u>Figures</u>	<u>Page</u>
7.1	A Ka-Band Circulator (Magnet Is Not Shown).....114
A.1	Microstrip Line.....118
A.2	Configuration of Wideband Stub-Tuned Microstrip Circulator.....120
A.3	Insertion Loss, Isolation and Return Loss of Wideband Stub Tuned Microstrip Circulator.....129
A.4	Insertion Loss, Isolation and Return Loss of Wideband Stub Tuned Microstrip Circulator.....130
B.1	3 to 6 Ports Active Coupler.....134
B.2	3-Port Junction Active Circulator Formed by a Delta Connection of Thru Elements.....135
B.3	Active Circulator Using Three MESFETs.....137
B.4	4-Port Circulator Using One Active Magic-T and One Coupler139

List of Tables

<u>Tables</u>	<u>Page</u>
1.1 Comparison of Proposed Tasks and Actural Achievements for Phase II.....	12
3.1 Ferrite Materials for Microwave and Millimeter Wave Circulator.....	35
3.2 Performance Parameters of Magnet at Room Temperature.....	40
3.3 Comparison of MMW Coaxial to Microstrip Launchers....	42
4.1 Summary of Resistivity Measurements, in Micro-Ohm-cm, For Electroplated and All-Sputtered Cr/Cu and Cr/Au Films.....	47
4.2 Ferrite Substrate Cleaning Procedure.....	58
4.3 Magnetic Field Measurement of Different Magnet Materials.....	60
5.1 Summarized the Results of Circulator 36 - 40 GHz Performance.....	92
B.1 Comparison of Active and Passive Circulator.....	142

1.0 Introduction

This report presents the investigation of high performance, millimeter-wave microstrip circulators. The circulators are to have an operation bandwidth of 36 to 40 GHz over the temperature range -20°C to $+50^{\circ}\text{C}$. This research and development project is a Fiscal year 1988 Small Business Innovation Research (SBIR) project, Phase II, supported by Jet Propulsion Laboratory Through Contract Number: NAS7-1035. The investigation was performed during the period of June 1988 through December 1989.

1.1 The Need for a Millimeter-Wave Microstrip Circulator

Millimeter-wave systems for communications, radar, and sensing systems have many attractive features, such as:

- Wide available bandwidth
- Small size/weight
- Excellent measurement accuracy
- High antenna gain, narrow beam width
- Low probability of interception/jamming,
high communication security

Therefore, they are viable for space satellite and military applications. Many millimeter-wave systems, such as Communications, radar and electronic warfare (EW) systems, require high performance miniature broadband circulators for diplexing,

switching, isolation, VSWR improvements and the fabrication of diode (IMPATT or Gunn) reflection amplifiers. Miniature broadband circulators are needed in solid state arrays for radar and EW systems to provide isolation between radiating elements and the solid state transmit/receive circuits.

For example, switchable circulators can provide path selection for phased-array beamforming networks, as depicted in Figure 1.1. Such switchable circulator-based beamforming networks are very practical for all EW, radar, and satellite communications systems. A transmit/receive module of an active phased-array antenna using four circulators is illustrated in Figure 1.2. One of the four circulators is switchable. In the transmit mode, the circulator routes the signal from exciter through the phase shifter and high power amplifier (HPA) to the radiating element, and dumps any power reflected from the radiating element into the load. In the receive mode, the signal travels from the antenna through the low noise amplifier (LNA) and phase shifter to the receiver. A slightly different application of circulators in the modules of a dual-channel active phased-array antenna is shown in Figure 1.3. Dual-channel active antennas are suitable for transmitting and receiving linear or circular polarization.

The trend of modern phased-array antennas is toward the effective use of mass-producible, miniature GaAs monolithic microwave integrated circuits (MMIC). Therefore, A millimeter-wave wideband circulator/isolator, fabricated in

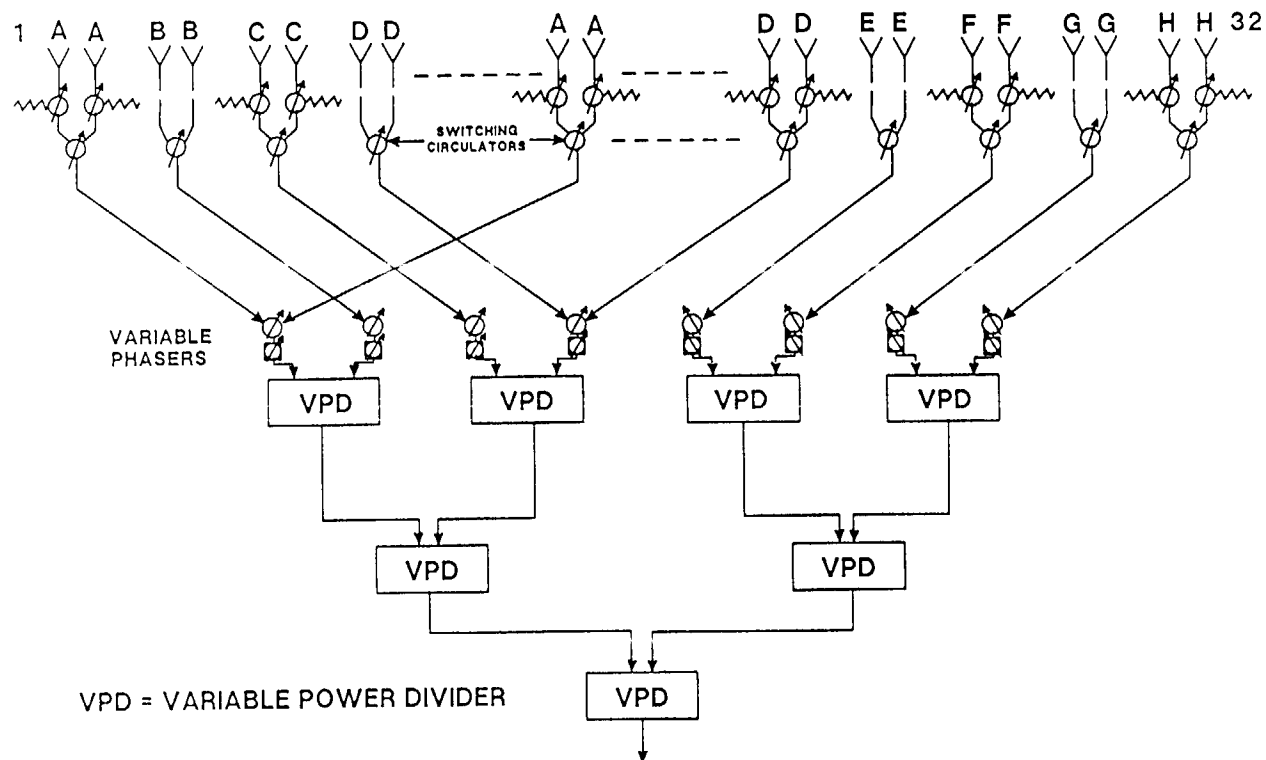


Figure 1.1 Beam Forming Network Employing Variable Power Dividers, Phase Shifters and Switching Circulators
(From Ford Aerospace Corporation and after G.P. Rodrigue)

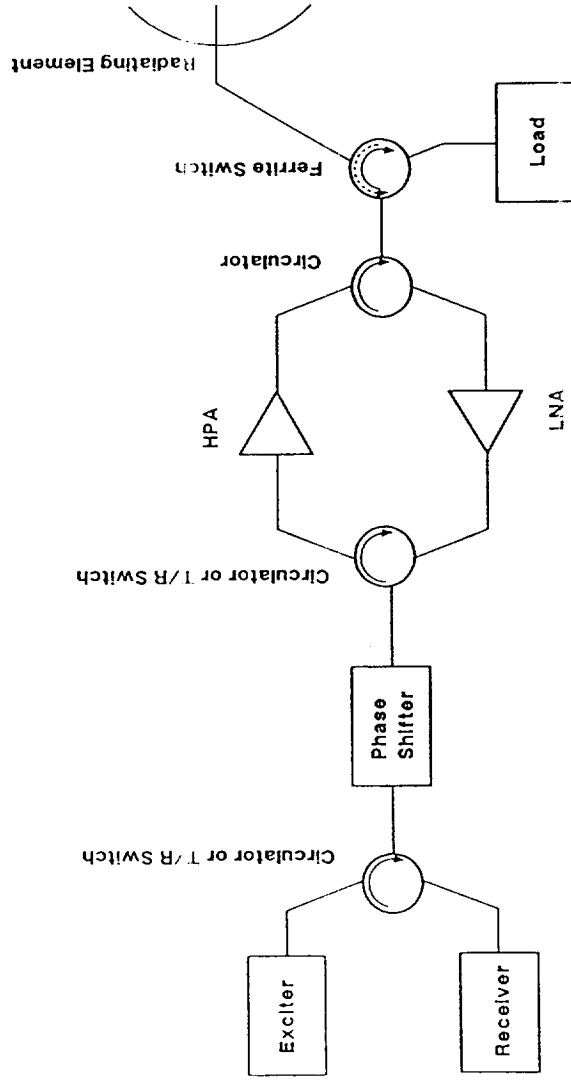


Figure 1.2 Schematic Diagram of Transmit/Receive Module
(After E.F. Schloemann)

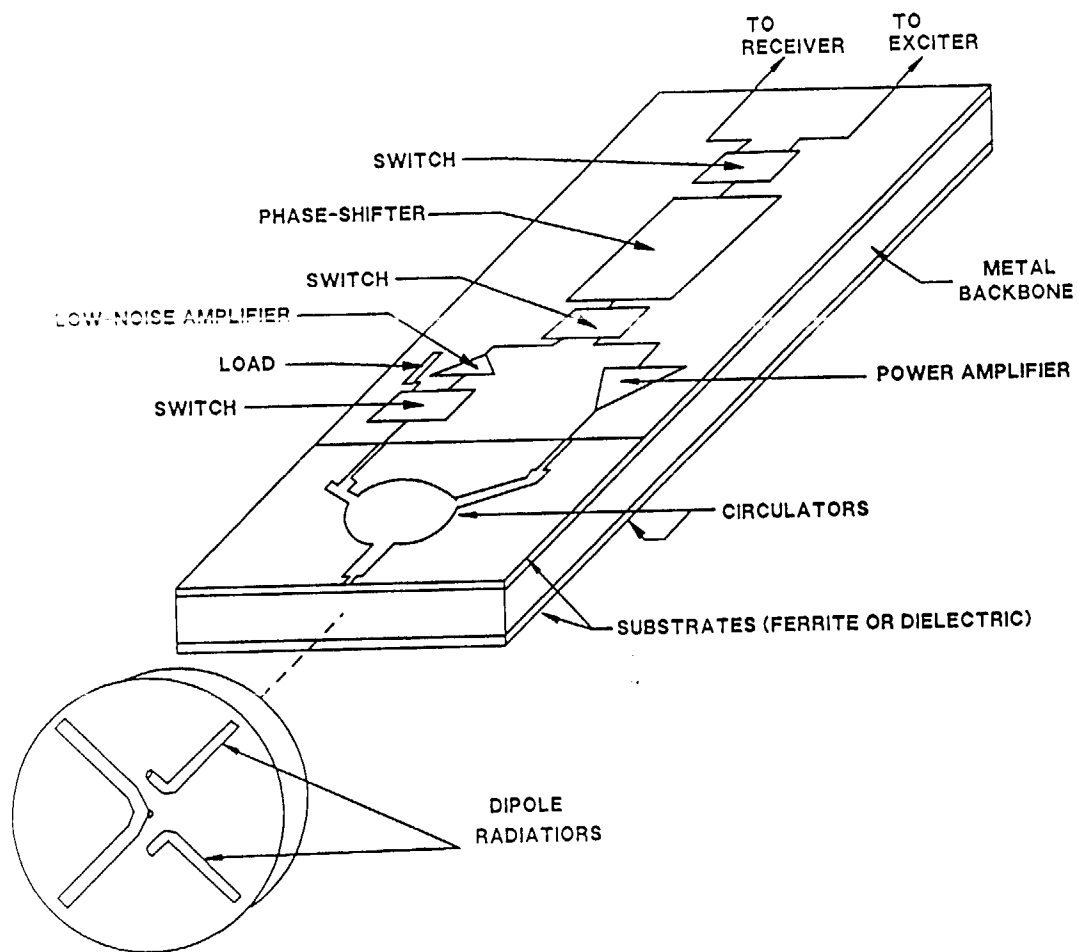


Figure 1.3 Dual-Channel Phased-Array Module Using a Circulator
(After E.F. Schloemann)

microstrip configuration and using a precision photolithographic method, will have the following advantages:

- Easy to interface with other millimeter-wave integrated circuits or MMIC
- Wide operational bandwidth
- Small size/weight
- Low cost, high reliability
- Less tuning work required, potential for production

1.2 Technical Tasks in Phase II R & D

In Phase II, E-Tek Dynamics, Inc., proposed to achieve the following technical objectives

- (1) Improve millimeter-wave microstrip circulator fabrication process
- (2) Improve millimeter-wave circulator performance. A new microstrip circulator will be designed to extend temperature range. For this task, a new test fixture must also be designed, fabricated, and evaluated. The new test fixture can accurately characterize the circulator up to a frequency of 40 GHz.
- (3) Design, fabricate, and evaluate a ruggedized circulator package.

- (4) Test millimeter-wave circulator over an extended operating temperature range.

In order to accomplish these technical objectives, E-Tek engineers proposed the following R&D tasks in phase II of this program:

1.2.1. Improve Millimeter-Wave Microstripe Circulator Fabrication Process

To improve the microstrip circulator fabrication process developed in Phase I R&D, efforts are necessary to ensure that the ferrite substrate metallization process would yield good conductivity and durable adhesion. The following metallization goals (or the equivalent) of ferrite substrate needed to be accomplished:

1. Ferrite substrate thickness: 0.010 inches
2. Ferrite substrate surface finish: $\leq 10 \mu\text{inches}$
3. Ti (or TiW) adhesion layer thickness: $500 \text{ \AA} \pm 100 \text{ \AA}$
4. Au sputter metallization thickness: 2000 \AA
5. Au plating thickness: $\geq 2 \mu\text{m}$
6. Adhesion of ferrite substrate metallization (over temperature range of -20° to $+50^\circ\text{C}$): satisfactorily pass the adhesive tape test [no metallic layer should peel off after Application of RT20 tape, or equivalent).

1.2.1.1. Dielectric Constant Measurement of Ferrite Substrate

In order to ensure the accurate design of circulator resonator, impedance matching transformer, and 50-Ohm transmission line, the dielectric constant of the ferrite substrate needed to be defined and measured prior to circulator design and fabrication.

1.2.1.2 Coaxial-to-Microstrip Launcher Evaluation

To prevent the introduction of large insertion loss during use and test of the millimeter-wave microstrip circulator, E-Tek will evaluate and select a coaxial-to-microstrip launcher which meets the following characteristics:

- Operation frequency range: DC to 45 GHz
- Insertion loss at 40 GHz: ≤ 0.5 dB (or ≤ 1.0 dB for two launchers connected back-to-back)
- VSWR in frequency range of 30-0 GHz: $\leq 1.3:1$
- Repeatability: Less than $\pm 10\%$ variation after 30 cycles of connection and disconnection

1.2.2 Millimeter-Wave Microstrip Circulator Performance Improvement

1.2.2.1 Design, Fabricate, and Test a Drop-In Microstrip Circulator

A drop-in microstrip circulator should be designed, fabricated, and tested to ensure operation over a temperature range of -20° to $+50^{\circ}\text{C}$ and to meet the following design goals:

● Frequency Range:	36 to 40 GHz
● Bandwidth:	4 GHz
● Input/Output Impedance:	50-Ohm
● VSWR:	1.5:1
● Insertion Loss:	0.7 dB
● Isolation:	≥ 15 dB
● Power Handling Capability (est.):	1 Watt
● Substrate:	Ferrite
● Substrate Thickness:	10 mils
● Operation Temperature Range:	-20° to $+50^{\circ}\text{C}$

1.2.2.2 High Performance Circulator Test Fixture

Design of the microstrip circulator test fixture, developed in Phase I R&D, need to be modified and improved using the coaxial-to-microstrip launcher specified in Paragraph 1.2.1.2. The test fixture modification and improvement shall emphasize and achieve the critical goals of:

- Adequate RF grounding
- Adequate contact between coaxial launcher center conductor and microstrip

- No insertion loss or VSWR degradation for each test

1.2.2.3 Loss Tangent of Ferrite Substrate

E-Tek should obtain the loss tangent test data of the ferrite substrate from the vendor to ensure that the loss tangent is equal to or smaller than 0.0002. In the event that loss tangent was larger than 0.0005, the ferrite disk embedding method will be used to reduce the dielectric loss.

1.2.3 Design, Fabricate, and Evaluate Circulator Package

A ruggedized package need to be designed, fabricated, and evaluated for the millimeter-wave microstrip circulator. The package must have the following features:

- Operating temperature (without generating stress on ferrite substrate and causing loss increases):
-20°C to +50°C
- Connector/launcher: Coaxial connector/launcher specified in Paragraph 1.2.1.2
- Provides adequate RF grounding to microstrip ferrite substrate
- Adequate dimension without resonance in the frequency range of 36 to 40 GHz
- Integration simplicity

1.2.4 Temperature Test of Millimeter-Wave Microstrip Circulator

The following microstrip circulator performance parameters should be tested in the temperature range of -20° to $+50^{\circ}\text{C}$ over the operation bandwidth to meet the design goals specified in the paragraph 1.2.2.1 :

- Insertion loss
- VSWR
- Isolation

Three temperature cyclings between -20° and 50°C are required and these measurements need to be recorded.

The measurement data is to exclude the temperature efforts of the transmission line used in the test setup. Necessary analysis and action shall be taken to improve the circulator performance and to meet the design goals if measurement results are different from theoretical predictions.

1.3 Accomplishments of Phase II R&D

E-Tek engineers have completely performed Phase II R&D tasks for this project. A comparison of proposed tasks and actual achievements for Phase II is summarized in Table 1.1.

In addition to the proposed Phase II tasks, E-Tek engineers also accomplished extra work:

Table 1.1

<u>Proposed Phase I Task</u>	<u>Task Accomplished?</u>	<u>Highlights of Phase Achievements</u>
● Material Selection	Yes	<ul style="list-style-type: none"> ● Investigated/selected materials <ul style="list-style-type: none"> - Ferrite substrate - Permanent magnet - Coaxial to microstrip launcher - Low temperature solder and highly conductive epoxy
● Improve millimeter Wave microstrip circulator fabrication process	Yes	<ul style="list-style-type: none"> ● Improved ferrite metallization adhesion by various approaches, e.g. E-Beam and sputtering. ● Optimized surface adhesion and minimized insertion loss by varying thickness of TiW, Cu and Au layers deposited on substrate improve performance.

Table 1.1

(Continued)

<u>Proposed Phase I Task</u>	<u>Task Accomplished?</u>	<u>Highlights of Phase Achievements</u>
		<ul style="list-style-type: none">● Prepared and inspected ferrite substrate in following critical areas<ul style="list-style-type: none">- Better cleaning procedure for substrate- Closer tolerance checks of surface finish- Improved photolithographic process- Proper assembly for drop-in circulator- Verified dielectric constants of ferrite substrate- Selected/purchased/evaluated all millimeter wave coaxial microstrip launchers, including:<ul style="list-style-type: none">* K-connectors* APC 2.4* V-connectors* K-connectors without glass bead

Table 1.1

(Continued)

<u>Proposed Phase I Task</u>	<u>Task Accomplished?</u>	<u>Highlights of Phase Achievements</u>
<ul style="list-style-type: none"> ● Improve millimeter wave microstrip circulator performance 	Yes	<ul style="list-style-type: none"> ● Designed and fabricated millimeter wave drop-in circulators with center frequency of 38 GHz and 4 GHz bandwidth ● Designed/fabricated high performance circulator test fixture ● Verified loss tangent of ferrite substrate ● Conducted tests on circulator parameter, including insertion loss, isolation loss and return loss. ● Improved drop-in circulator performance ● Tested/demonstrated that improve drop-in unit meets design goals

Table 1.1

(Continued)

<u>Proposed Phase I Task</u>	<u>Task Accomplished?</u>	<u>Highlights of Phase Achievements</u>
<ul style="list-style-type: none"> ● Design/fabricate and evaluate circulator package 	Yes	<ul style="list-style-type: none"> ● Designed/fabricated ruggedized circulator package with very close tolerance, s i.e., < 1 mil, between coaxial microstrip launcher and microstrip transmission line ● Improved assembly/soldering techniques to optimize overall performance ● Optimized circulator package for operation within temperature range -20°C to +50°C ● Optimized circulator package enclosure to avoid resonance ● Designed/fabricated rapid temp. change fixture to permit rapid temperature cycling tests

Table 1.1
(Continued)

<u>Proposed Phase I Task</u>	<u>Task Accomplished?</u>	<u>Highlights of Phase Achievements</u>
		<ul style="list-style-type: none"> ● Performed temp. cycling tests, from +50°C to -20°C, on each ports of circulator components and package to reduce/minimize temperature impact ● Improved circulator components and package to reduce/minimize temperature impact
o Submit Quarterly Technical Reports	Yes	<ul style="list-style-type: none"> ● Five (5) quarterly technical reports were submitted to the Administrative Contracting Office
o Design Review and Critical Design Review	Yes	<ul style="list-style-type: none"> ● Design Review was held at E-Tek's physical plant; the critical design review was held at JPL, pasadena, CA.
o Final Report	Yes	<ul style="list-style-type: none"> ● One (1) Final Technical Report was completed.

- Investigated various approaches to increase the circulator operation bandwidth, including:

- (i) Configured microstrip line circulator with attached¹ dome shape ferrite substrate (Figure 1.4) which may uniformly distribute the internal magnetic field, and eliminate low field loss to achieve the broad band operation frequency.
- (ii) Modified the stub tuned nonreciprocal stripline circulator design,² which initially used the disk configuration shown in Figure 1.5. E-Tek engineer's investigated and designed different disk configurations, Figures 1.6(a),(b),(c),(d), to change the resonant mode and achieve the wideband operation.
- (iii) Investigated wideband, miniature four port lange coupler-circulator approach: a four-port catching circulator, Figure 1.7 (a),(b) (DPOT switch), proposed by G.T. Roome³, has been reviewed. This lange coupler

-
1. E. Scholemann and R. Blight, "Broad-Band Stripline Circulations Based on YIG and Li-Ferrite Single Crystals", IEE Transactions on Microwave Theory and Techniques, Vol. MTT-34, No. 12, Dec. 1986.
 2. Yansheng Xu and Jianyong Miao, Theory and Design of Stub Tuned Nonreciprocal Stripline Junctions and Circulators", Microwave and Optical Technology Letters, Vol. 1, No. 9 Nov. 1988
 3. G.T. Roome, H.A. Hair and C.W. Gerst, "A planar four-port switchable circulator for microwave integrated circuits", the 1967 Internat'l Solid-State Conf., Philadelphia, Pa, Feb. 1967

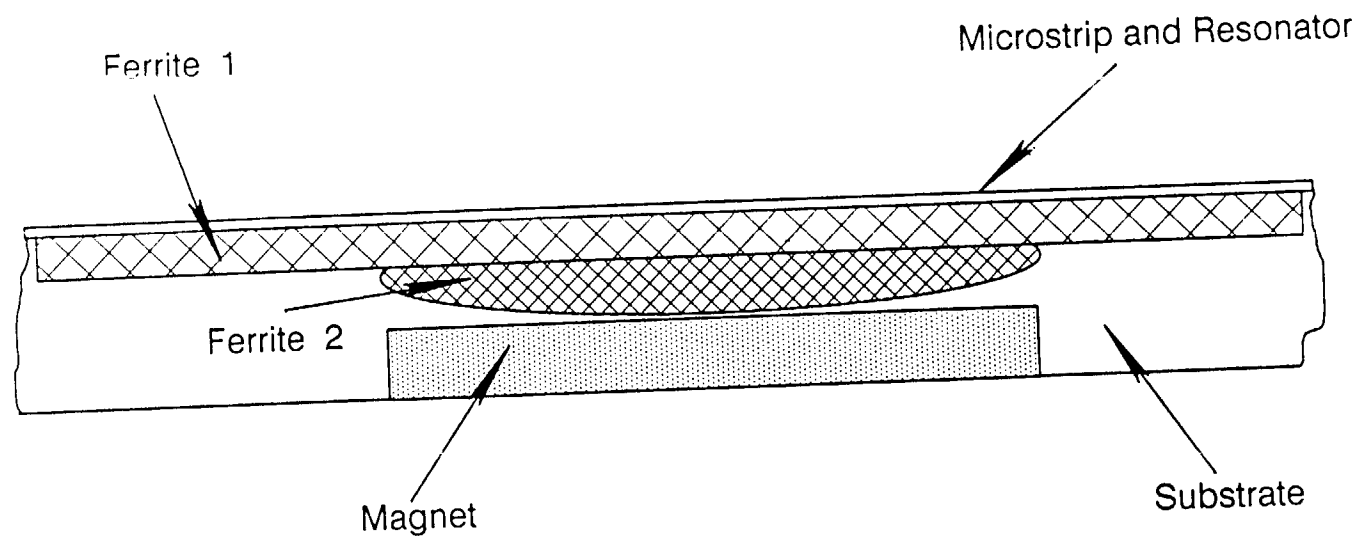


Figure 1.4 Schematic Diagram of a Magnetic Field
Redistribution Broadband Circulator

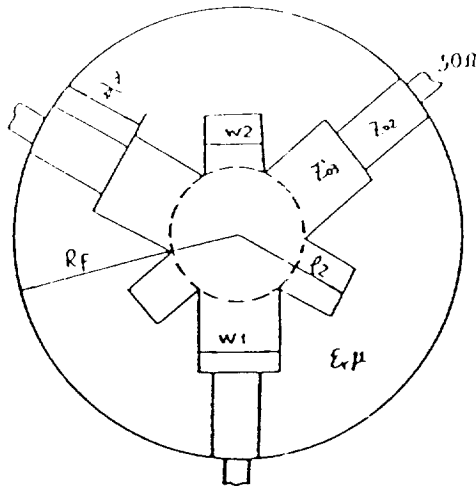


Figure 1.5 Experimental Model of a Stub Tuned Stripline Circulator
(After Y. Xu and J. Miao)

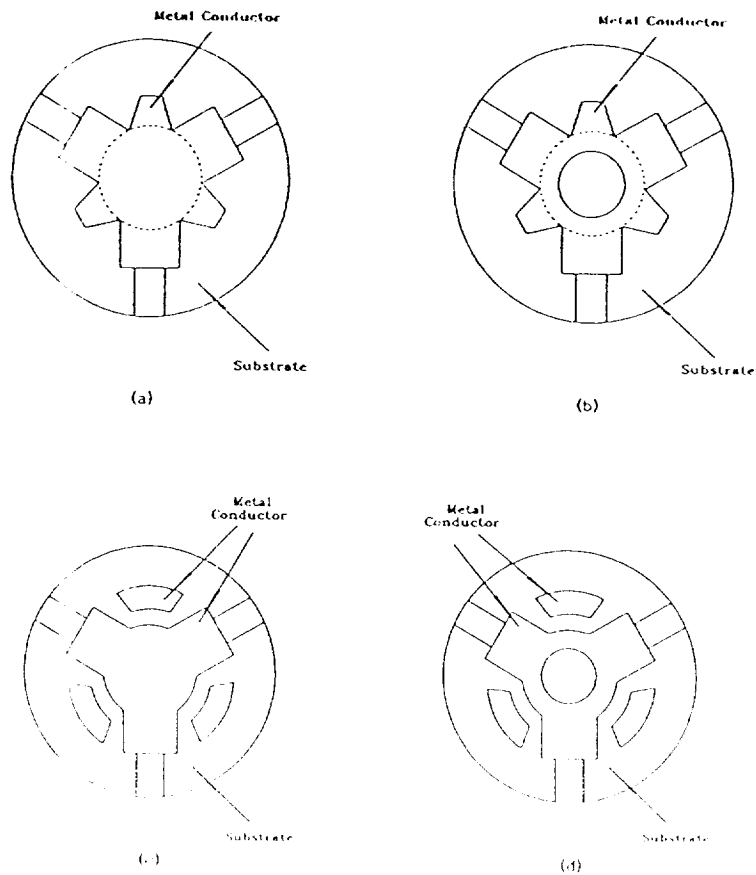


Figure 1.6 Schematics of Some Configurations Studied by E-Tek

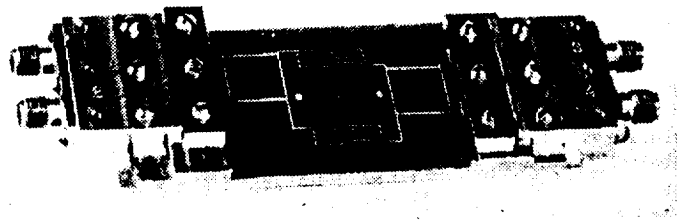


Figure 1.7 (a) Four-port Switchable Circulator (After G.T. Roome, H. A. Hair and C. W. Gerst)

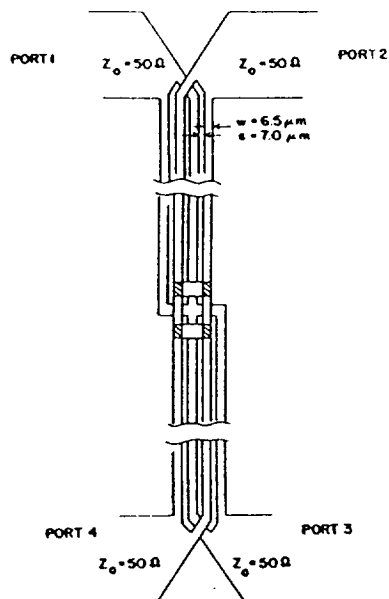


Figure 1.7 (b) Layout of 7-17 GHz Lange Coupler on a GaAs Substrate

approach has many advantages, such as extremely small size (less than 0.1" x 0.01"), the potential to eliminate the requirement for a magnet, and very wide bandwidth (7-17GHz lange coupler was achieved eight year age). However, for the Ka band applications, advanced photolithographic fabrication techniques are mandatory and future studies are required.

- Performed theoretical analysis and computer simulation for Ka band stub tuned microstrip circulator design. (For detailed analysis and results, please refer to appendix A.)
- Investigated active circulator approaches and their potential for Ka band applications. (Please refer to the appendix B for more details.)
- Designed, fabricated and evaluated the 31-37 GHz circulator for deep space applications. The circulator has a calibrated insertion loss less than 1.0dB, and both insolation and return loss of 17dB or better.
- Purchased and set-up a thin film sputtering system to improve the adhesion between Ti/Au and ferrite substrate; the critical factors which will impact substrate adhesion are: substrate cleanliness condition, chamber contamination, material selection, stress, temperature, argon pressure.

- Designed and fabricated an enclosure for temperature cycling tests which provides for: (i) quick temperature rise/drop from -20°C to $+50^{\circ}\text{C}$ within 5 minutes, and (ii) Elimination of extension semi-rigid or flexible cables, since a circulator under test can be directly connected to the network analyzer during the test.

2.0 Fabrication Considerations of High Performance Millimeter-Wave Microstrip Circulation

Among the key considerations for high performance millimeter-wave microstrip circulator fabrication are:

- Wide operation frequency and bandwidth
- Low insertion loss for the operation band at 50 ohm input/output impedance
- High isolation among ports
- Low VSWR
- Minimum temperature impact
- Power handling capability
- Performance uniformity
- High yield rate

2.1 Wide Operation Frequency and Bandwidth

The operation frequency and bandwidth of a millimeter wave circulation are determined by the following elements:

- Resonator geometry and shape
- Saturation magnetization($4\pi M_s$) of ferrite substrate
- Magnetic bias condition and uniformity of internal magnetic field
- Junction admittance (and equalization network for broad band circulator)
- Fringing or parasitic effects

- Material and modal dispersion

2.2 Low Insertion Loss

Insertion loss of the microstrip transmission line and resonator at millimeter-wave frequencies is determined by :

- Conductor loss
- Scattering loss due to substrate surface roughness
- Dielectric loss
- Resonance loss
- Dispersion loss
- Electromagnetic surface wave generation and radiation
- Anisotropic effect

Losses due to the first two mechanisms can be expressed as:

$$\alpha_c = \frac{0.072\sqrt{f\lambda_g}}{wZ_0} \left[1 + 2/\pi \arctan \left\{ 1.4 (\Delta/\delta_s)^2 \right\} \right]$$

(dB/Wavelength)

where f is in GHz and Z_0 is in Ohms

Δ = rms surface roughness

$\delta_s = 1/(R_s \sigma)$ is the skin depth at the appropriate operating frequency

R_s = surface resistance

To minimize the scattering loss and resonance loss, E-Tek has utilized a narrow linewidth nickel ferrite substrate which has a flat surface finish with less than 1 μm finish. The substrate is magnetically biased at saturated condition.

To minimize conductor loss, E-Tek employed the following steps to metallize the substrate:

- (1) Sputter thin layer of titanium (Ti) on ferrite substrate for a good adhesion bond
- (2) Sputter a 2000-3000 Å thick gold (Au) layer on Ti layer
- (3) Plate a 1-2 μm thick of (Au) on top of sputtered Au

Dielectric loss depends on composition and construction of the ferrite components. New technology can produce MMW application ferrites which have dielectric loss tangents at 10 GHz $\tan \delta = \epsilon''/\epsilon$ in 10^{-4} range. Under conditions anticipated, such a dielectric loss would be acceptable for our application.

Resonant loss can be expressed as

$$\chi'' \pm = M_s \frac{\Delta H/2}{(H_r \pm f/\gamma)^2 (\Delta H/2)^2}$$

where f is the operating frequency

H_r is the applied field

γ is the ferromagnetic ratio $\gamma = 3,51.10^4 \text{ m/A.s}$

$$= 2,8 \text{ MHz/Oe}$$

M_s is the saturation magnetization

ΔH is the mid point width of the Lorentz curve $\chi'' + (f)$
centered around $f_r = \gamma H_r$

The relation between the resonant loss and applied static field(H) is a Lorentz curve, as depicted in Figure 2.1. Due to substrate magneto-crystalline, the actual loss $\chi'' + (H)$ is deflected away from the resonant frequency with an effective line width $\Delta H_{eff} \leq \Delta H$. For circulator design purposes, ΔH_{eff} can be used to calculate the loss outside the resonant zone, the width of which is determined by ΔH . E-Tek intends to select a ferrite substrate for which both ΔH_{eff} and ΔH are as low as possible.

2.3 High Isolation among Parts

In order to achieve isolation between components of greater than 15 dB in the millimeter wave frequency band, the following elements must be carefully determined.

- Ferrite material and magnetic bias
- Resonator size, shape, thickness
- Junction admittance and equalization network for broadband circulator
- Fringing or parasitic effects
- Material and mode dispersion

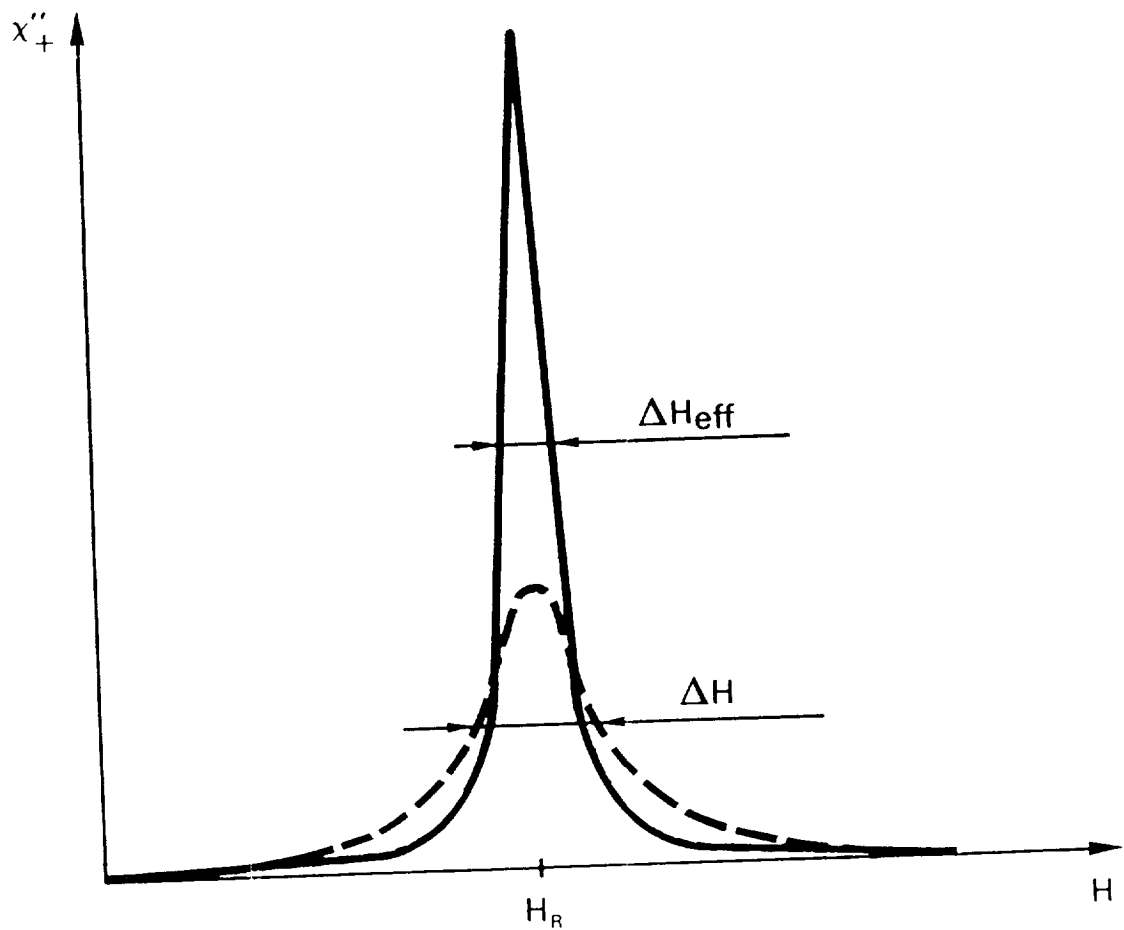


FIG. 3

• experimental points

Figure 2.1 Resonant Loss Curve vs Applied Static Force
(After Thomson Semiconductor)

2.4 Low VSWR

Frequency response flatness and VSWR of the microstrip millimeter-wave are related to the following factors:

- 50-Ohm microstrip line fabrication accuracy
- Ferrite material and magnetic bias
- Junction admittance
- Resonator mode-conversion
- Mutual coupling among high-order hybrid modes (electromagnetic surface wave modes)

Because the propagation velocities of millimeter-waves are different in ferrite substrate than in air, high-order hybrid modes of electromagnetic surface waves are generated and the microstrip is no longer in a TEM mode. Interaction among these high-order hybrid modes introduces both extra insertion loss and spurious response. E-Tek minimizes hybrid mode generation and radiation by proper design between resonator and microstrip.

2.5 Minimum Temperature Impact

As the temperature of the ferrite is increased, the saturation magnetization of ferrite substrate decreases (as shown in Figure 2.2) for Trans-Tech TT86-6000 nickel ferrite substrate and so does the anisotropy ratio, k/μ . Thus, junction performance will decline as the operating temperature increases. Likewise,

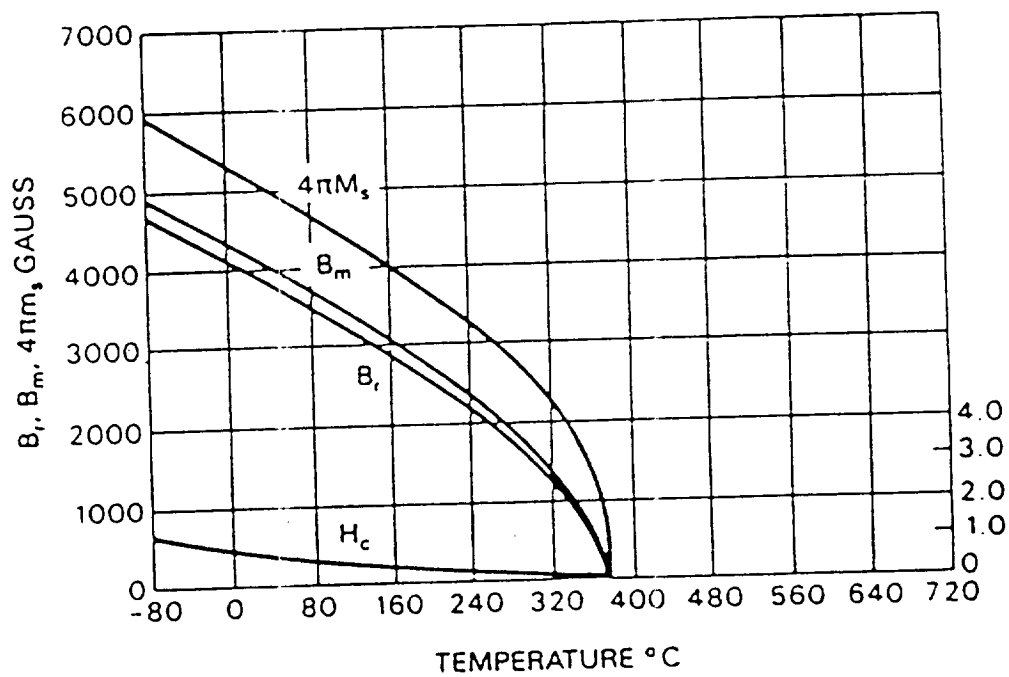


Figure 2.2 Saturation Magnetization ($4\pi M_s$) as a Function of Temperature of Trans-Tech TT 86-6000 Ferrite

the junction resonance will shift to lower frequency. Therefore, the 36 to 40 GHz Circulator must be designed with an adequate bandwidth to accommodate the change in $4\pi M_s$, impedance, and resonance frequency due to the temperature change.

The magnetic characteristics of a magnet also change drastically with temperature. Figure 2.3 illustrates a typical demagnetization curve as a function of temperature. Hence, the design of a millimeter-wave circulator, operating over a wide temperature range, must incorporate the temperature effects of the magnet.

2.6 Power Handling Capability

The average power handling capability of microstrip is primarily a function of the permissible temperature rise of the center conductor and surrounding laminate. It is, therefore, related to the dielectric substrate used, its thermal conductivity and electrical loss, the cross section of the microstrip, the supporting material, the maximum allowable temperature, and the ambient temperature.

Dissipative losses of the stripline must be minimized to maximize CW power handling capability. Since conductor losses are a function of the line cross section (which is a function of substrate thickness), circulator dimensions must be chosen carefully. Thermal considerations suggest that wide microstrip and thin

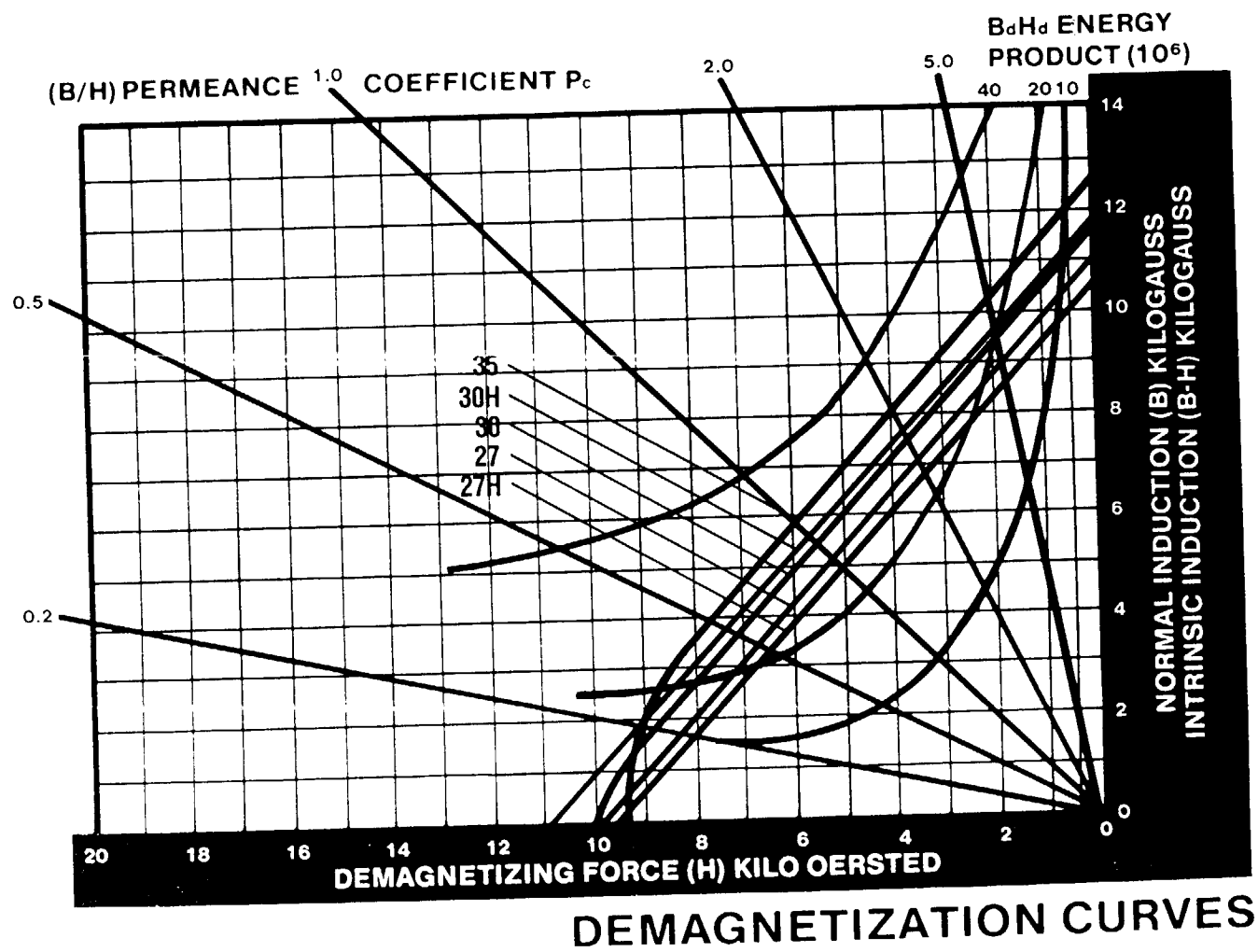


Figure 2.3 Demagnetizing Curve at Different Temperatures
(After I.G. Technologies, Inc.)

substrate thickness provide good heat conduction to the package housing (or supporting material for the microstrip substrate). This condition can be achieved by performing the tradeoff of substrate thickness and losses caused by hybrid mode generation. At millimeter-wave frequency, microstrip cannot maintain a pure TEM mode propagation. Hybrid TE and TM will be generated. Cut-off frequencies of higher-order TE and TM modes impose an upper limit on cross section dimensions. For a given frequency band, maximum ground plane spacing should be such that neither the TE or TM modes can propagate at the upper frequency limit.

For design of a medium power microstrip circuit (up to 10 W, including circulator), the following guidelines are recommended:

- Select cross sectional dimension to limit higher-order modes and to achieve both smooth transitions (microstrip-microstrip and microstrip-coaxial launcher) and good impedance matching.
- Determine the total transmission line losses at the highest operating frequency. Minimize conductor loss by using TiW/Au microstrip, and minimize dielectric loss by choosing a substrate with low loss tangent.
- Consider the worst operating conditions, and compute the maximum safe operating temperature of the dielectric substrate.

- Select ferrite substrate with high spin wave line width (ΔH_k)

2.7 Performance Uniformity and High Yield Rate

In order to achieve uniform performance and high yield rate for MMW circulators, the following processes must be carefully controlled.

- Design of circulator resonator (size, shape, symmetry) transformer (size, length, levels), and transmission line (size, bending, length).
- Selection of ferrite substrate with suitable physical properties (purity, magneto-crystalline anisotropy, porosity)
- Preparation of substrate including substrate cleaning, polishing, cutting
- Metallization of material, thickness, quality and process conditions
- Photolithograph processing techniques and tolerance
- Housing design and mechanical tolerance
- Solder selection and assembly procedure
- Coaxial to launcher selection and assembly procedure

3.0 Material Selection

3.1 Ferrite Substrate Selection Guide

High performance microwave and millimeter-wave circulators, with wide bandwidth and low insertion loss, require magnetic substrates with low FMR (ferromagnetic resonance) linewidth. Low insertion loss circulators need a ferrite substrate with small values of linewidth. High operational frequencies require a substrate with high saturation magnetism.

3.1.1 Microwave and Millimeter Wave Ferrite Materials

Single crystals and polycrystalline ferrite thin films for microwave and millimeter wave circulator substrates can be classified into three groups, as described in Table 3.1. Lithium ferrite and Ni-Zn ferrite are the spinel ferrites; barium ferrite ($\text{BaFe}_{12}\text{O}_{19}$) is a hexagonal ferrite. This hexagonal ferrite is very attractive for millimeter wave applications because of its high magneto crystalline anisotropy field, which reduces the external field required for resonance. The linewidth of the best hexagonal ferrite sphere is 15 Oe at 60 GHz, with a predicted value 10 Oe for Mn-doped materials.^{1,2} Although single-crystal ferrites have

-
1. M. Labeyrie, J.C. Mage, W. Simonet, J.M. Desvignes, and H. Le Gall, "FMR linewidth of barium hexaferrite at millimeter wavelengths", IEEE Trans. Magan., vol. MAG-20, pp. 1224-1226, 1984.
 2. L.M. Silber and W.D. Wilber, "Temperature and frequency dependence of linewidth in $\text{BaFe}_{12}\text{O}_{19}$ ", IEEE Trans. Magan., vol. MAG-22, pp. 984-986, 1986.

Table 3.1
 Ferrite Materials for Microwave and Millimeter Wave Circulator
 (After H.L. Glass)

<u>Material</u>	<u>Typical Compositions</u>	<u>Characteristics</u>
Garnets	$Y_3Fe_5O_{12}$ $(La, Y)_3(Ga, Fe)_5O_{12}$	Low magnetization: 1780G for YIG, less with substitution Low Curie temperature: 280°C for YIG, less with Ga substitution Excellent crystal quality, low linewidth, low losses
Spinel	$LiFe_5O_8$ $(Ni, Zn)Fe_2O_4$	High magnetization: 3750 G for Li ferrite, 5000 G for Ni-Zn ferrite High Curie temperature: 640°C for Li ferrite 375°C for Ni-Zn ferrite Fairly low linewidths, losses: Generally higher than garnets (crystal quality needs improvement)
Hexagonal Ferrites	$BaFe_{12}O_{19}$	High magnetization: 4500G Fairly high Curie temperature: 450°C Potential for fairly low loss crystal quality (needs improvement high magnetocrystalline anisotropy: Can reduce need for magnets).

important roles to play in certain components, polycrystalline materials are more feasible for microwave and millimeter wave circulators and isolators.

3.1.2 New Commercially Available Ferrite Substrates for Millimeter-Wave Circulators

The characteristics of three new commercially available ferrite substrates are presented in Figure 3.1. Saturation magnetism versus temperature variation of these three substrates is depicted in Figure 3.2. The new ferrite materials have a low loss tangent of less than 0.0002 measured at 9.4 GHz.

WRDC/ELMT has aggressively sponsored a project to investigate Millimeter Wave Ferrites. Several ferrites, including LiCu, LiZn and barium ferrites, were grown and characterized by TRW, Colorado State University, Alfred University, Washington University, Countis Laboratory and Ampex. The main objective of the project was development of millimeter wave ferrite materials. The investigation results are reported elsewhere.¹

3.2 Magnets

A permanent magnet for high performance wide bandwidth, miniature microwave circulators require the following characteristics:

1. J.E. Rave and W. S. Piotrowski, Millimeter Wave Ferrites, Final Tech. Report, AFWAL-TR-88-1026.

- Saturation magnetization ($4\pi M_s$) in Gauss @ 23°C
- g-effective @ 9.4 GHz
- Linewidth (ΔH) in oersteds @ -3 dB and 9.4 GHz
- Dielectric constant (ϵ') @ 9.4 GHz
- Dielectric loss tangent ($\tan\delta$) @ 9.4 GHz
- Curie Temperature in °C
- Initial permeability (μ_0) KHz

	Transtech TT86-6000	Transtech TT2-111	Thomson A50
	4900	5000	5000
	2.11	2.11	2.06
	160	160	170
	12.5	12.5	15.3
	< 0.0002	< 0.0010	< 0.0005
	363	375	450
	317	317	398

Figure 3.1 Characteristics of Three High Performance Ferrite Substrate for Microwave Circulators

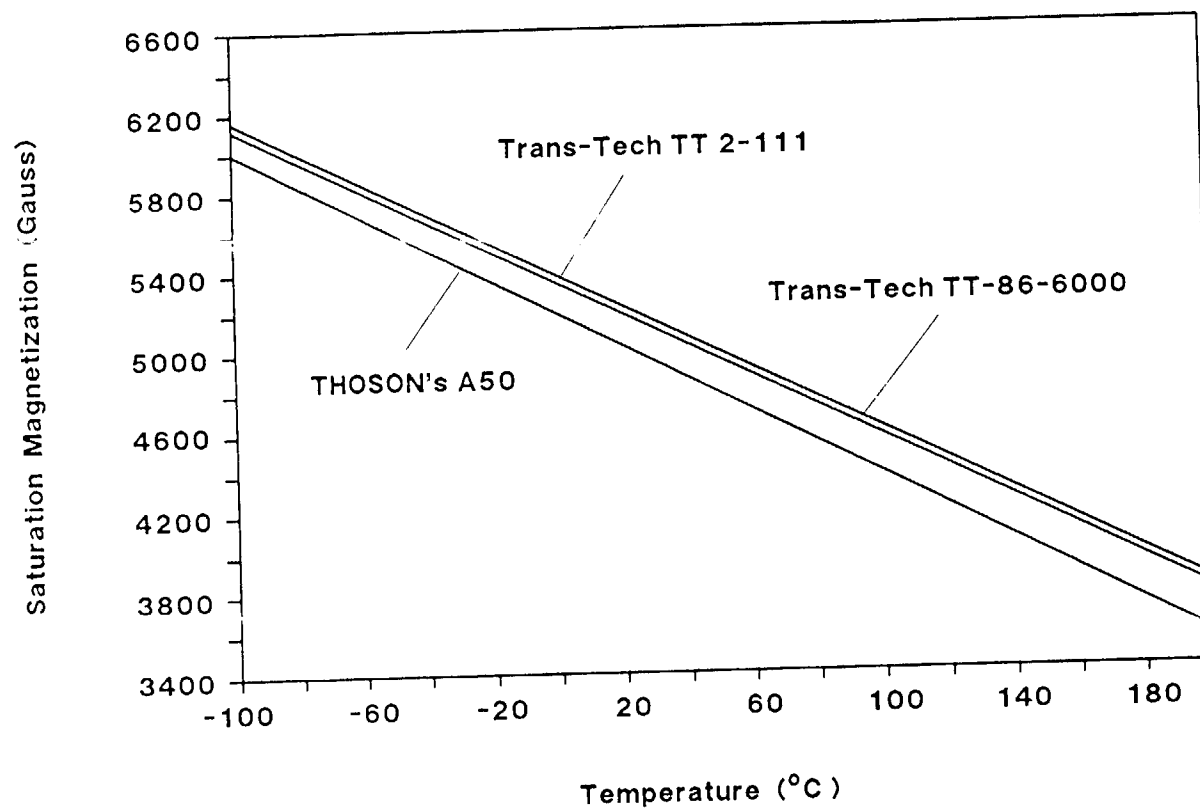


Figure 3.2 Comparison of Saturation Magnetization Vs Temperature of Ferrites

- High magnetism with small physical size
- Good temperature stability
- High resistance to demagnetization
- Low reversible losses

Several commercial high performance magnets were investigated in Phase II R&D. Performance parameters of the magnets are listed in Table 3.2.

Among these permanent magnets, permag's SM_2O_{17} -28 was selected and used in this project for the following reasons:

- High energy product (28 MGD) and high residual induction (10,750 Gauss) will allow device to use smaller volume of magnet and provide high flux density in the gap. These properties will improve device operation frequency and provide better RF grounding
- Excellent temperature stability - the SM_2O_{17} magnet provide the best temperature stability; it can survive within a wide temperature range and has the lowest temperature coefficient, which allows minimum flux density change over our designed temperature range.
- High resistance to demagnetization SM_2O_{17} virtually immune to accidental demagnetizing effect, since it allows the user to magnetize the magnet and then assemble it into the

Table 3.2

Performance Parameters of Magnet at Room Temperature

Magnetic Characteristic	Hitachi H-96B	Permag SM ₂ CO ₁₇ -28	IE Tech INCOR21	Arnold NdFeB35H
Peak Energy Product-(BdHd) Max. $\times 10^6$	21.5	28.0	21.0	35
Residual Induction B _r - Gauss	9,400	10,750	9,400	12,100
Coercive Force H _c - Oersteds	8,800	8,400	8,300	11,300
Intrinsic Coercive Force H _{ci} - Oersteds	15,000	10,000	10,000	>14,000
Curie Temperature - C°	680	800	680	300
Temperature Affecting Material - C°	150	350	300	150
Reversible Temperature Coefficient-%/C° For Magnets Operating at (BH) Max.	0.05	0.025	0.045	.10
Magnetizing Force H _s -KO _E	>20	>15	>15	>28

device without using a magnet keeper.

3.3 RF Launcher Selections

Coaxial-to-microstrip launcher for MMW circulator project should have the following features:

- o Operation Frequency: DC to 45 GHz
- o Insertion Loss at 40 GHz ≤ 0.5 dB (or ≤ 1.0 dB)
for Two Launchers
Connected Back to Back)
- o VSWR in Frequency Range: $\leq 1.3 : 1$
- o Repeatability: Less than $\pm 10\%$
Variation within 30 Time of Mating

Table 3.3 compares the two millimeter wave coaxial to microstrip launchers which currently are commercially available . Apc 2.4 mm connector launchers are manufactured by M/A COM OMNI spectra, Inc. K-connector launchers are manufactured by Wiltron. The typical back-to-back return loss of two connector launchers, joined by 0.5" microstrip transmission line, is depicted in Figure 3.3 (a) and (b) for Apx 2.4 mm connector and K connector, respectively. The performance of both of these connector launchers meets the project's requirements. Therefore, in phase II R & D, E-Tek selected and tested both connector launchers for the MMW circulator fabrication.

Table 3.3
Comparison of MMW Coaxial to Microstrip Launchers

Description	K Connector Launcher		APC 2.4mm Connector Launcher
	W/Glass Beads	W/O Glass Beads	
● Operation Frequency Range	DC-46 GHz	DC-46 GHz	DC-50 GHz
● VSWR			
DC-18 GHz	-	-	1.08 (Max)
18-26.5 GHz	-	-	1.13 (Max)
26.5 46 GHz	1.35 (Max)	1.25	1.29 (Max)
● Field Replaceable Interface	Yes	No	Yes
● Connector Durability	500 Cycles	N/A	500 Cycles
● Electrical and Mechanical Compatibility with SMA, APC 3.5 mm	Yes	Yes	No
● Operating Temperature	-65C °-125 C °	-65°C-125°C	-55°-125°C

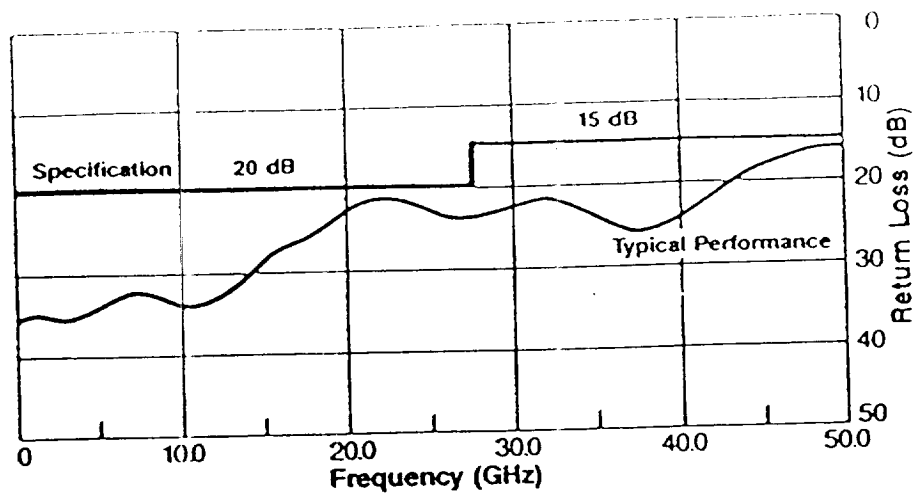


Figure 3.3 (a) Typical Return Loss of 2.4 mm Launchers Joined by Microstrip Transmission Line

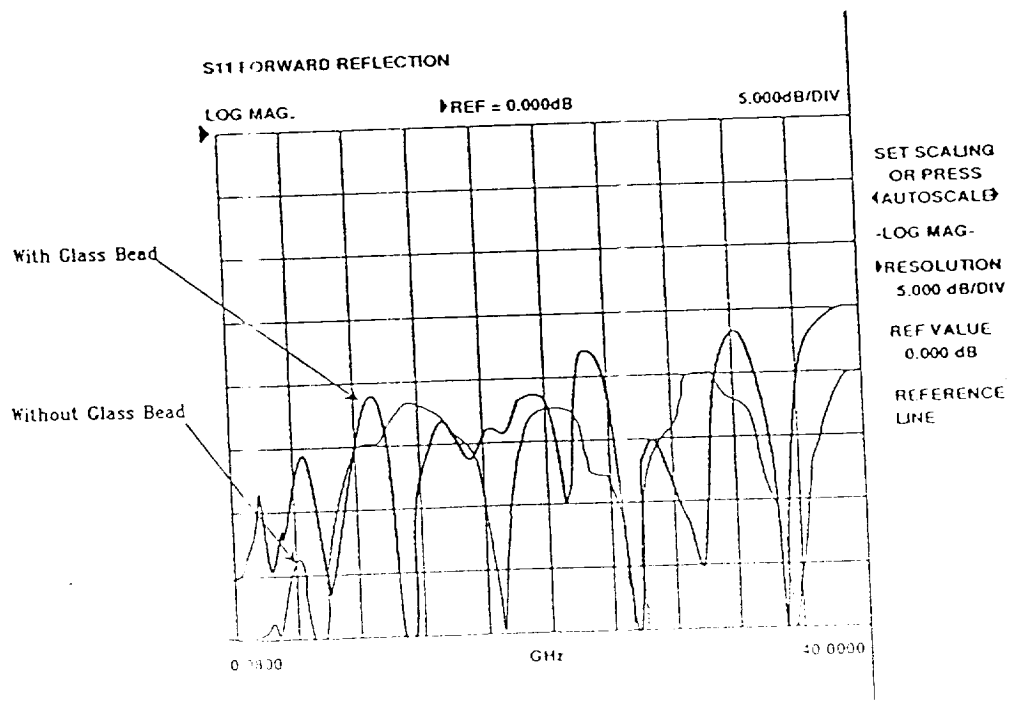


Figure 3.3 (b) Typical Return Loss of K Connector Launcher Joined by Microstrip Transmission Line

4.0 Fabrication Assembly Process Improvement Evaluation and Optimization

Critical factors in the 36-40 GHz high performance microstrip circulator fabrication and assembly process have been improved, evaluated, and optimized in order to achieve the design goals. These factors are:

- Proper ferrite substrate metallization, with low conductor resistance; strong and durable adhesion
- Proper ferrite substrate preparation and cleaning procedure
- Adequate photolithographic process with precise line width control and no undercut.
- Permanent magnet evaluation for different type, shape, size, bias condition, and magnetic field density over a wide operation temperature.
- Coaxial to microstrip launcher performance evaluation

4.1 Ferrite Substrate Metallization

During phase I circulator development, three layers of Cr/Cu/Au were metallized on the ferrite substrate. The reason for using Cr/Cu/Au instead of Cr/Au is that Cu provides a better

conductivity than Au and thus reduces the circulator's metallic loss. The purpose of sputtering a thin layer of Au on top of Cu is to protect Cu from oxidization. However, the results proved to be unsatisfactory for the following reasons:

- (i) Metallization process complexity
- (ii) Adhesion between layers was not strong; etching undercut occurred during the photolithograph process
- (iii) Cr etching solution will significantly attack the ferrite substrate

Therefore, in phase II R & D, E-Tek used Ti/Au metallization for circulator fabrication instead of Cr/Au for following reasons:

- (i) Ti (Titanium) has a strong adhesion bond with ferrite, LiNbO_3 , Al_2O_3 , etc.
- (ii) Ti metallization is a well established and recognized techniques
- (iii) E-Tek has an in-house sputtering system (CVC 6000 series) with 8" Ti target which provides very good uniformity. Also, E-Tek process engineers have great deal of experience with Ti. Therefore, Ti layer quality can be assured.
- (IV) Fabrication simplicity (only two metallization layers required for Ti/Au instead of three layers required Cr/Cu/Au)
- (V) Ti layer can be etched off by hydrogen Peroxide (H_2O_2)

which will not degrade the ferrite substrate. Cr etching solution, on the other hand, contains strong acid such as Ceric surface, Nitric acid, sulfuric acid, which will significantly damage ferrite substrate.

(VI) From a recent study (see table 4.1) Ti/Au (or TiW/Au) sputtered metallization provides low resistivity

Sputtered copper (Cu) (see Table 4.1) has a substantially lower resistivity than electroplated Cu (although it has 1.8 times the resistivity of the bulk Cu). The high resistivity of sputtered gold (Au), relative to the plated gold, is due to the diffusion of chromium (Cr) into the gold during the sputtering process (Subsequent removal of the Au revealed that the Cr adhesive layer was indeed dissolved by the gold). The resistivity of all sputtered Ti/Au (or TiW/Au) is 3.0×10^{-6} ohm-cm, which is slightly higher than sputtered Cu, but also much better than plated Cu or sputtered Au.

Determining the proper thickness of the adhesion layer is a trade-off between better conductivity on the one hand, and better adhesion bond of substrate and metallization on the other. For a thin adhesion layer, which was used in phase I R&D, it was found that the adhesion layer partially migrated into the gold (or copper) layer, due to the sputtering process, timing, and wide operating temperature range. These migrations result in poor adhesion and cause severe undercut during the etching process. A thick adhesion layer increased the resistivity which, in turn,

Table 4.1 Summary of Resistivity Measurements, in Micro-Ohm-cm,
For Electroplated and All-Sputtered Cr/Cu and Cr/Au Films
(After R. Tramposch)

Cu, Sputtered	Cu, Plated	Au, Sputtered	Au, Plated
2.93	12.4	6.64	3.26
Bulk Cu	Bulk Au	TiW/Au, Sputtered	
1.65	2.45	3.0	

increased the insertion loss of circulator performance. To optimize these two factors, E-Tek employed the following metallization sequence in phase II ferrite substrate metallization:

- (i) Sputter a layer of Ti on a well cleaned ferrite substrate with Ti thickness of $500 \text{ \AA} \pm 50 \text{ \AA}$. Figure 4.1 shows the substrate holder during the sputtering process.
- (ii) Sputter a 2000 \AA thick gold (Au) layer on top of the Ti layer (wait 20 minutes to cool down the temperature of substrate to avoid Ti migration into Au layer.)
- (iii) Au plate substrate to a proper thickness. (Please note that the plating is done after photolithograph work in order to ensure the best linewidth control.) A special gold plating substrate holder and set up (Figure 4.2) was made to provide uniform plating results for such a small device.

The metallization chamber environment is critically important to achieving a strong adhesion between metal layers. E-Tek process engineers optimized the metallization conditions as follows:

● Base pressure	5.0×10^{-7} Torr or lower
● Sputtering rate	10 \AA/sec
● Substrate heating temperature	95°C
● Ar gas pressure	5.0 Millitorr
● Substrate/Target distance	4.0 inches for Ti

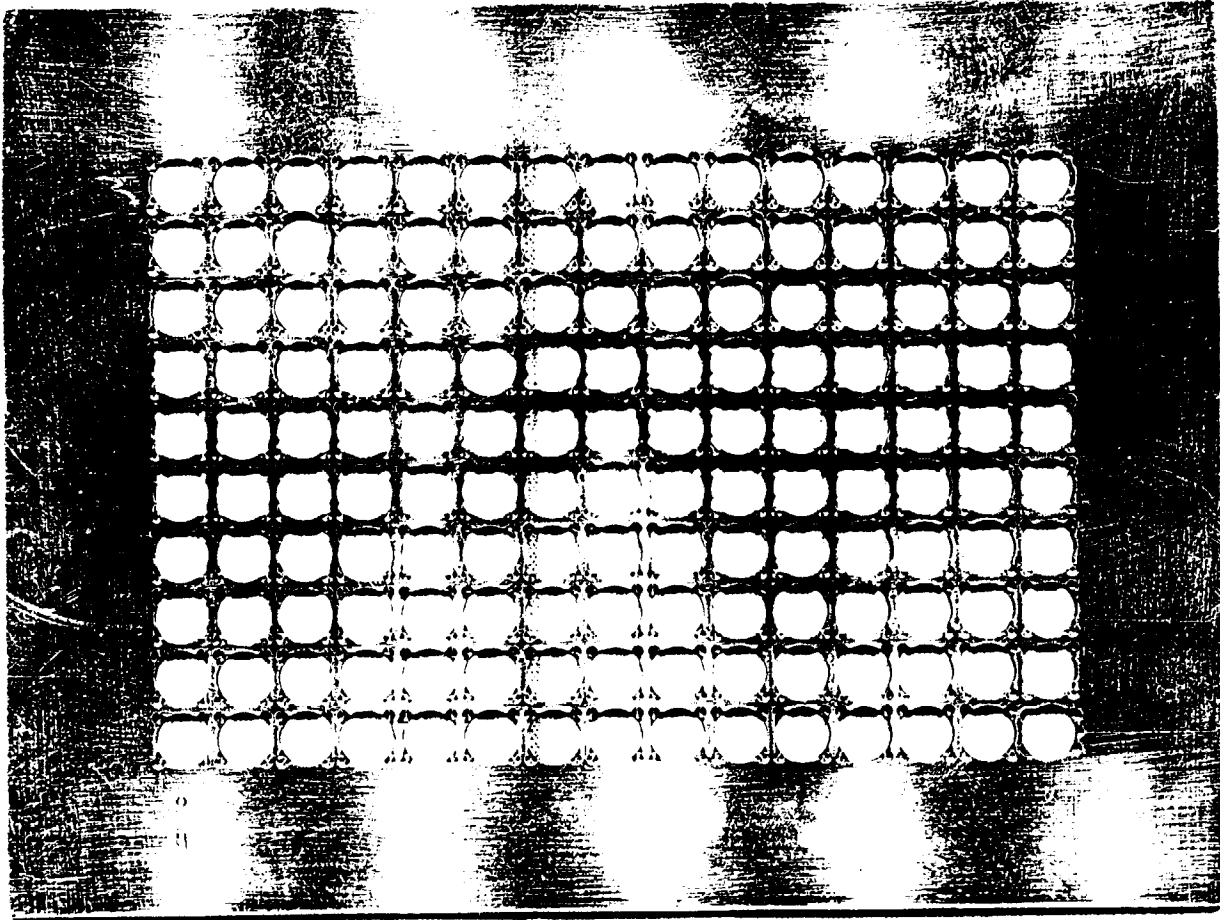
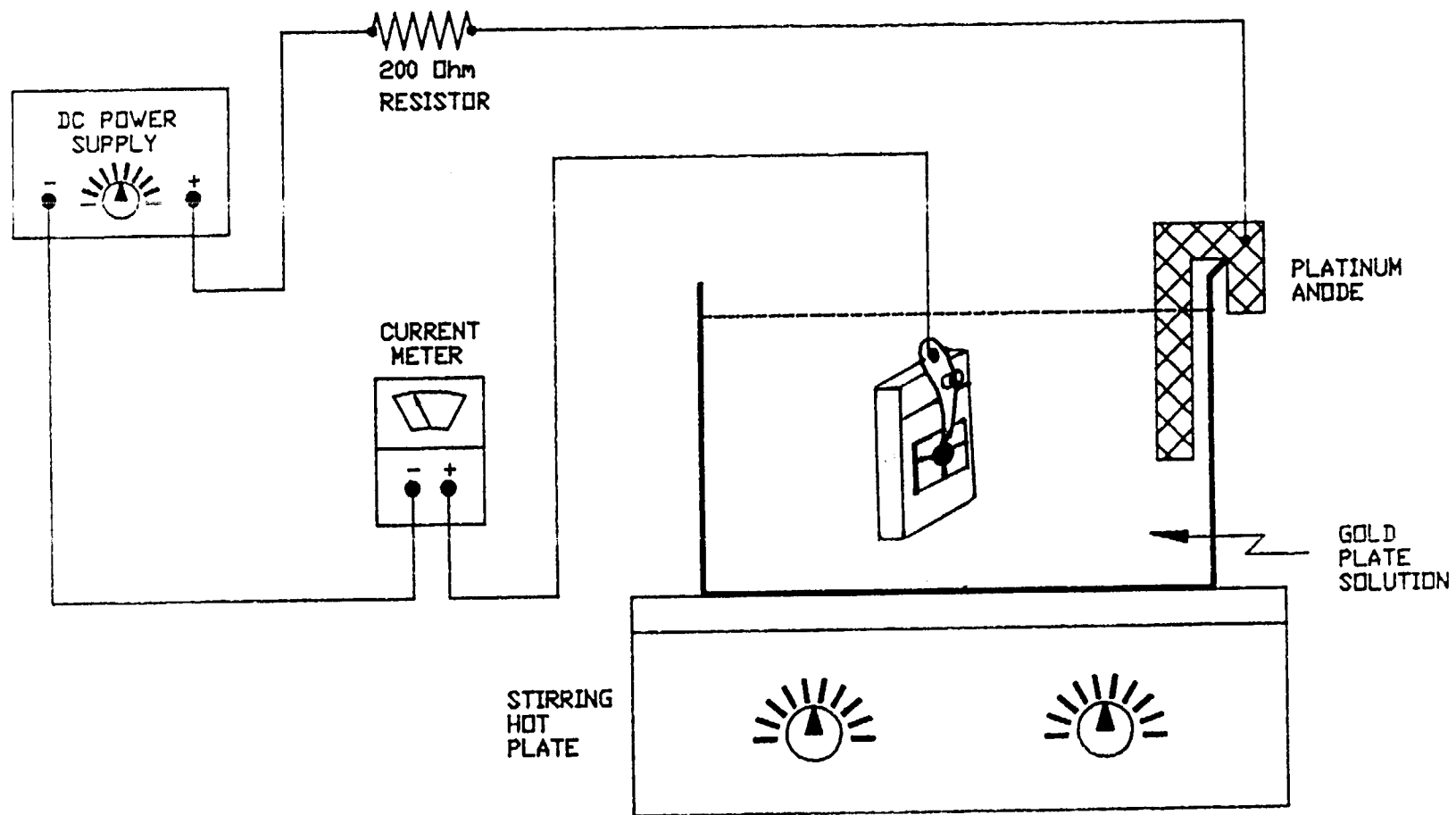


Figure 4.1 Substrate Holder during the Sputtering Porcess

ORIGINAL PAGE IS
OF POOR QUALITY



SETUP FOR GOLD PLATING ON BRASS BLOCK

Figure 4.2

5.0 inches for Au

- Substrate rotation speed 6 rpm

4.2 Substrate Preparation and Inspection

The practical impacts on circulator performance due to substrate preparation (such as thickness deviation, size deviation, surface finish, dielectric constant variation, loss tangent, substrate cleaning) are:

<u>Parameter</u>	<u>Performance Impact</u>
● Substrate thickness deviation	Impedance miscalculation: degradation of VSWR, insertion loss, and isolation
● Substrate size deviation	cannot correctly interface with test fixture, or package increase of insertion loss, VSWR, isolation and bandwidth
● Surface finish	Increased insertion loss, induced by rough surface scattering. Five μ inch finish is recommended for 40 GHz circulator substrate.
● Dielectric constant	Miscalculation of impedance: degradation of VSWR, insertion loss, and isolation. The measured value should be used in

the design

- Loss tangent Induce the dielectric loss
- Substrate cleaning process Directly affects the adhesion of metallization and photolithographic quality.

The standard ferrite substrate preparation and inspection flow diagram is depicted in Figure 4.3.

4.2.1 Ferrite Substrate Dielectric Constant & Loss Tangent

Upon receiving the ferrite substrate, E-Tek obtained and verified the measured ferrite dielectric constant, which was measured using standard microwave test methods in X-band (the setup is depicted in Figure 4.4) and dielectric loss tangent. The measured dielectric constant value is 12.27, which was used in the circulator design, and loss tangent has the value 0.0002 which will induce minimum dielectric loss, thus the ferrite disk embedding approach will not be necessary

4.2.2 Ferrite Substrate Size and Thickness Deviation

E-Tek has an in-house substrate cutter with 4"Dia x 0.006" thick diamond wheel which will precisely cut substrate within the tolerance $\pm 0.002"$. A polish procedure should be followed by using a 12 μm micropolish disc to keep the size tolerance within $\pm 0.001"$. The thickness and size measurement were taken with a Mitutoyo

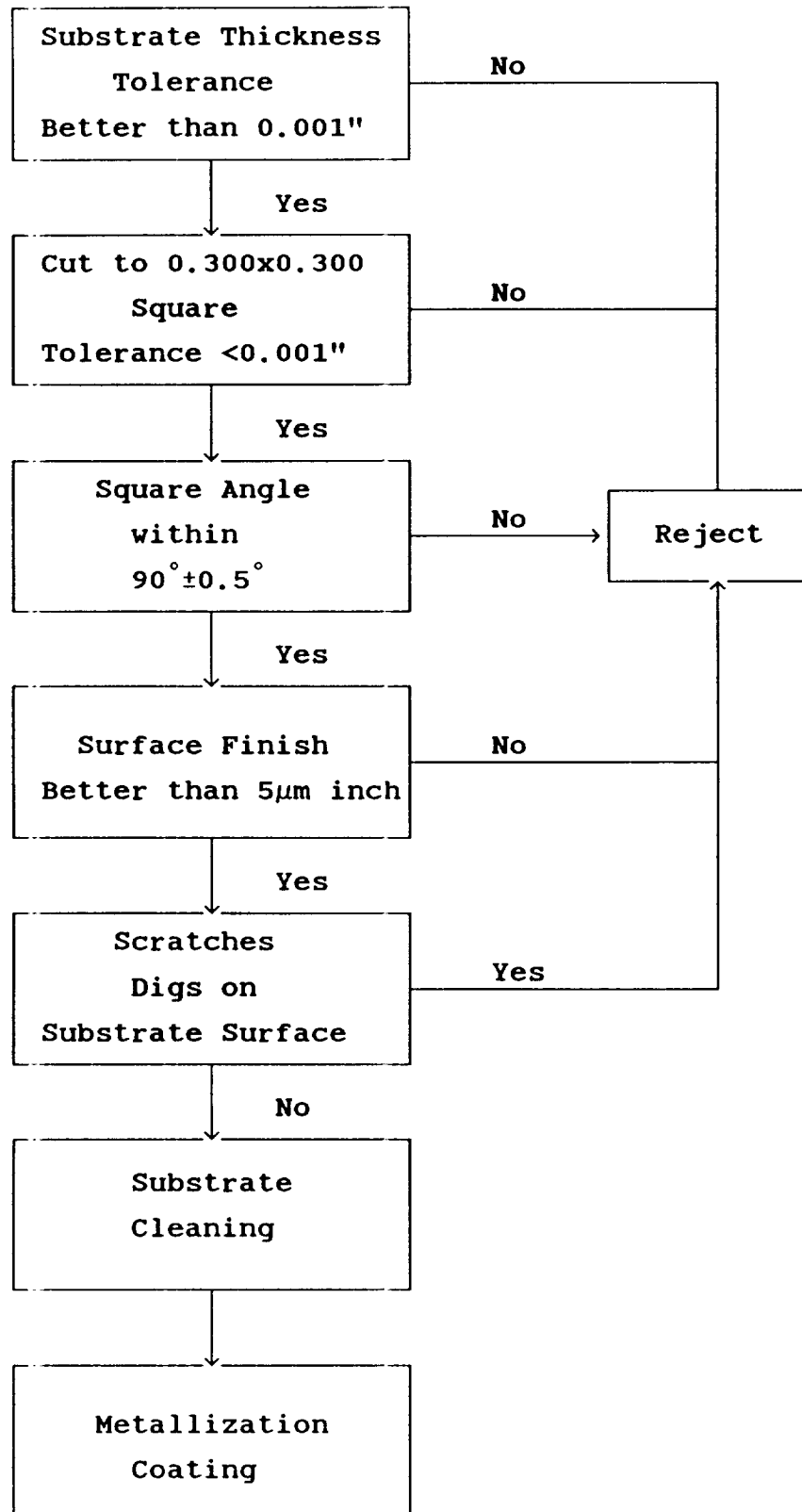


Figure 4.3 Substrate Preparation and Inspection Procedure

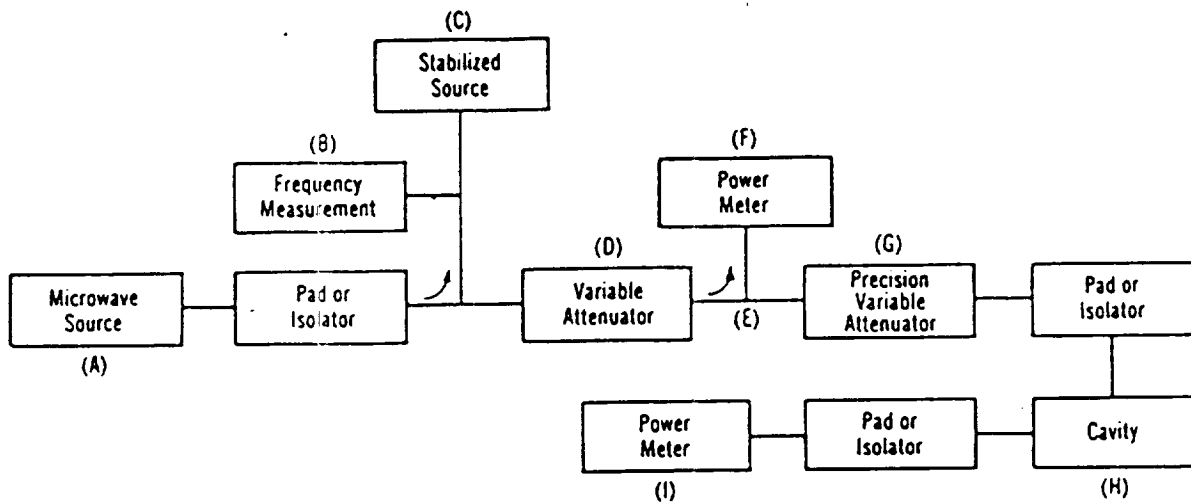


Figure 4.4 Setup for Ferrite Substrate Dielectric Constant Measurement

micrometer, which has the resolution capability of 0.00005", in order to make certain the dimensions are accurately established.

4.2.3 Ferrite Substrate Surface Finish

To improve circulator insertion loss due to surface scattering, it is essential to obtain well finished ferrite substrate. Due to its spinel structure and the thickness required, ferrite substrate is very difficult to polish down to 10 μ inch uniformity.

Only recently have a few manufacturers have promised to polish the ferrite substrate down to 5 μ inch range: a typical ferrite substrate polish procedure is depicted in Figure 4.5. E-Tek engineers use a comparison method to check the condition of the substrate surface finish. The ferrite substrate is compared, under a 50x microscope, with LiNbO₃ substrate to make sure the flatness, scratch and dig conditions meet our proposed requirements.

4.2.4 Ferrite Substrate Cleaning Procedure

The cleanliness of the oxide substrate decisively influences the adhesion, film growth, sintering and electrical performance of the metal films deposited. Therefore, a thoroughly cleaned substrate is an absolute prerequisite for the preparation of films with acceptable results.

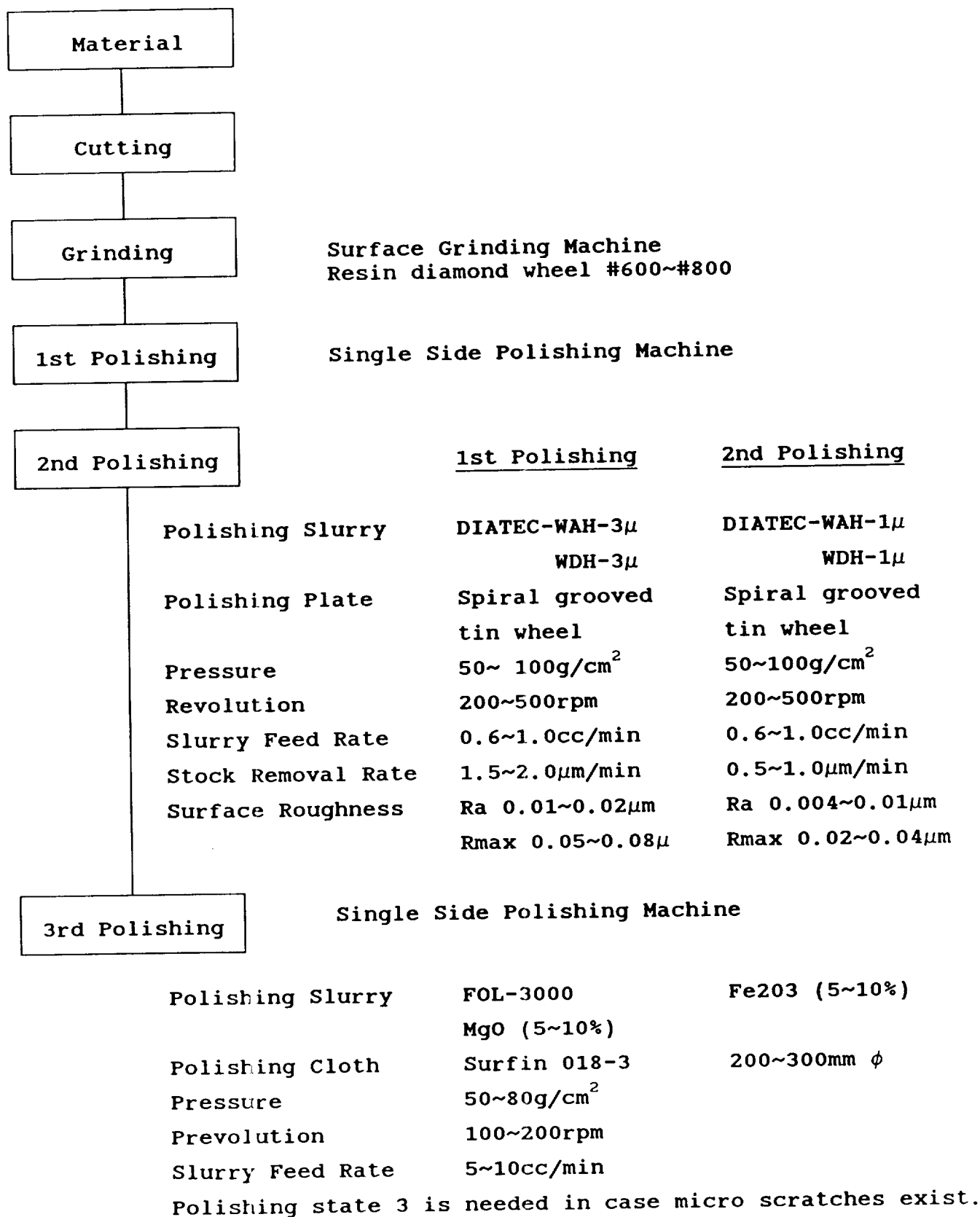


Figure 4.5 Ferrite Process

25-43-19FR-FG45

Residues from manufacturing and packaging, lint, fingerprints, oil, grease and airborne dust are examples of contaminants frequently encountered on substrates. Accordingly their identification and effective removal, by methods that will not harm the substrate, is a critical preliminary step. In general, ferrite substrates are more readily attacked by strong acids (HCl, HF, HNO₃, chromic acid) and alkaline (NaOH, KOH) than alumina substrate; therefore, it is important to avoid the use of these cleaning agents.

The sequence of the cleaning process is also important. Organic residues (oils greases, waxes, and adhesives) have to be removed first, since they will prevent the wetting of other inorganic soils. To remove water-soluble and some organic contaminants, the ferrite substrate was cleaned with ultrasonic agitation in an aqueous, mild alkaline detergent (such as Alconox, PH of 9-10). Thorough rinsing and drying by water displacement was employed to remove the alkaline or other ionic salts derived from the detergent.

During the cleaning process, mechanical scrubbing and all toxic cleaning solutions were avoided. Table 4.2 shows the ferrite substrate cleaning steps after diamond sawing and before metallization.

4.3 Optimized Photolithograph Process

Table 4.2 Ferrite Substrate Cleaning Procedure

Step	Operation	Time
1	Immersion in trichlorotrifluoroethane with ultrasonic agitation	5 minutes
2	Ultrasonically agitate substrate in Alconox detergent (ph. 9-10, temperature 50° - 60°C)	30 minutes
3	Rinse in running deionize water	2 minutes
4	Nitrogen gas blow dry	1 minute
5	Ultrasonic rinse ethanol	5 minutes
6	Vapor rinse in ethanol	1 minute

A photolithograph process for achieving a high performance MMW circulator has been evaluated and optimized to meet the following goals:

- No undercut or overcut allowed between metallization layers or substrate
- All critical linewidth tolerances are better than 0.2 mil
- Pattern misalignment tolerances are better than 1 mil, especially those interfacing with connector launchers
- All etching plating cleaning solutions utilized must not attack the ferrite substrate
- No scratch or digs allowed

The process was performed in E-Tek's new clean room to ensure repeatability; optimized procedure flow is depicted in Figure 4.6.

4.4 Permanent Magnets

Several high energy product permanent magnets (listed in Table 4.3) were measured for flux density. Neodymium Iron Boron ($\text{Nd}_2\text{Fe}_{14}\text{B}$) and Submarine cobalt ($\text{Sm}_2\text{Co}_{17}$) have the best magnetic fields. However, the Neodymium Iron Boron material suffers more from temperature variation than does submarine cobalt material. Figure 4.7 shows four different magnet Normal Flux density measurements at various temperatures. Figure 4.8 demonstrates the same measurement with 0.010" thick ferrite on top of the magnet $\text{Sm}_2\text{Co}_{17}$ has better overall performance.

Table 4.3

Magnetic Field Measurement of Different Magnet Materials

Magnet Material	Direct Conduct	With Ferrite
NdFeB-35(.125DX.125H)	5.00	3.85
SM2CO17-28(.125DX.125H)	4.10	2.94
SM2CO17-28(.100DX.100H)	3.50	2.20
Hicorex-96(.125DX.125H)	3.65	2.50
Hicorex-96(.04DX.10H)	1.20	0.28
Hicorex-90(.125DX.125H)	3.65	2.50

*All Measurement in KGauss

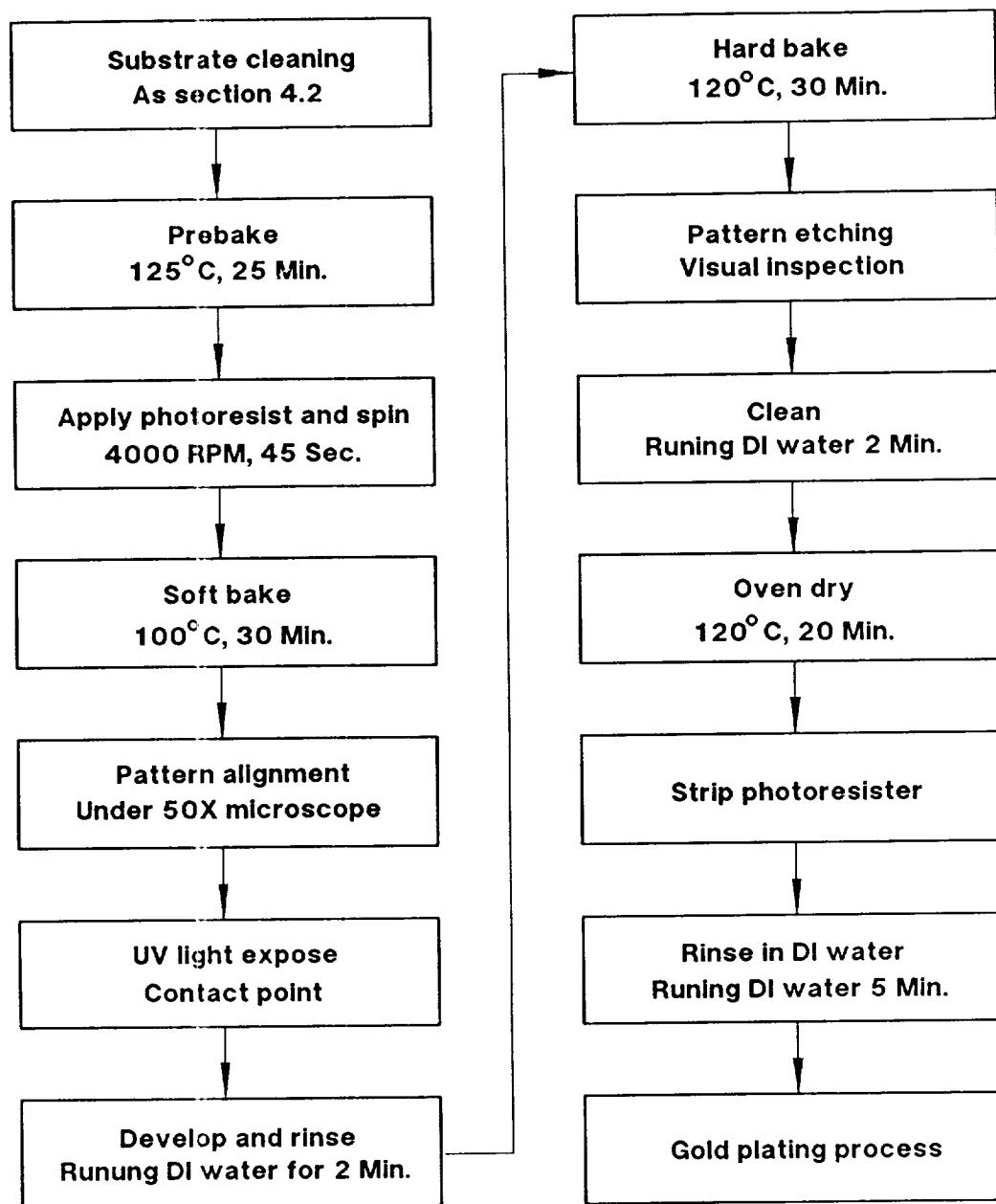


Figure 4.6. Photolithograph Process

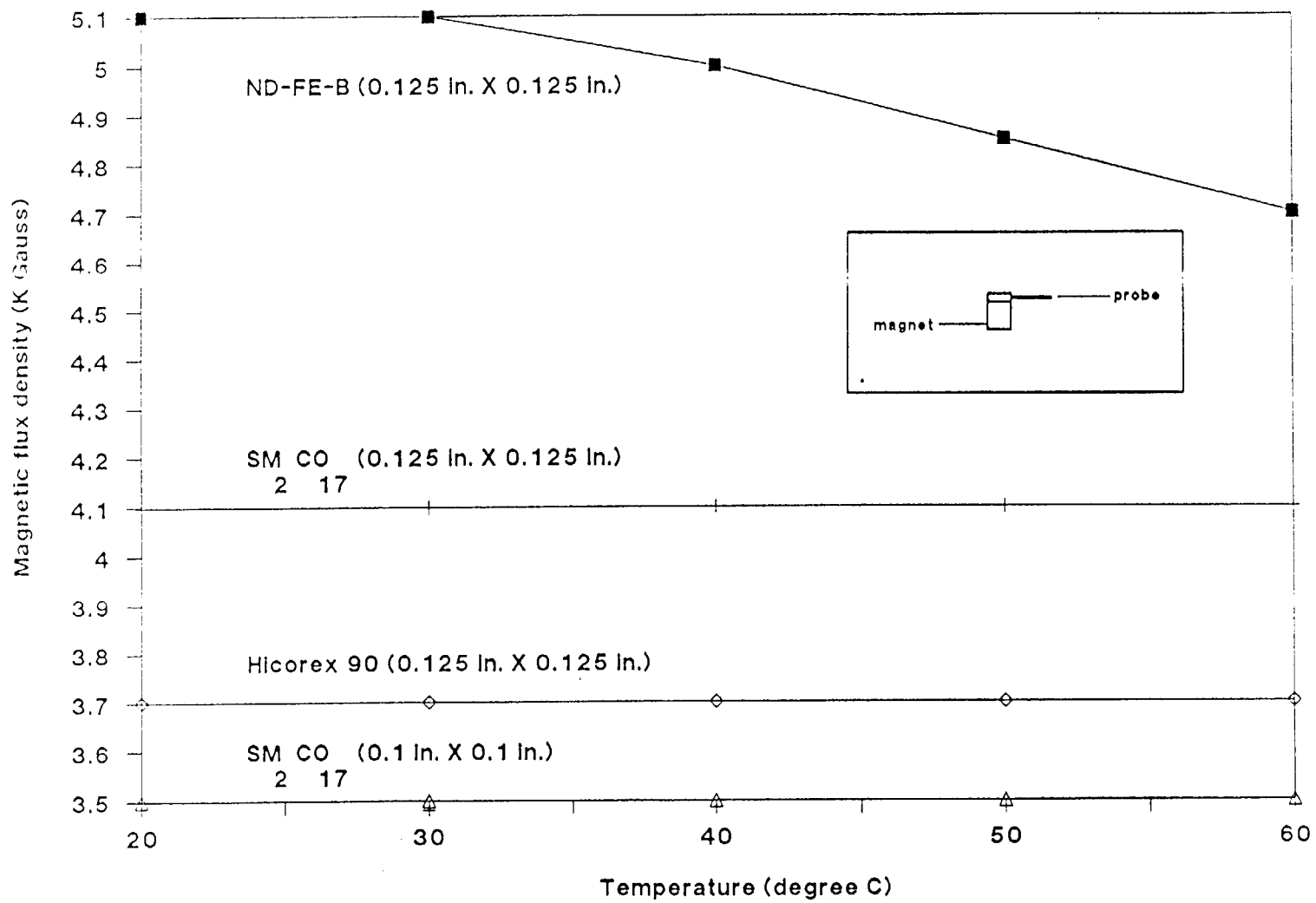


Figure 4.7 Magnetic Flux Density of Different Magnet Materials (without ferrite) Vs. Temperature

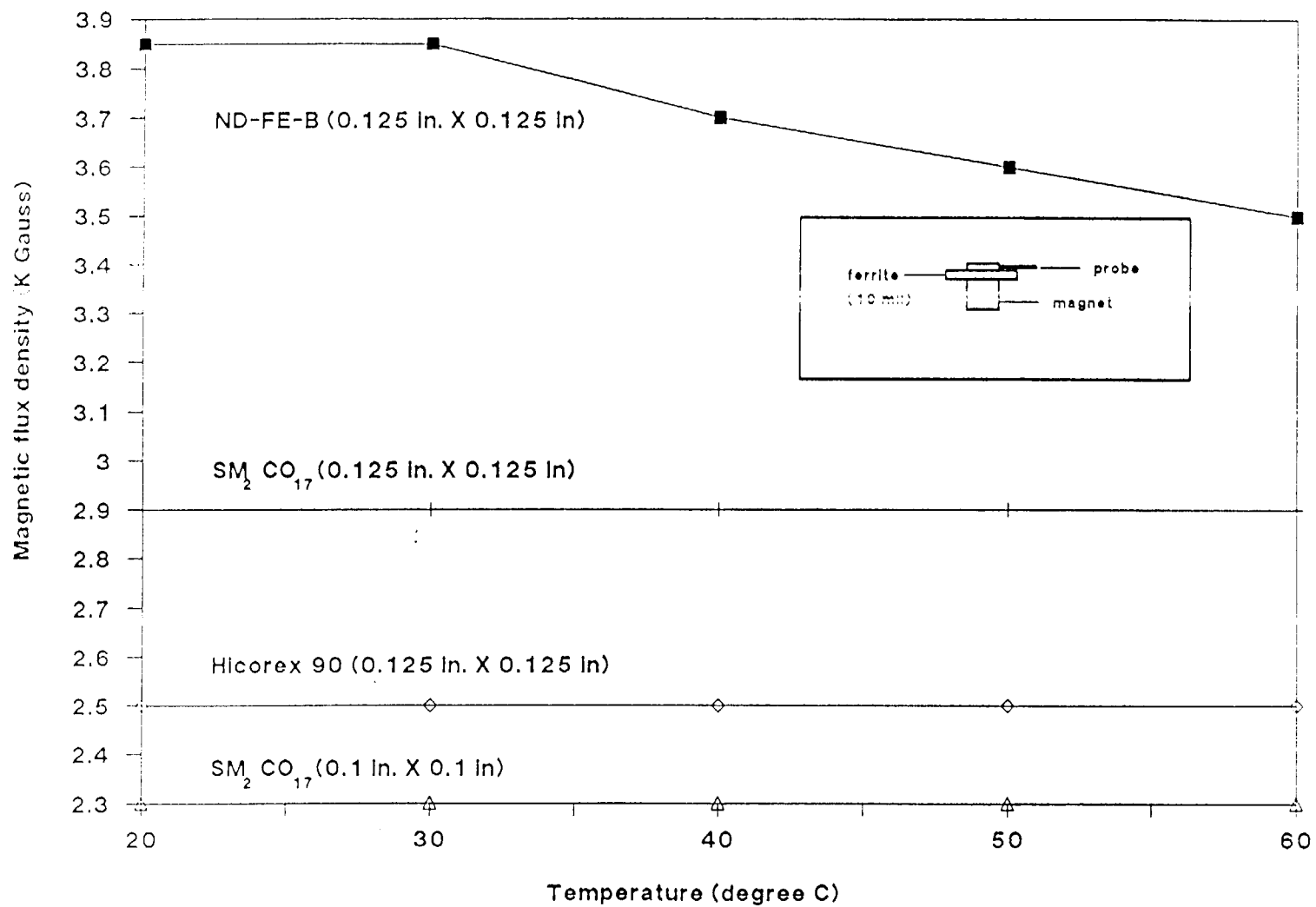


Figure 4.8 Magnetic Flux Density of Different Magnet Materials
(with ferrite) Vs. Temperature

The magnetic flux density decreases when the spacing between magnet and ferrite substrate increases, as measured and illustrated in Figure 4.9.

To obtain a strong magnetic flux density, one magnet can be placed above the ferrite substrate and one magnet placed below the substrate. As illustrated in Figure 4.10, a magnetic flux density of 6800 Gauss was achieved by using two small magnets.

4.5 Coaxial to Microstrip Launcher Performance Evaluation

In order to accurately and respectively measure/evaluate the 36-40 GHz circulator performance, E-Tek engineers have tested both modified K-connectors and APC 2.4 mm connector launchers using a test fixture. Due to limitations of the equipment, the tests were performed with two connector launchers and a 50 Ohm transmission line under ungated conditions. Figure 4.11 shows performance results of the K connector test setup with a 0.3 inch 50 Ohm transmission line on aluminum substrate. Figure 4.12 shows the performance results of the APC 2.4 connector test setup with a 0.5 inch 50 Ohm transmission line on aluminum substrate, plus two APC 2.4 mm male-to-K female adapters. The poor results of the APC 2.4 mm setup occurred mainly because the two extra adapters and the network analyzer were equipped and calibrated for the K connector setup instead of APC 2.4 mm. Vendor data and other lab reports indicate that the performance of APC 2.4 mm can exceed the

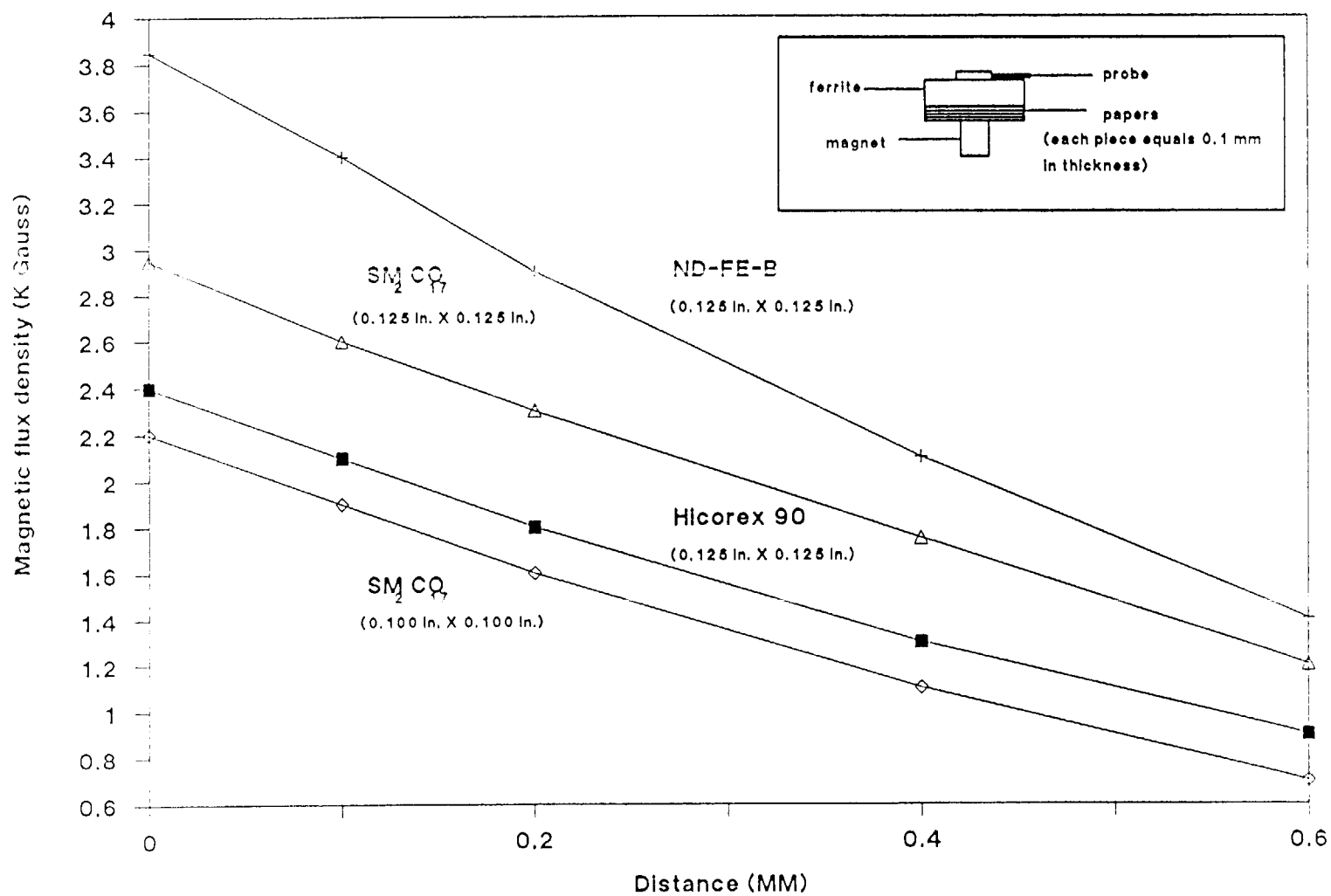


Figure 4.9 Magnetic Flux Density of Varying Magnets with Ferrite (10 mil.) Vs. Distance

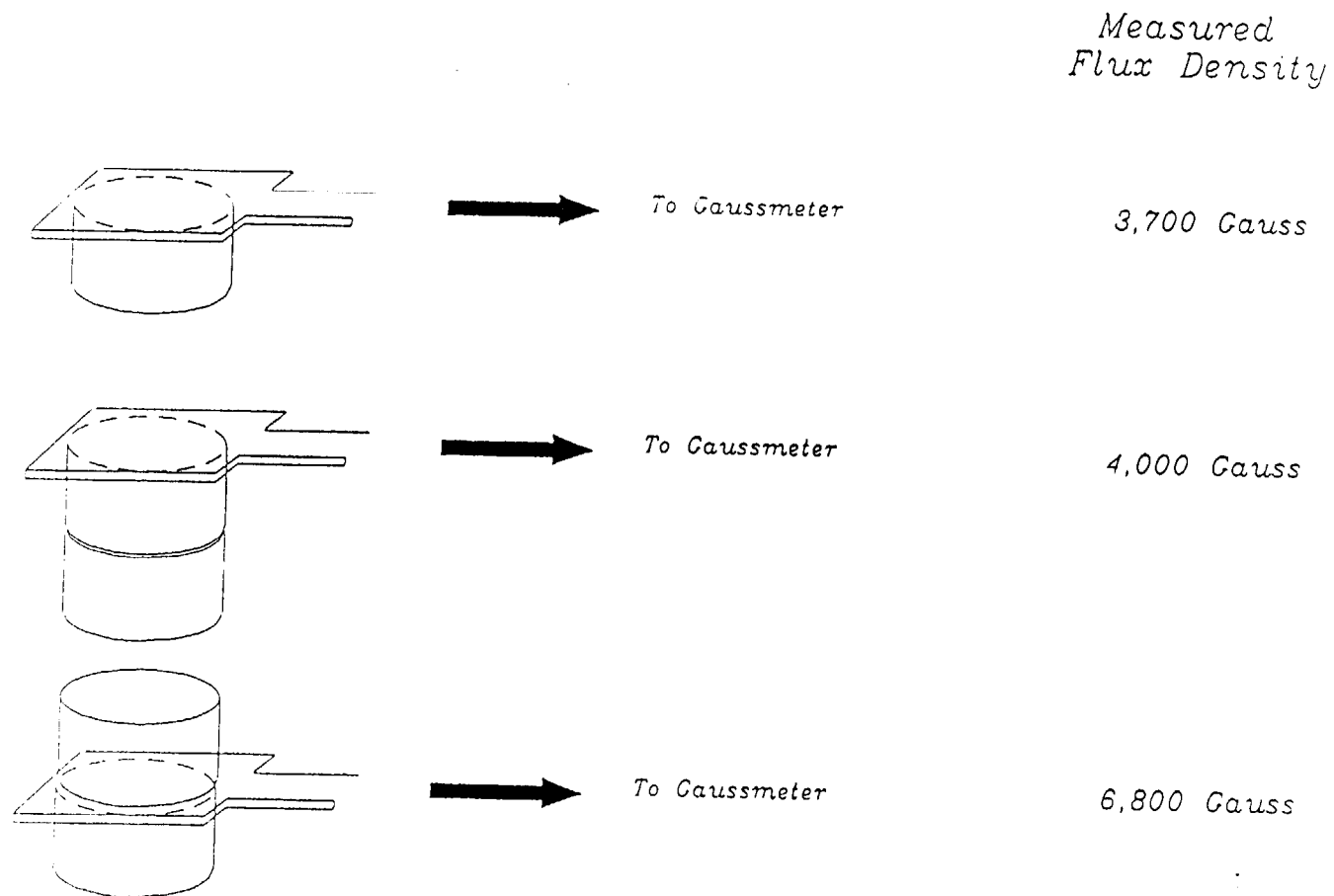


Figure 4.10 Magnet Flux Density Measurement vs Bias Conditions

Identify: 30-40GHZ

Test Device: WILTRON TST

Date: 10-12-89

2: RETN LOSS (B)

5.0 dB/DIV

OFFSET +0.0 dB

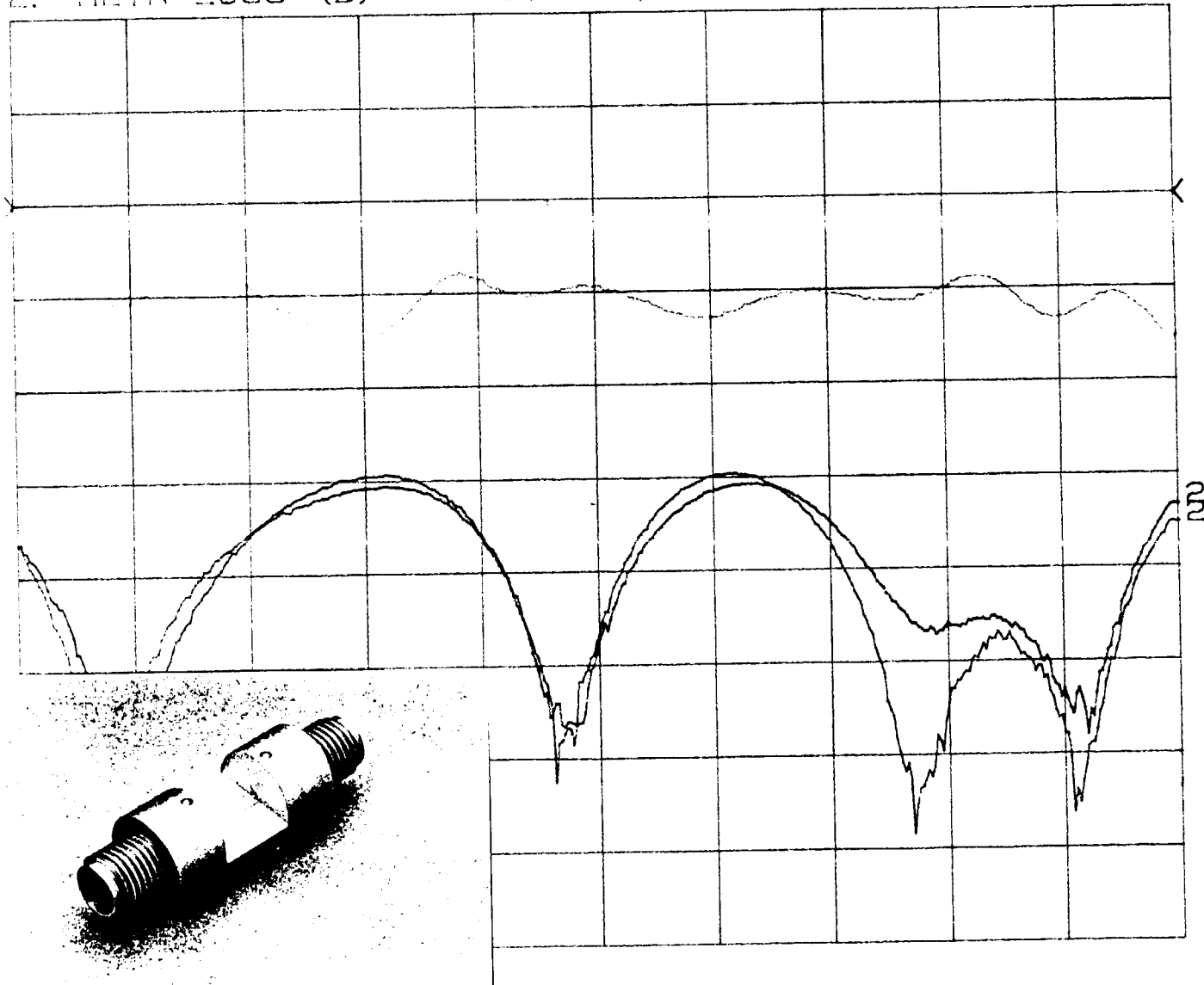


Figure 4.11 Performance of K Connector Test Setup with Two K Connector Launchers and 0.3 " 50 Ohm Transmission Line

Identify: 30-40GHZ

Test Device: OMNI TST#1

Date: 10-12-89

2: RETN LOSS (B)

5.0 dB/DIV

OFFSET +0.0 dB

OFFSET +0.0 dB

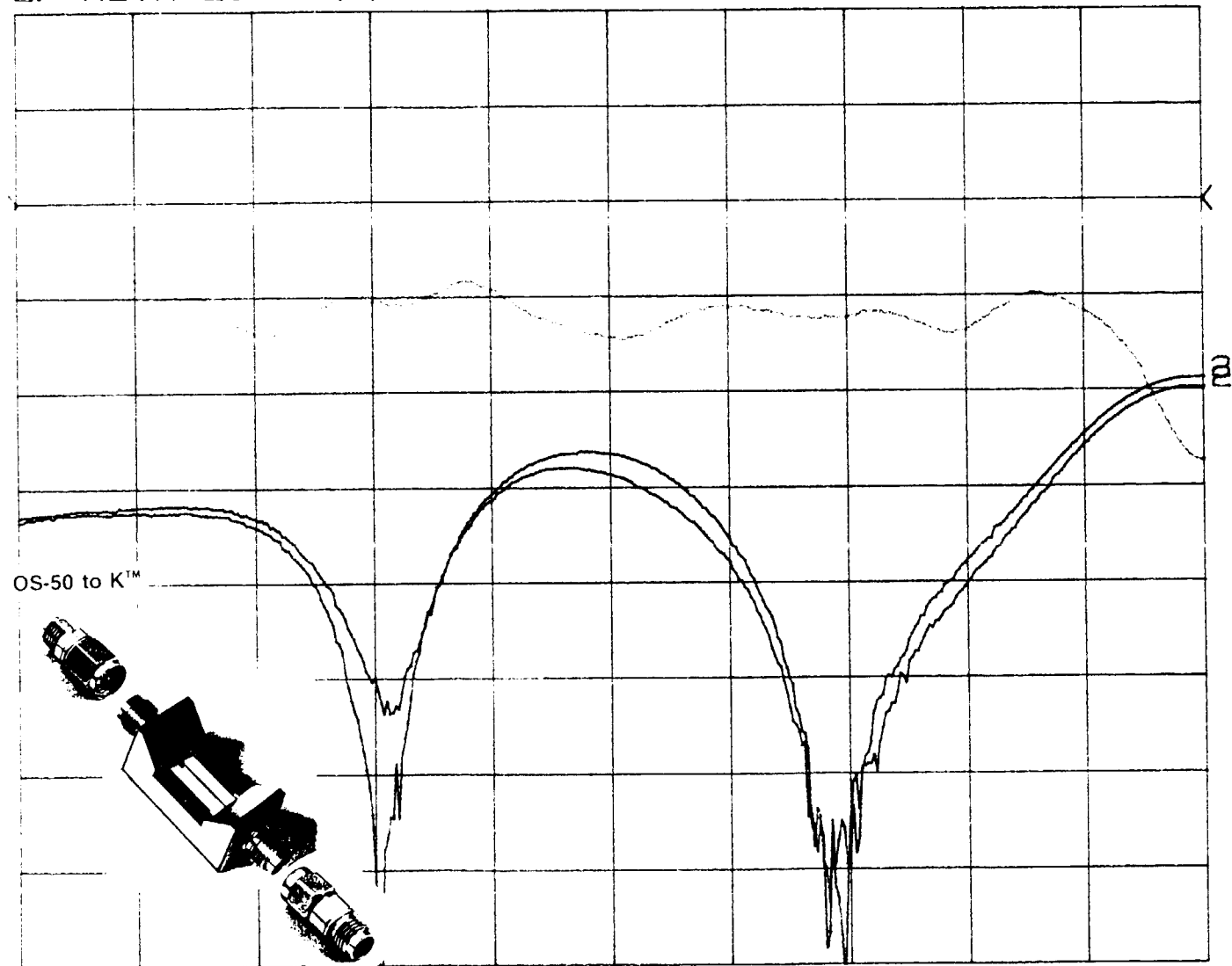
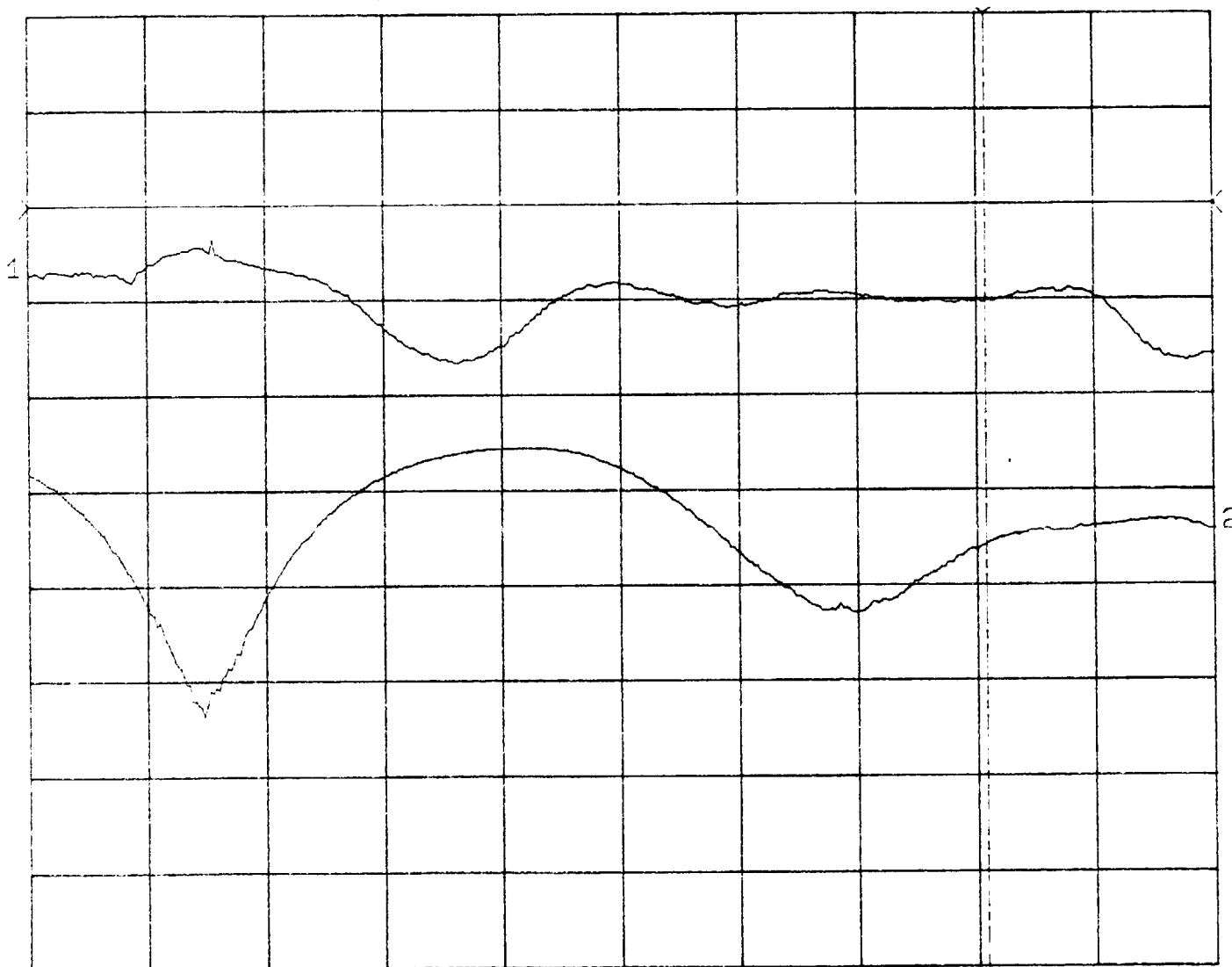


Figure 4.12 Performance of APC 2.4 Connector Test Setup with Two K to APC 2.4 Adapter, Two APC 2.4 Connector Launchers and 0.5" 50 Ohm Transmission Line

performance of K connector in the 30 to 40 GHz range. Thus, apprised of the modified K connector's potential performance, E-Tek engineers built a test fixture with two K connectors and a 0.3 inch 50 Ω transmission line on ferrite substrate. Figure 4.13 shows the performance of this revised setup. The major overall insertion loss is about 1.5 dB and consists of the two connectors' loss and ferrite substrate transmission loss; it will be used to calibrate circulator performance.

Identify: 30-40GHZ Test Device: FERRITE TST Date: 10-12-89
 2: RETN LOSS (B) 5.0 dB/DIV OFFSET +0.0 dB



CURSOR

1: -1.01 dB

Figure 4.13 Performance of K Connector Test Setup with Two K Connector Launchers and 0.3" Ferrite Substrate 50 Ohm Transmission Line

5.0 Millimeterwave Microstrip Circulator Experimental Results

To demonstrate the performance of the designed microstrip circulator, several drop-in circulators were designed, fabricated and evaluated. In this chapter, the mask design generation, test fixture design, test set and performance optimization are described.

5.1 Mask Design Generation and Drop In Circulator Fabrication

Using the actual ferrite substrate test data (i.e. dielectric constants, loss tangent, magnetic field saturation) and a computer simulation program, several circulator configurations and transmission lines were analyzed, laid out and plotted by CAD program (Figures 5.1, 5.2).

The resonator disc size, microstrip linewidth, and impedance transformer section varied slightly to allow for performance parameters adjustments. A 50-Ohm straight line is included to serve as a reference line for the circulator. The dimension of the reduced photomask has been checked with a tolerance of $\pm 3 \mu\text{m}$, which surpasses the fabrication accuracy requirement.

After the mask was designed and generated, a drop in circulator unit (Figure 5.3) was carefully fabricated with tight tolerances, the circulator drop in unit has overall size of 0.3" x 0.3" x 0.16" with a small circular bay, 1.25" in diameter,

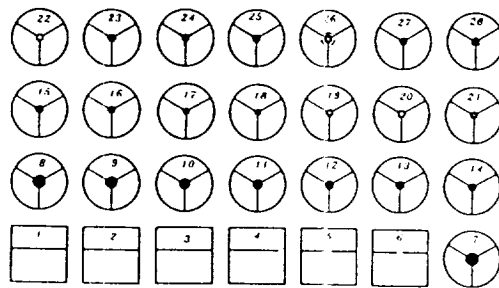
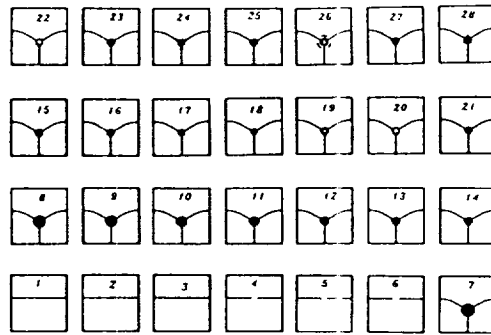


Figure 5.1 Mask Layout of MMW Circulator

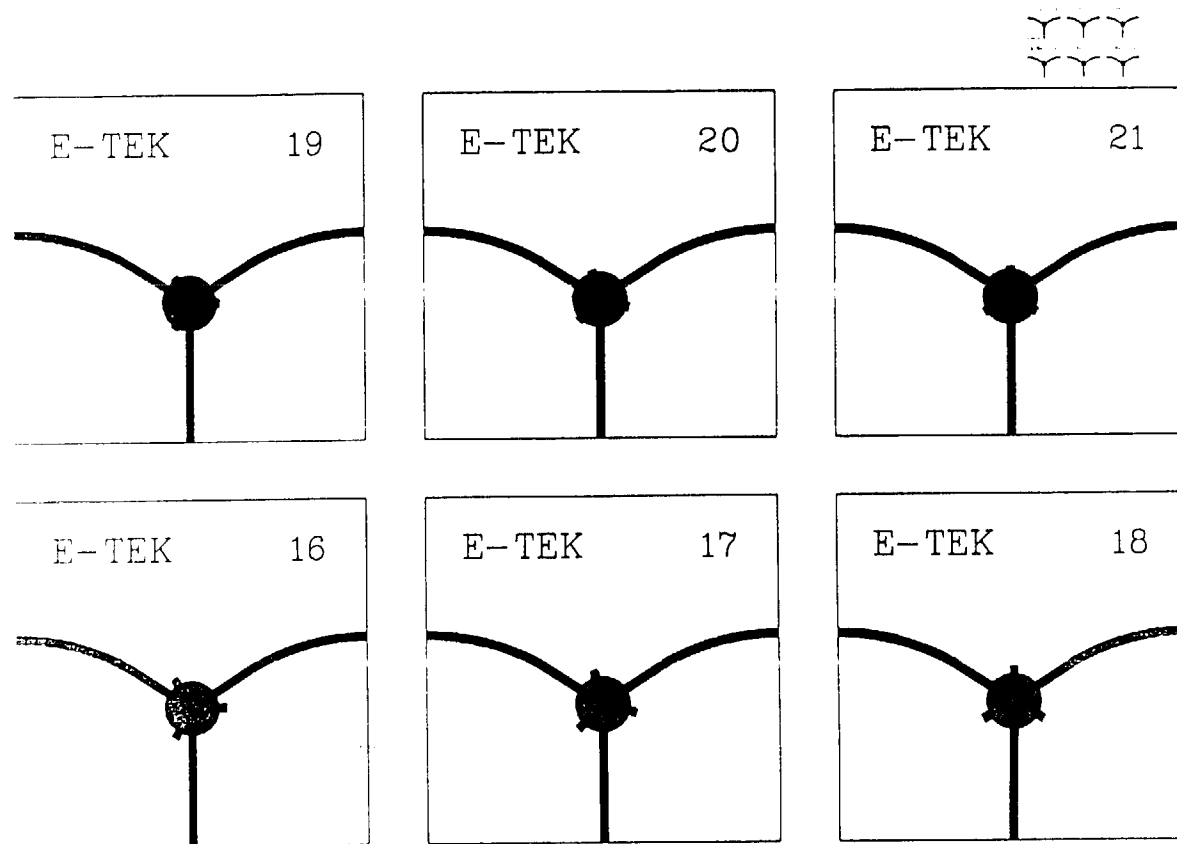


Figure 5.2 Mask Layout of MMW Circulator with Stubtuned configurations

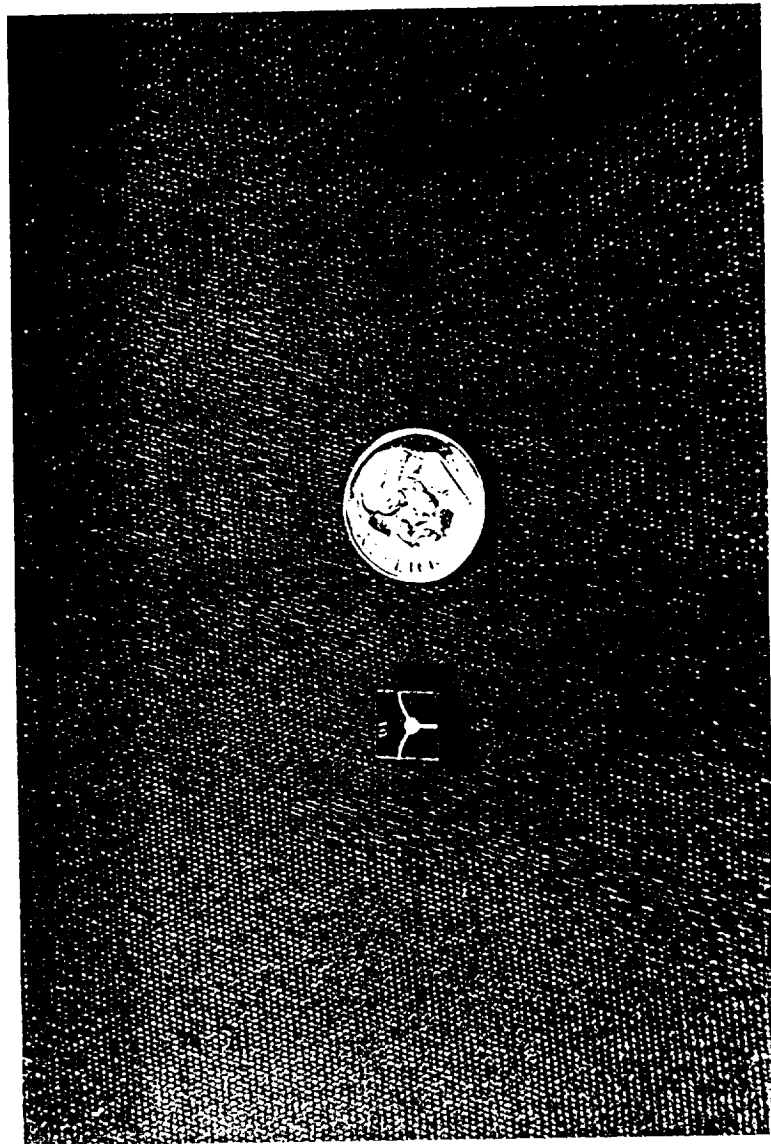


Figure 5.3 36-40 GHz Drop-In Circulator Unit

ORIGINAL PAGE IS
OF POOR QUALITY

underneath the resonator test drive for permanent magnet installation.

5.2 Drop-In Circulator Test Fixture Design and Fabrication

The test fixture will significantly affect the performance of the circulator. The easy access package will simplify adjustment and tuning during circulator-package integration. The design features and fabrication of the test fixture are described below:

- Connectors: Modified Wiltron K-connectors/launchers have been selected for this project. The data sheet for the K-connector/launcher indicates that it can respond up to 46 GHz; however, repeatability and maintainability are still critical issues.
- The connecting section between the microstrip line and K-connector: The microstrip linewidth is about 7.5 mils, and the diameter of the K-connector pin is 12 mils. Alignment for excellent connections between the three connectors and the three microstrip lines, simultaneously, is very difficult. Any misalignment, interruption or discontinuity between the coaxial launcher and the microstrip will cause malfunction in the circulator, with extremely high insertion loss, poor VSWR and isolation as a result. To ensure alignment accuracy for all three connectors vs transmission lines, all machine work and

photolithograph patterns the critical dimensions have to be within a tolerance ± 1 mil, and the alignment work must be performed under a microscope to perfectly align all the critical connections. The gap between connector pin and microstrip line should be less than 1 mil, with no bending or compression forces against each other. Pure silver Epoxy (84-1LMI-T from Ablestick) is then applied and allowed to cure at 125°C for 2 hours to achieve optimum connections.

- RF Grounding: Good RF grounding is extremely important in the circulator package design in order to avoid parasitic effects. Package housing fabrication tolerances, surface flatness, surface finish, conductivity of the adhesive materials, substrate attachment techniques, and substrate/housing cleaning processes all affect RF grounding quality. By considering the above factors, a carefully designed mechanical contact approach was selected and evaluated. A complete circulator test fixture and package was designed, fabricated, Au plated, and evaluated. A sketch of the package components is depicted in Figure 5.4. The totally assembled circulator is illustrated in the Figure 5.5 drop-in unit with test fixture.

5.3 Circulator Performance Evaluation and Test Results

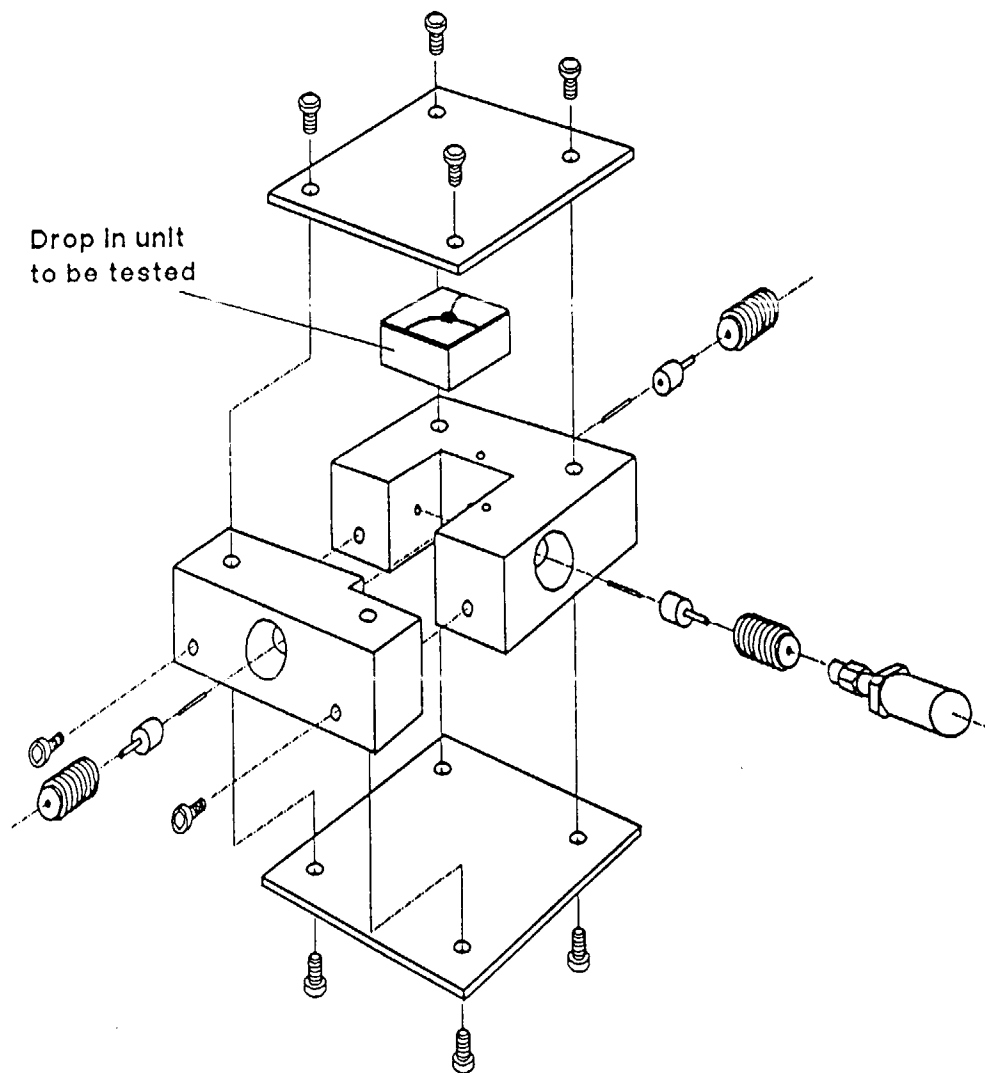


Figure 5.4 Drop-In Circulator/Isolator Test Fixture

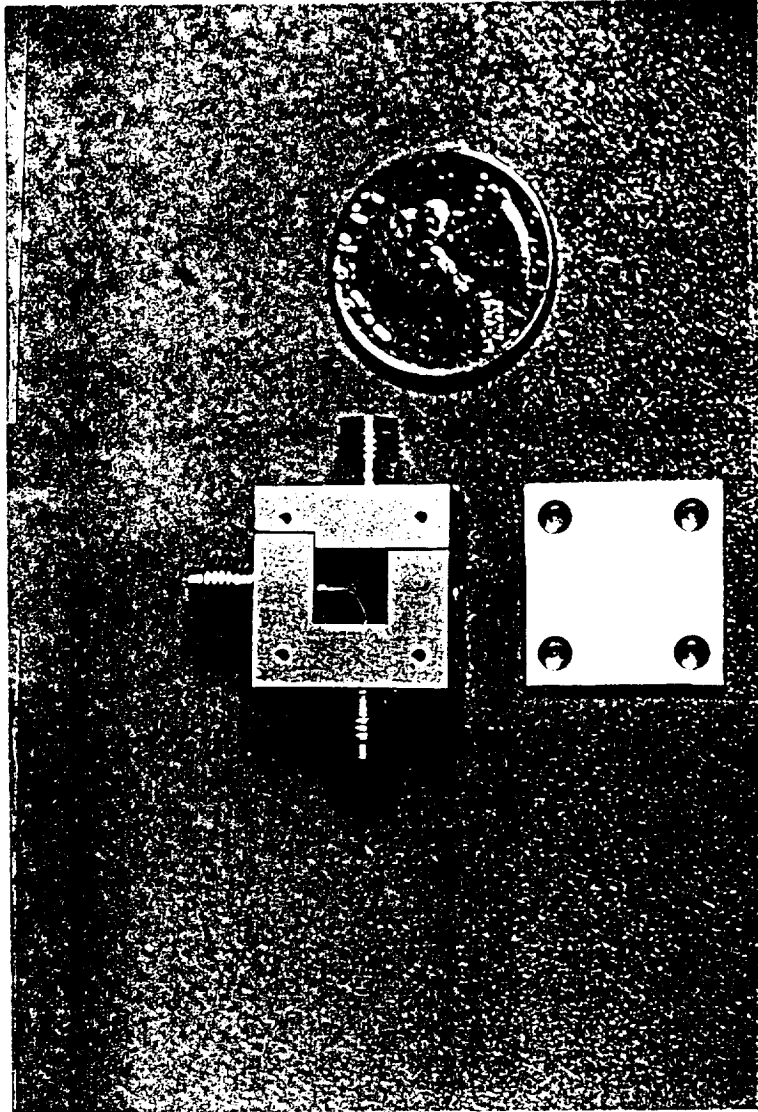


Figure 5.5 Assembled Circulator Drop-In Unit with Test Fixture

ORIGINAL PAGE IS
OF POOR QUALITY

5.3.1 Performance Test Setup

Insertion loss, isolation and return loss of the millimeter-wave microstrip circulator were measured from 36 to 40 GHz, using the setup depicted in Figure 5.6 and Figure 5.7. A Wiltron scalar network analyzer (Model 561), and HP sweep oscillator (HP 8350B), with 26.5-40 GHz RF plug in, were used to record the measurements. The waveguide directional coupler with power feedback, waveguide to coaxial adapter and 50-Ohm terminator were also included in the measurement system with a calibrated operation range from 30 to 40 GHz.

5.3.2 Experimental Results of 36 - 40 GHz Circulator

The circulator devices were tested with different configurations of magnetic bias to achieve optimum results. During insertion loss and isolation measurement, one port was terminated by a 50 Ohm terminator. For VSWR (return loss) measurement, two ports were terminated by 50 Ohm terminators. With 1/8" diameter x 1/8" thick Samarium cobalt ($\text{Sm}_2\text{CO}_{17}$), the overall measurement results were considered to be most stable and acceptable. The optimized test measurements of insertion loss, isolation, and return loss are shown in Figures 5.8 through 5.10 for each of the circulator ports respectively. To improve performance, a set of tuning chips made by ferrite and absorbing rubber were used and added onto the resonator. Figures 5.11 through 5.16 show the improved results. Comparison of

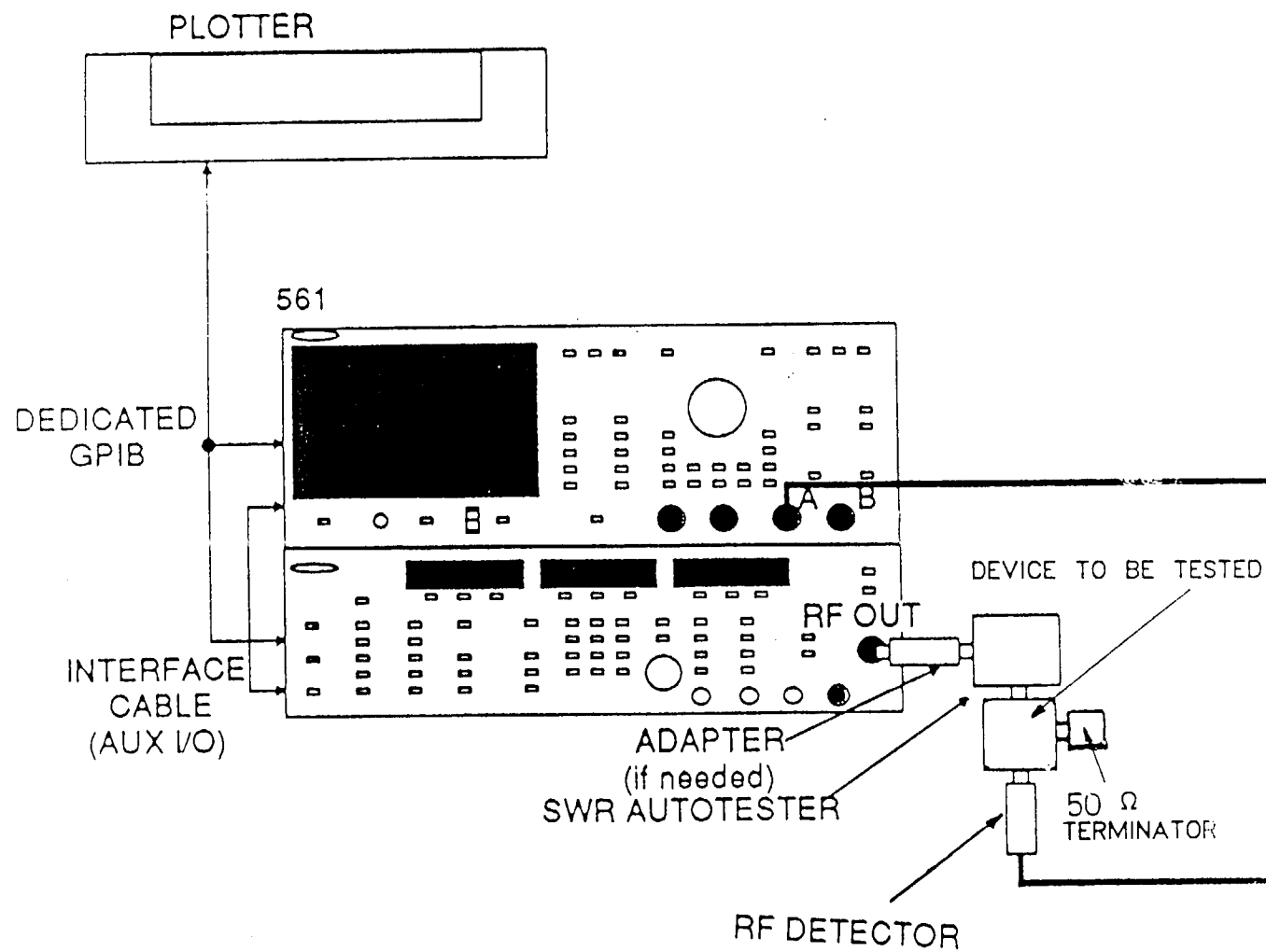


Figure 5.6 Circulator Insertion Loss/Isolation Testing Setup

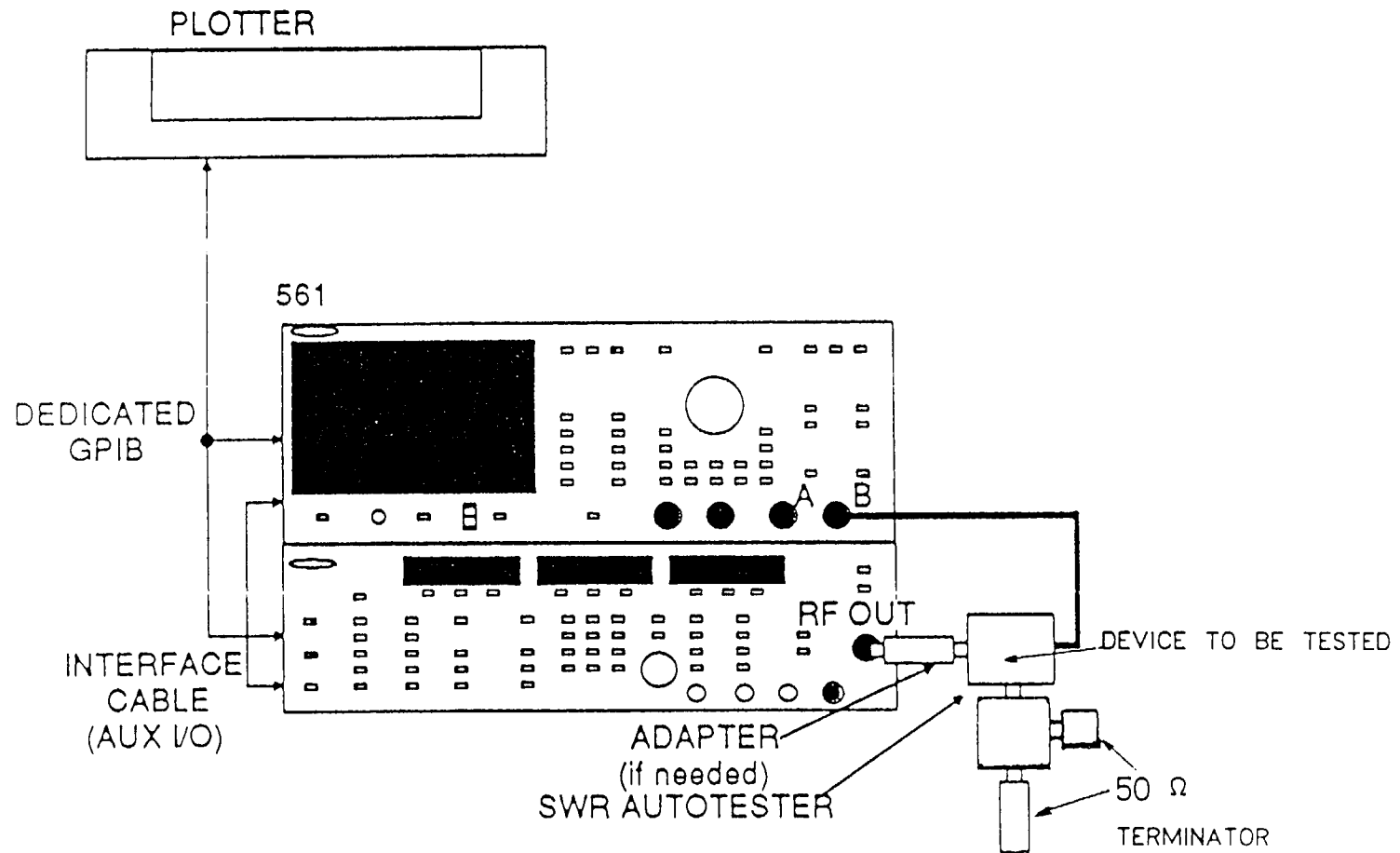


Figure 5.7 Circulator Return Loss Test Setup

Identify: 30-40GHZ Test Device: Date: 10-25-89
 1: TRANSMSSN (A) 1.0 dB/DIV OFFSET +0.0 dB
 2: RETN LOSS (B) 5.0 dB/DIV OFFSET +0.0 dB

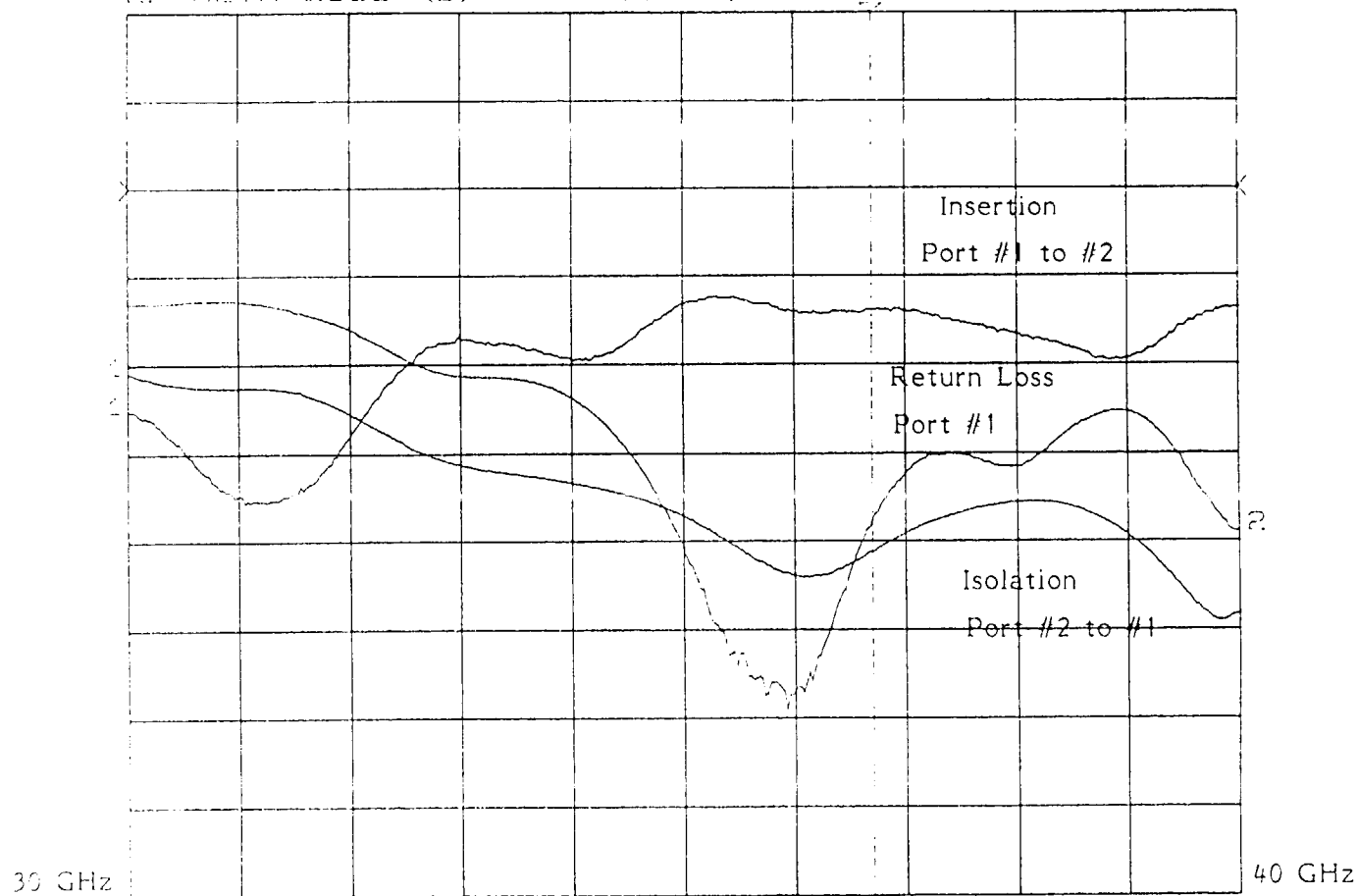


Figure 5.8 Performance Parameters of Microstrip Circulator at Port # 1 (W/O Tuning)

Identify: 30-40GHZ Test Device: Date: 10-25-89
 1: TRANSMSSN (A) 1.0 dB/DIV OFFSET +0.0 dB
 2: RETN LOSS (B) 5.0 dB/DIV OFFSET +0.0 dB

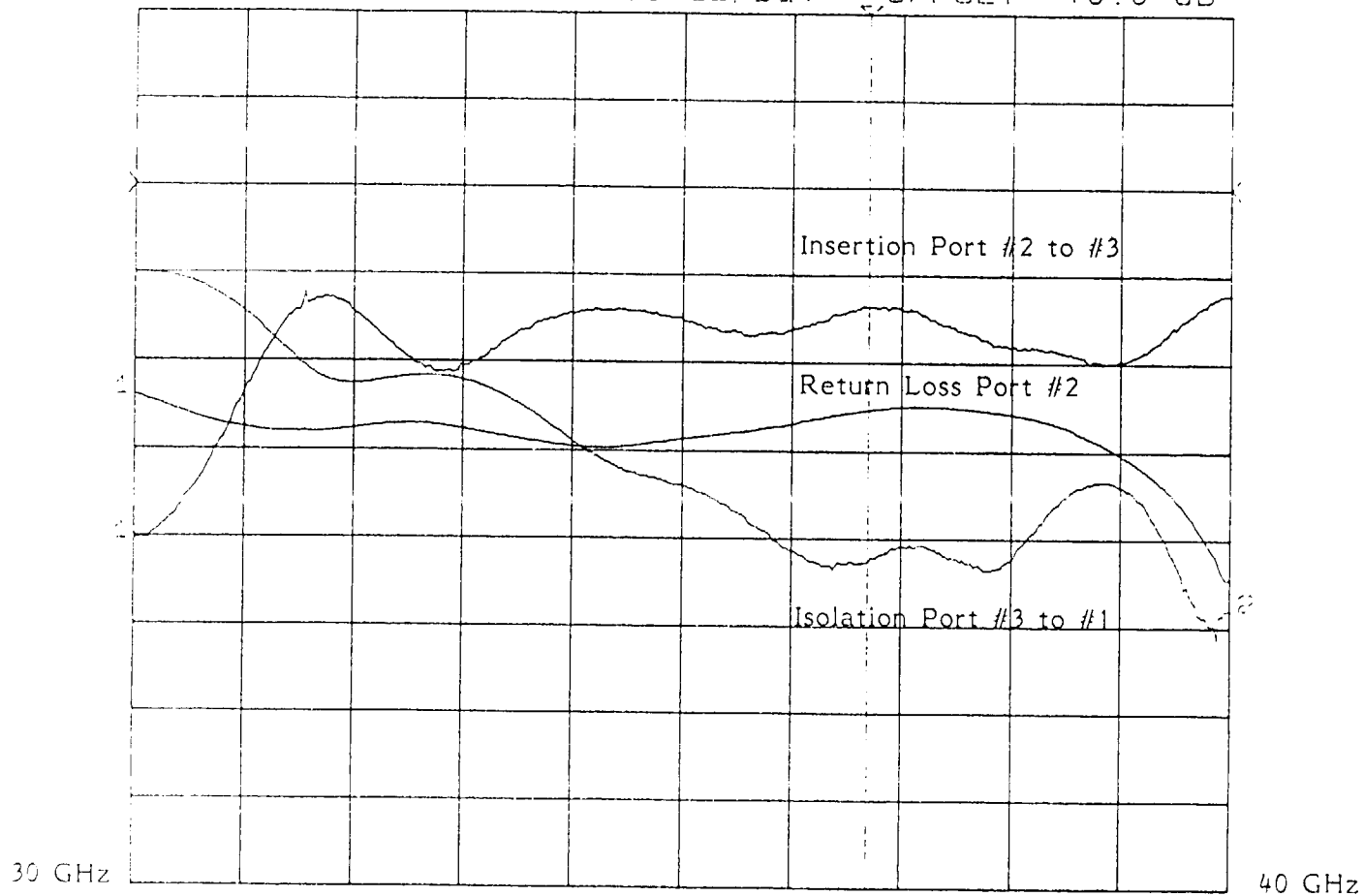


Figure 5.9 Performance parameters of Microstrip Circulator at Port # 2
 (W/O Tuning)

Identify: 30-40GHZ Test Device: Date: 10-25-89
 1: TRANSMSSN (A) 1.0 dB/DIV OFFSET +0.0 dB
 2: RETN LOSS (B) 5.0 dB/DIV OFFSET +0.0 dB

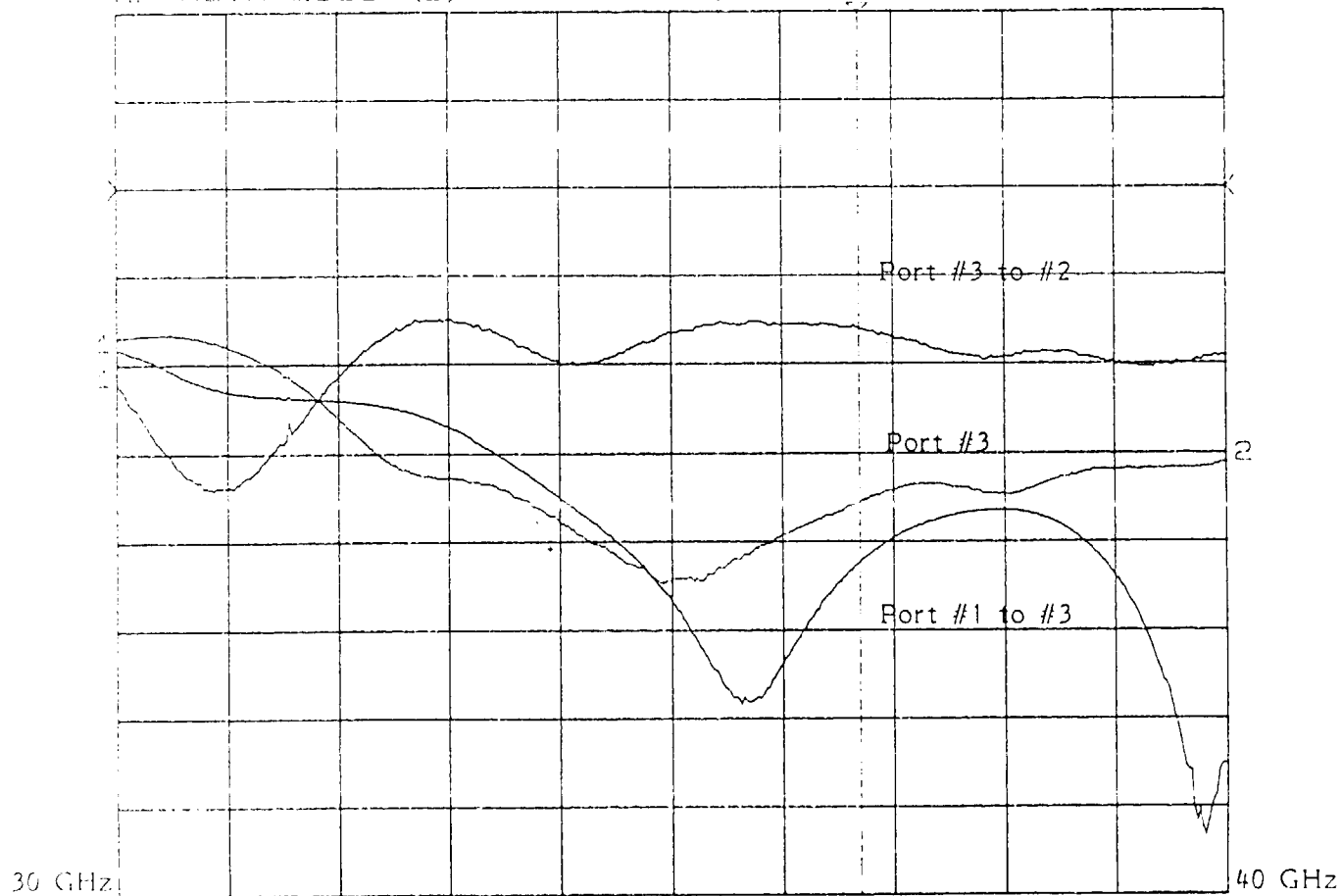


Figure 5.10 Performance Parameters of Microstrip Circulator at Port # 3
 (W/O Tuning)

1: TRANSMSSN (A) 5.0 dB/DIV OFFSET +0.0 dB
 2: RETN LOSS (B) 5.0 dB/DIV OFFSET +0.0 dB

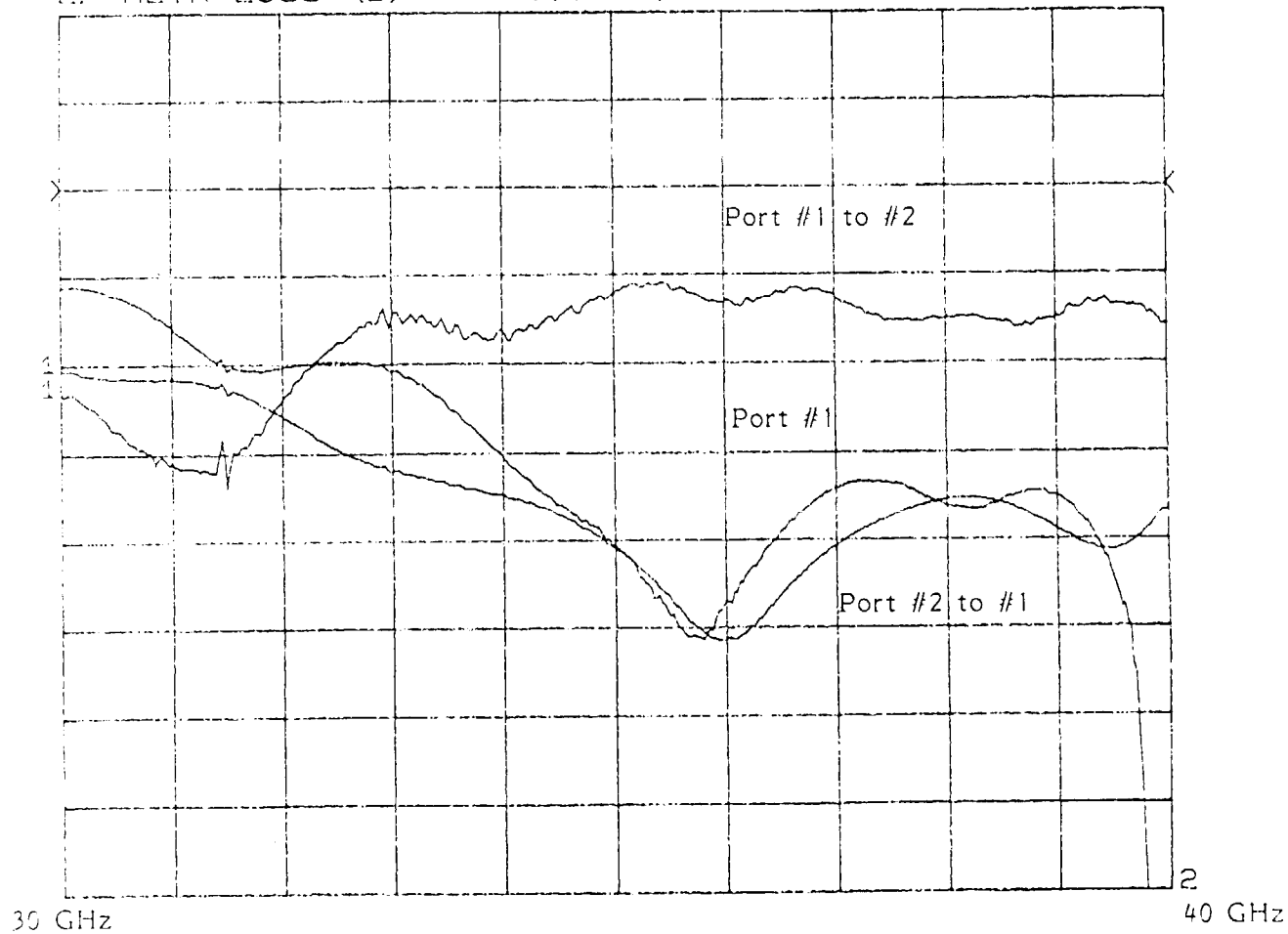


Figure 5.11 Performance Parameters of Microstrip Circulators at Port # 1
 (Tuning Using Metal Chips)

ORIGINAL PAGE IS
 OF POOR QUALITY

85
 C-2

1: TRANSMSSN (A) 5.0 dB/DIV OFFSET +0.0 dB
 2: RETN LOSS (B) 5.0 dB/DIV OFFSET +0.0 dB

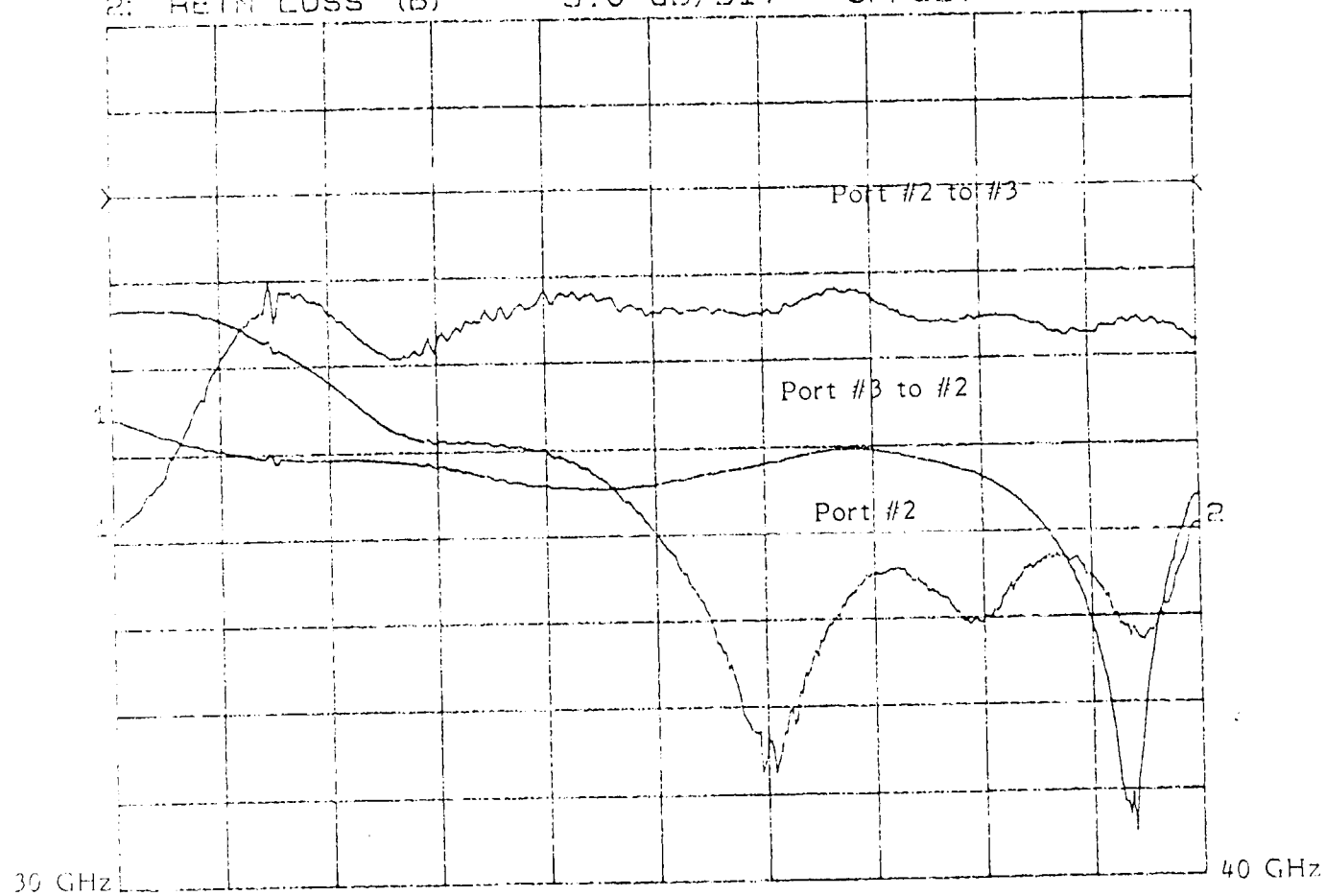


Figure 5.12 Performance Parameters of Microstrip Circulator at Port # 2
 (Tuning Using Metal Chips)

1: TRANSMSSN (A) 5.0 dB/DIV OFFSET +0.0 dB
 2: RETN LOSS (B) 5.0 dB/DIV OFFSET +0.0 dB

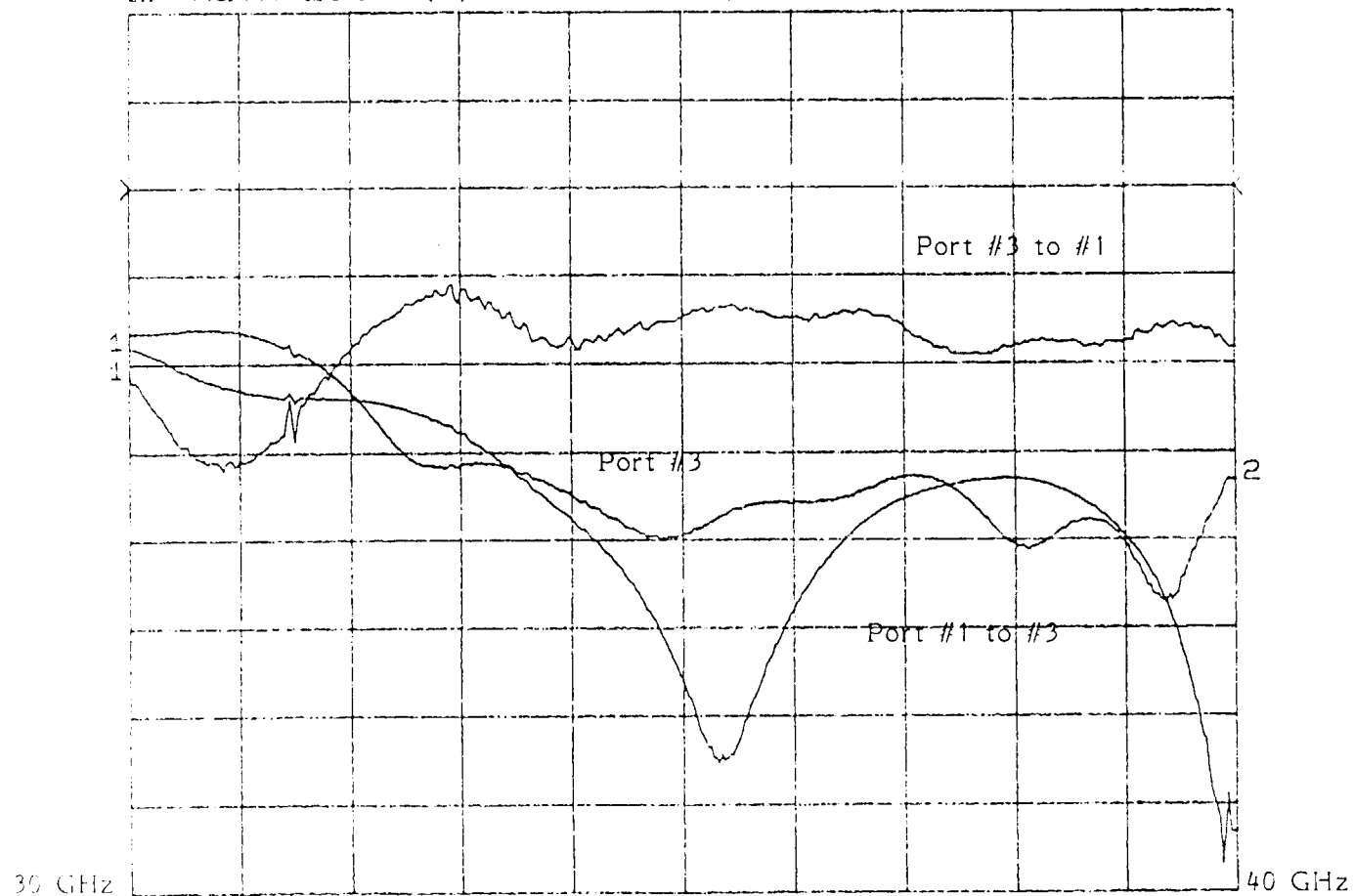


Figure 5.13 Performance parameters of Microstrip Circulator at Port # 3
 (Tuning Using Metal Chips)

Identify: 30-40GHz Test Device: CIRCULATOR Date: 01-06-90
 1: TRANSMSSN (A) 1.0 dB/DIV OFFSET +0.0 dB
 2: RETN LOSS (B) 5.0 dB/DIV OFFSET +0.0 dB

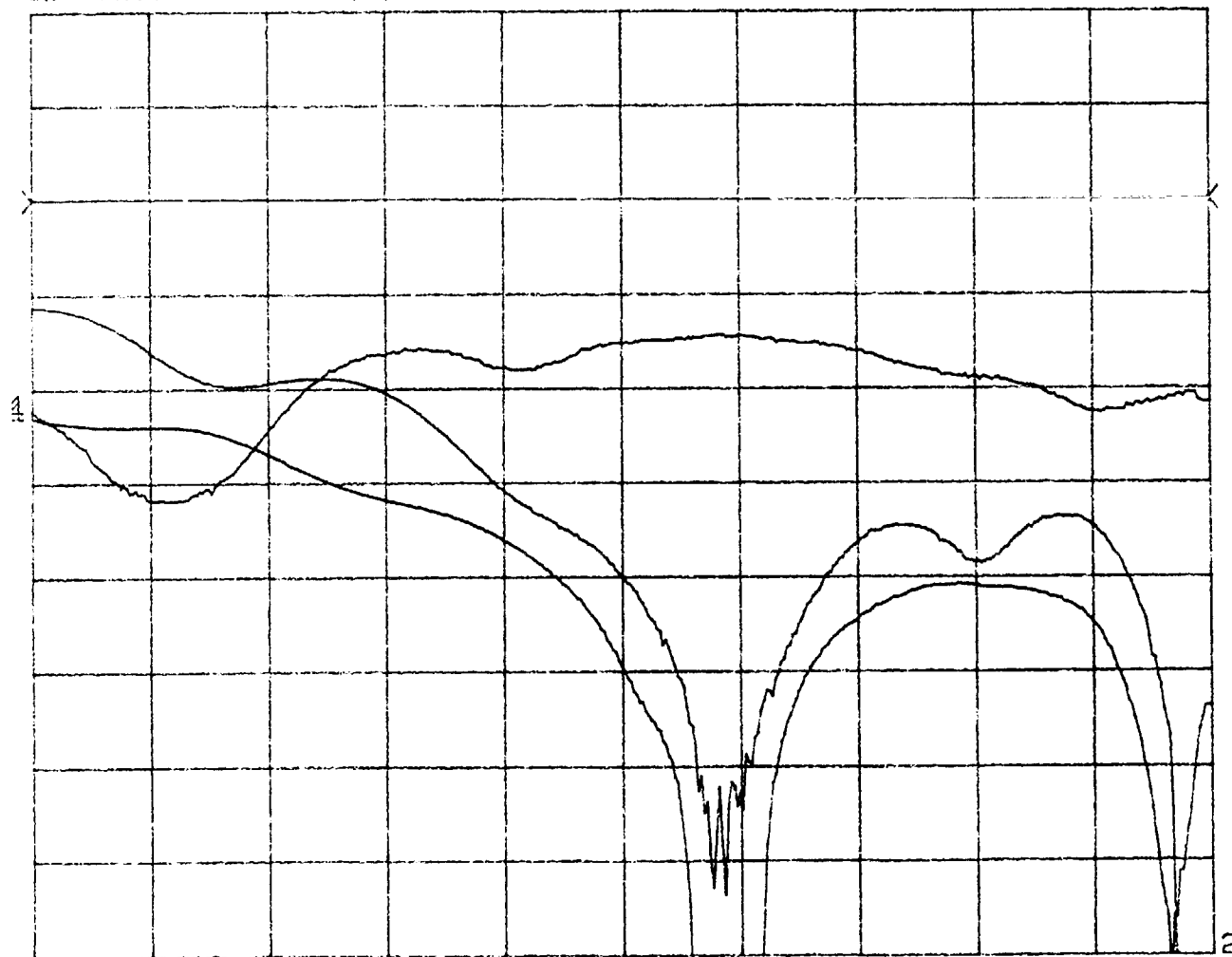


Figure 5.14 Performance Parameters of Microstrip Circulator at Port # 1
 (After Tuning by Using Absorbing Material)

Identify: 30-40GHz	Test Device: CIRCULATOR	Date: 01-06-90
1: TRANSMSSN (A)	1.0 dB/DIV	OFFSET +0.0 dB
2: RETN LOSS (B)	5.0 dB/DIV	OFFSET +0.0 dB

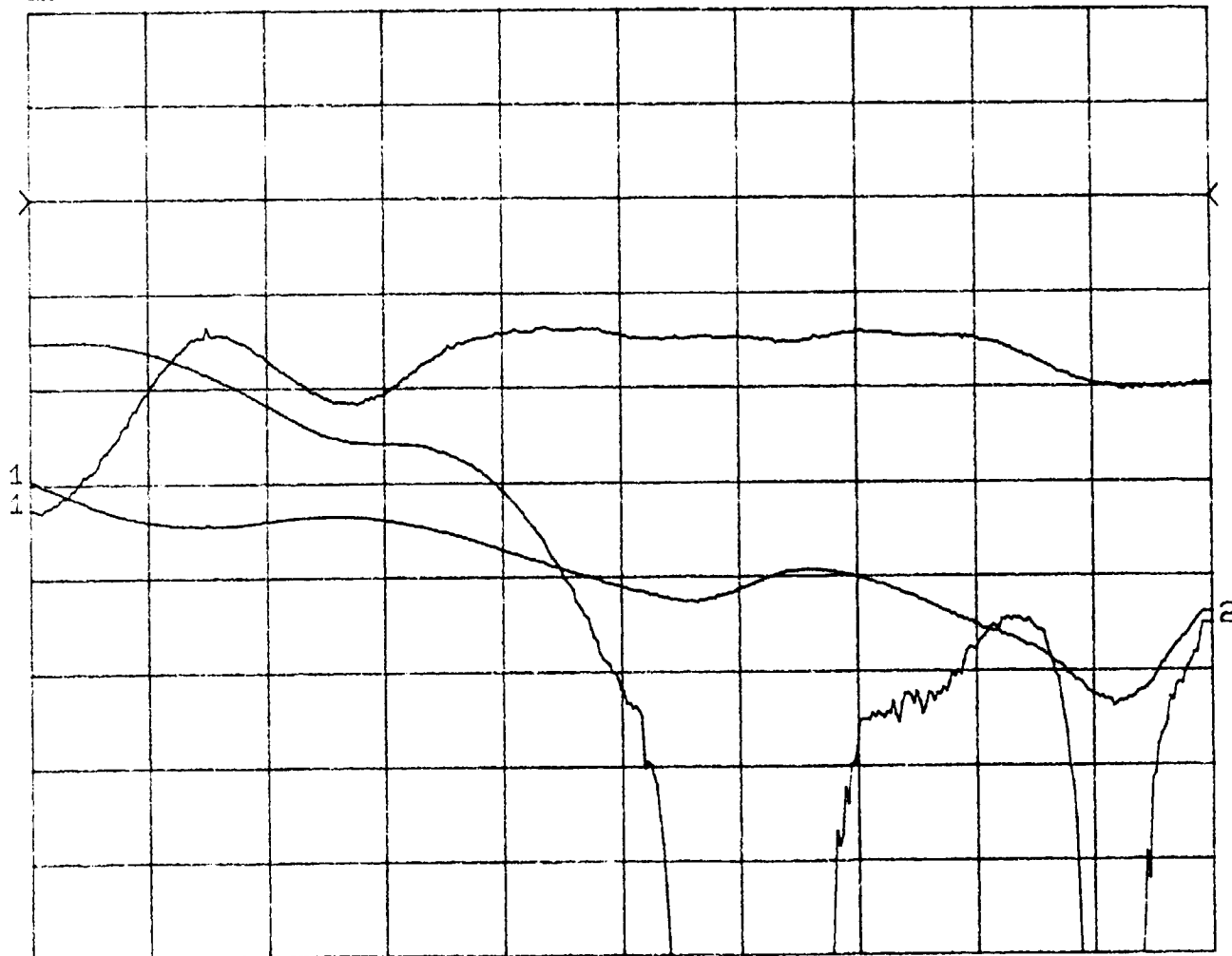


Figure 5.15 Performance Parameters of Microstrip Circulator at Port # 2
(After Tuning by Using Absorbing Material)

Identify: 30-40GHZ Test Device: CIRCULATOR Date: 01-06-90
 1: TRANSMSSN (A) 1.0 dB/DIV OFFSET +0.0 dB
 2: RETN LOSS (B) 5.0 dB/DIV OFFSET +0.0 dB

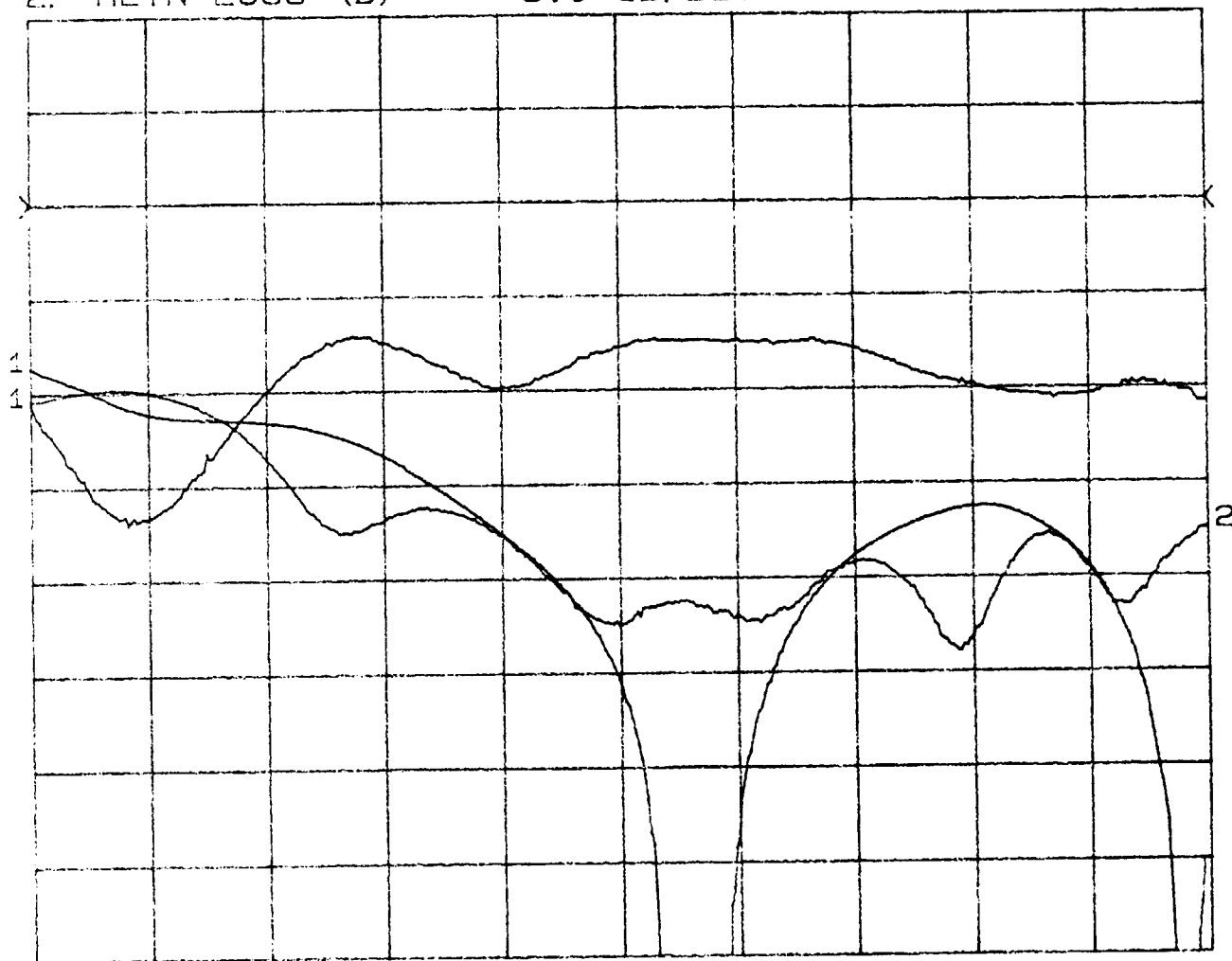


Figure 5.16 Performance Parameters of Microstrip Circulator at Port # 3
 (After Tuning by Using Absorbing Material)

circulator performance test data, before and after tuning, are listed in Table 5.1. Because the value of insertion loss was determined in conjunction with a comparison of the 0.3" 50 Ohm transmission and the test fixture, the insertion loss, by tuning the circulator, can be better than 0.8 dB. Achievable values for isolation loss and return loss can be better than 17dB, and operation bandwidth can be as wide as GHz.

5.3.3 Experimental Results of 31 - 37 GHz Circulator

To demonstrate the performance of a broadband microstrip circulator, a 31-37 GHz stub-tuned circulator was designed, fabricated and evaluated for deep space applications. This task was not required in the project R&D; however, E-Tek's engineers expressed their interest in expanding the applications that could result from this project. Figure 5.17 through Figure 5.19 show performance of the 31-37 GHz microstrip circulator. The values of the insertion loss were 0.8 or less (minus connector loss). The values for isolation loss were better than 15 dB, and the values for the return loss were better than 14 dB for all three ports, without any tuning required.

Table 5.1
Summarized the Results of Circulator 36 - 40 GHz Performance

	Insertion Loss* (dB)	Isolation (dB)	Return Loss (dB)
Port 1	< 0.9	> 17	> 12
Port 2	< 0.9	> 17	> 12
Port 3	< 0.9	> 18	> 16
Tuning w/Metal Chips			
#1	< 0.6	> 17	> 17
#2	< 0.7	> 15	> 19
#3	< 0.8	> 16	> 17
Tuning w/Absorbing Rubber			
#1	< 0.8	> 17	> 20
#2	< 0.7	> 22	> 19
#3	< 0.8	> 17	> 17

Identify: 30-40GHZ

Test Device: FERRITE TST

Date: 10-12-89

1: TRANSMSSN (A)

1.0 dB/DIV

OFFSET

+0.0 dB

2: RETN LOSS (B)

5.0 dB/DIV

OFFSET

+0.0 dB

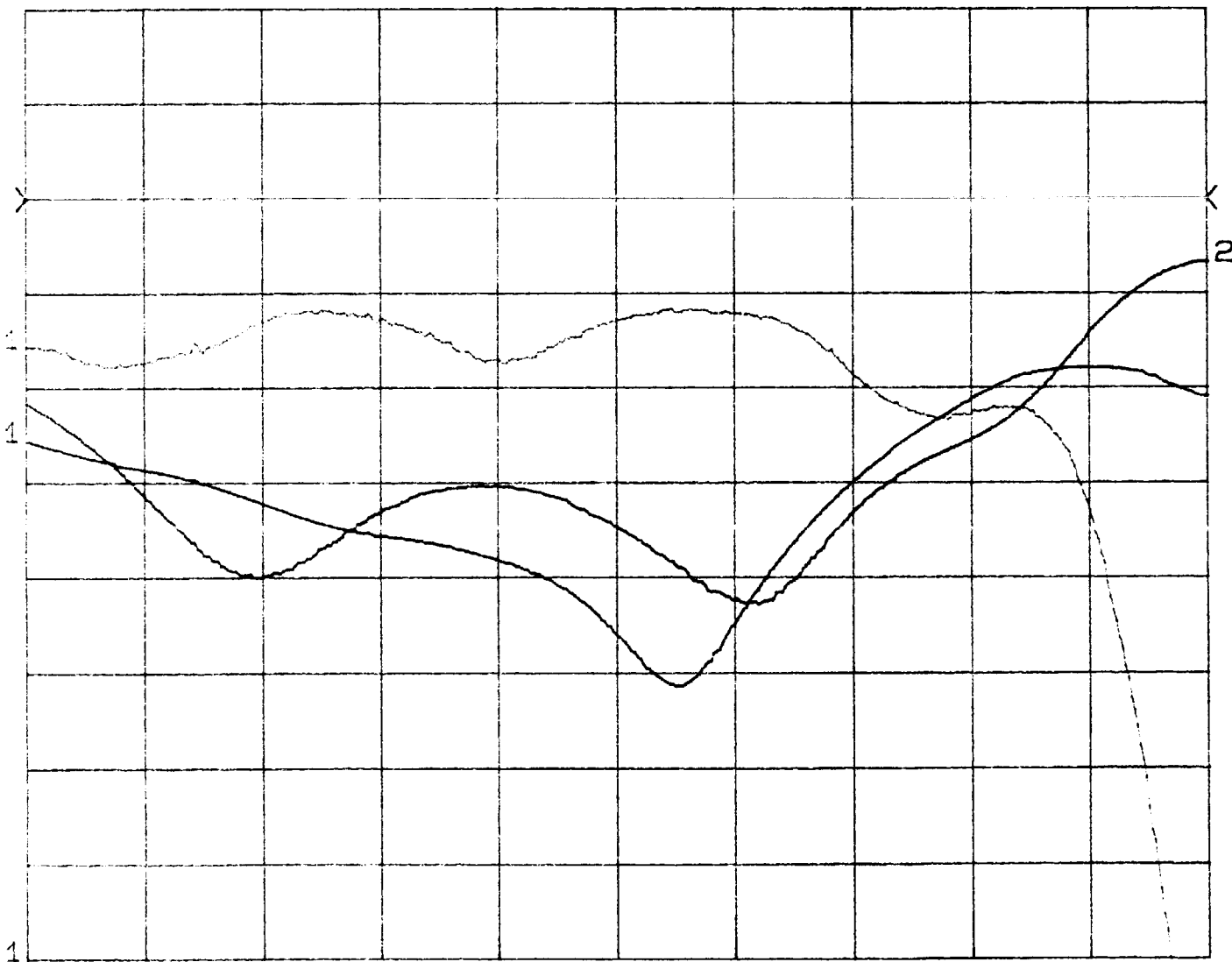


Figure 5.17 Performance of 31 to 40 GHz Broadband Microstrip Circulator at Port #1

Identify: 30-40GHZ

Test Device: FERRITE TST

Date: 10-12-89

1: RETN LOSS (A)
2: RETN LOSS (B)

1.0 dB/DIV

OFFSET +0.0 dB

5.0 dB/DIV

OFFSET +0.0 dB

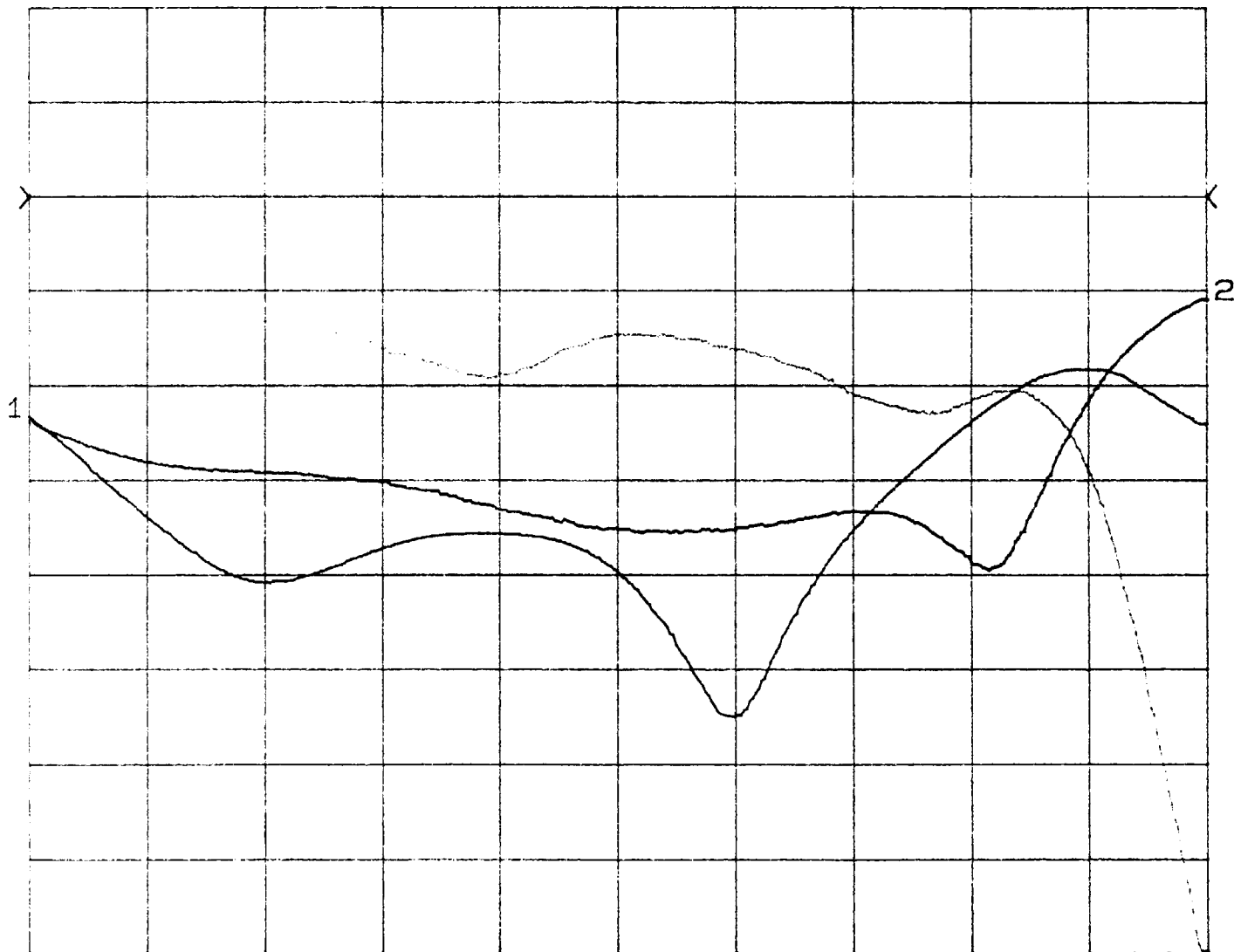


Figure 5.18 Performance of 31 to 37 GHz Broadband Microstrip Circulator at Port #2

Identify: 30-40GHZ Test Device: FERRITE TST Date: 10-12-89
 1: TRANSMISS (A) 2.0 dB/DIV OFFSET +0.0 dB
 2: RETN LOSS (B) 5.0 dB/DIV OFFSET +0.0 dB

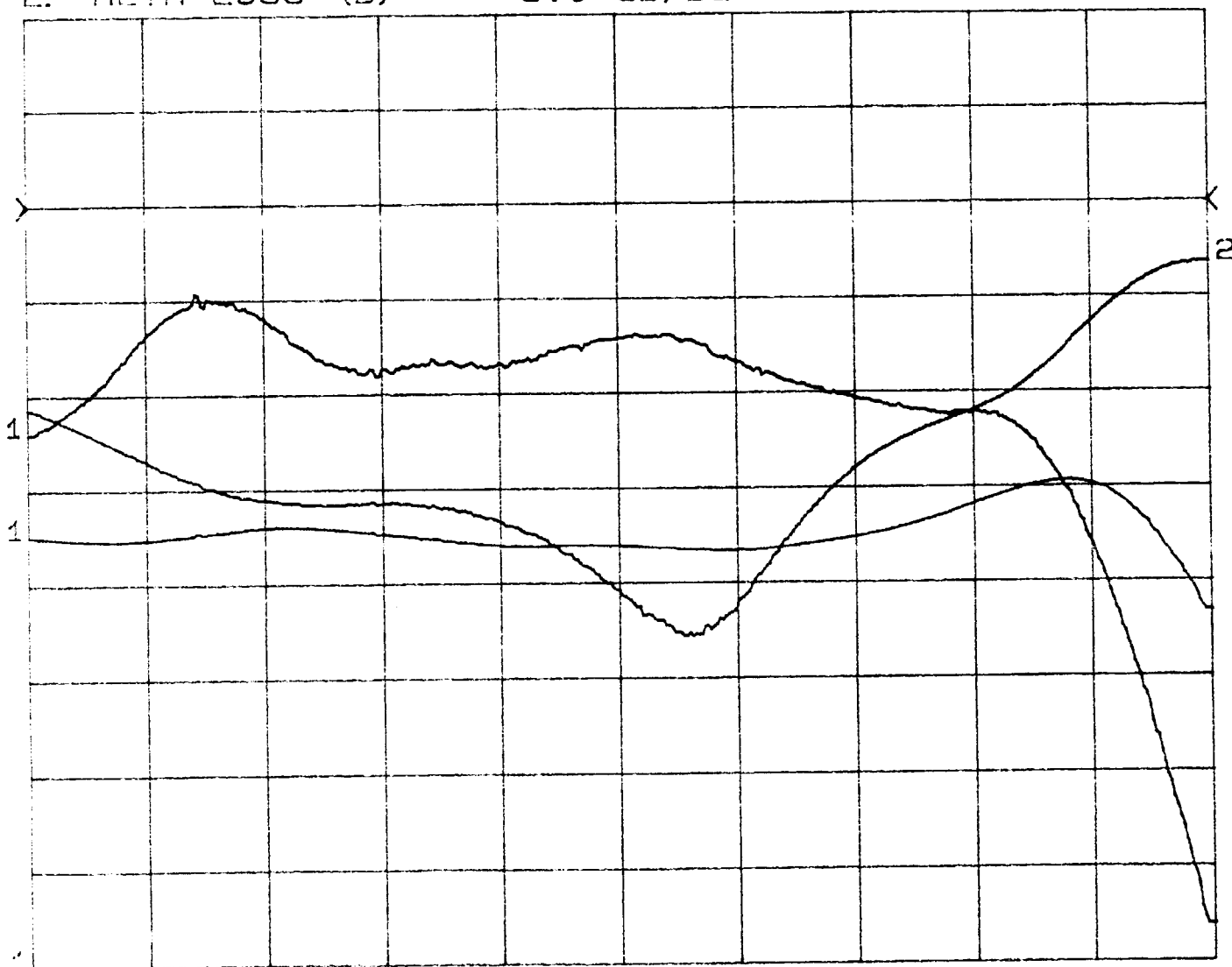


Figure 5.19 Performance of 31 to 37 GHz Broadband Microstrip Circulator at Port 3

6.0 Design, Fabrication and Evaluation of Ruggedized Circulator Package

The purpose in designing a ruggedized millimeter wave circulator package is to ensure the good and reliable performance against changing environmental conditions such as temperature variation, vibration, etc.. Since there is a close relationship between mechanical tolerance limitation and maximum electrical performance, it is a challenging task to design a ruggedized package which can simultaneously optimize all mechanical and electrical requirements.

6.1 Design of Ruggedized Circulator Package

The design of millimeter circulator package requires input from several different points of view, including material, mechanical, electrical and processing. In order to meet project needs, design of an adequate millimeter circulator package should satisfy the requirements listed below:

- Good electrical performance of RF transitions
- good transitions between internal assemblies with high dimensional precision and ground plane continuity.
- Wide operational temperature range, no thermal stress or strain should occur to the substrate or transition locales during thermal shock/cycling.
- Adequate dimension for cover and no response in the

operating frequency range.

- High reliability, unit can survive vibration, shock, and environmental moisture
- Coaxial connector launchers for input and output ports
- Integration simplicity, no special equipment required.
- Low cost

Of all above requirements, grounding continuity is of the most vital importance to sustained high frequency performance. If proper ground is not maintained, performance will be affected in various ways, such as increased insertion loss at discrete frequencies, isolator jump and poor VSWR. Bearing these factors in mind, E-Tek designed a ruggedized circulator package (Figure 6.1) which has an overall size 0.75" x 0.75" x 0.40" (less coaxial connector).

6.2 Fabrication of Circulator Package

Fabrication procedure for the high frequency circulator package must satisfy both electrical and mechanical requirements. Electrically, the gaps between circulator and package should be minimized and held to the closest possible tolerances. Mechanically, the considerations are more closely involved with machine limitations, and thermal/dynamic impacts to the package during fabrication. By optimizing both requirements, E-Tek's engineers and machinists have fabricated a circulator package with the following tolerances:

Ruggedized Circulator Package Design

Size : .75" X .75" X .40" (without connector)

Material : Brass

Finish : 30u inch polish, Au plated

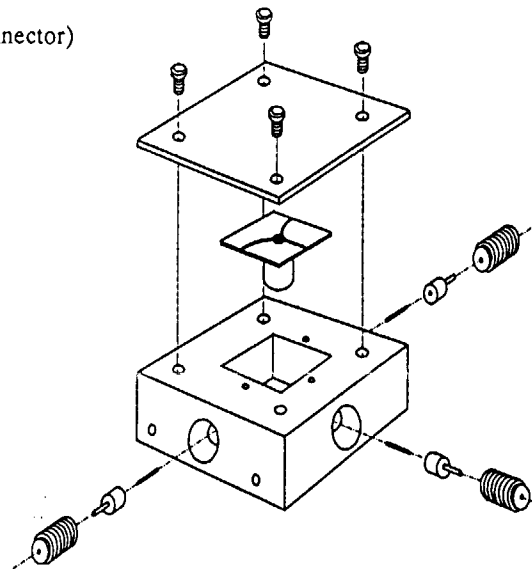


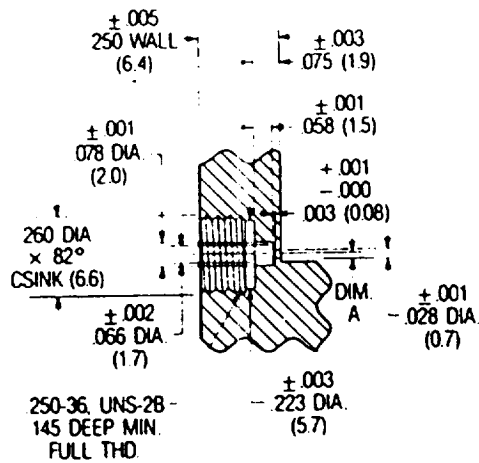
Figure 6.1 Ruggedized Millimeter-Wave Microstrip Circulator package

- Concentricity of Connector Housing and Glass Bead:
better than 0.0005"
- Center of Connector to Datum: < 0.001"
- Center of the Connector to Substrate Ground: < 0.001"
- Thread Taping Angle: < 0.2 degree
- All other Critical Dimensions: < 0.002"

E-Tek has achieved the above tolerances, which are more stringent than called for in the original connector design specifications (Figure 6.2 (a) and (b)). In order to guarantee optimum performance in high frequency operation, a millimeterwave microstrip circulator package was carefully fabricated according to the specified requirements. A fully assembled package with connector launchers, resonator, and magnet is depicted in Figure 6.3 (a) and (b).

6.3 Temperature Cycling Test

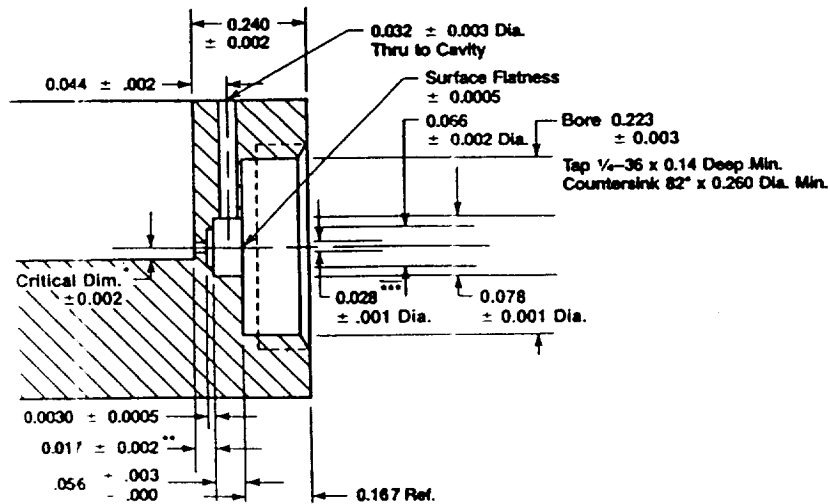
The 36 to 40 GHz ruggedized circulator should withstand a cyclic temperature change from -20°C to $+50^{\circ}\text{C}$ for three cycles without damage to its performance. In order to carry out these temperature cycling tests, a temperature chamber, together with two flexible, high frequency, high performance test cables, was used. Figure 6.4 and Figure 6.5 show the insertion/isolation and return loss measurement test setup. The proposed temperature chamber was a model "Tenny Jr"., manufactured by Tenny Industries.



NOTE: Diameters Concentric Within .002 T.I.R

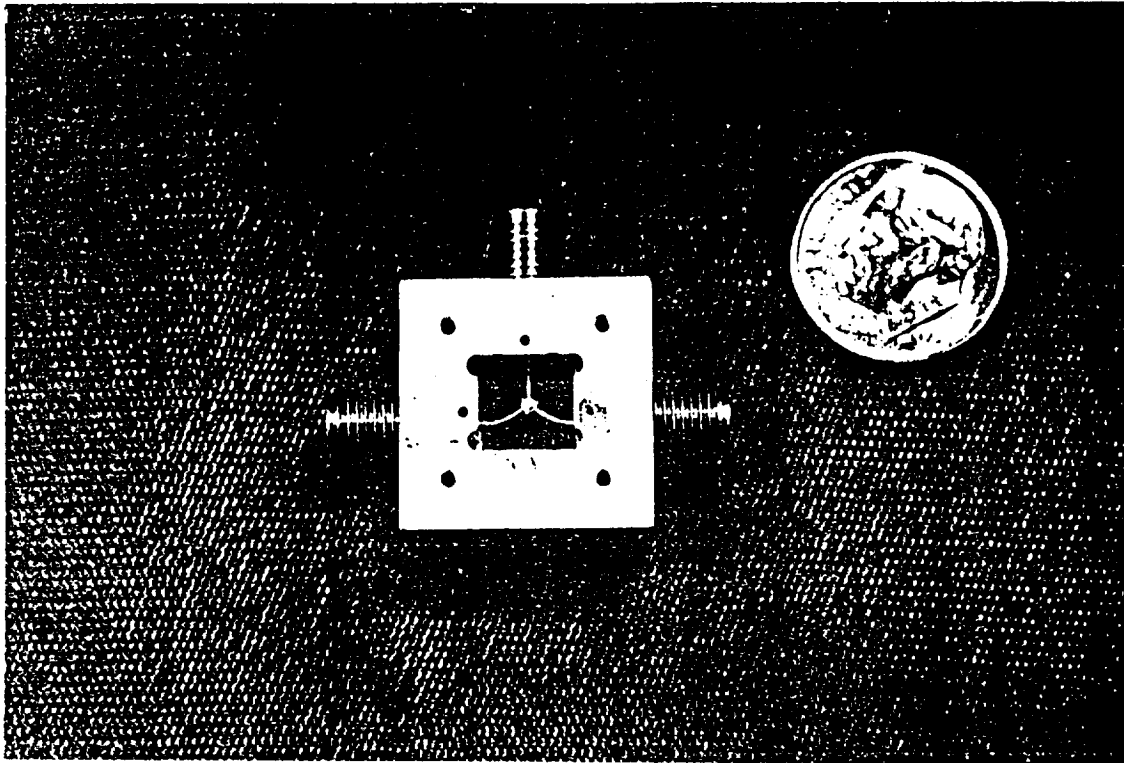
Board Thickness	Dim A $\pm .001$
.010	.019
.015	.024
.020	.029
.025	.034

(a) APC 2.4 mm Launcher Housing Dimensions
List of Figures



(b) K-Connector Launcher Housing Dimensions

Figure 6.2 Connector Launcher Housing Dimensions



(a)



(b)

Figure 6.3 Fully Assembled 36-40 GHz Circulator Package

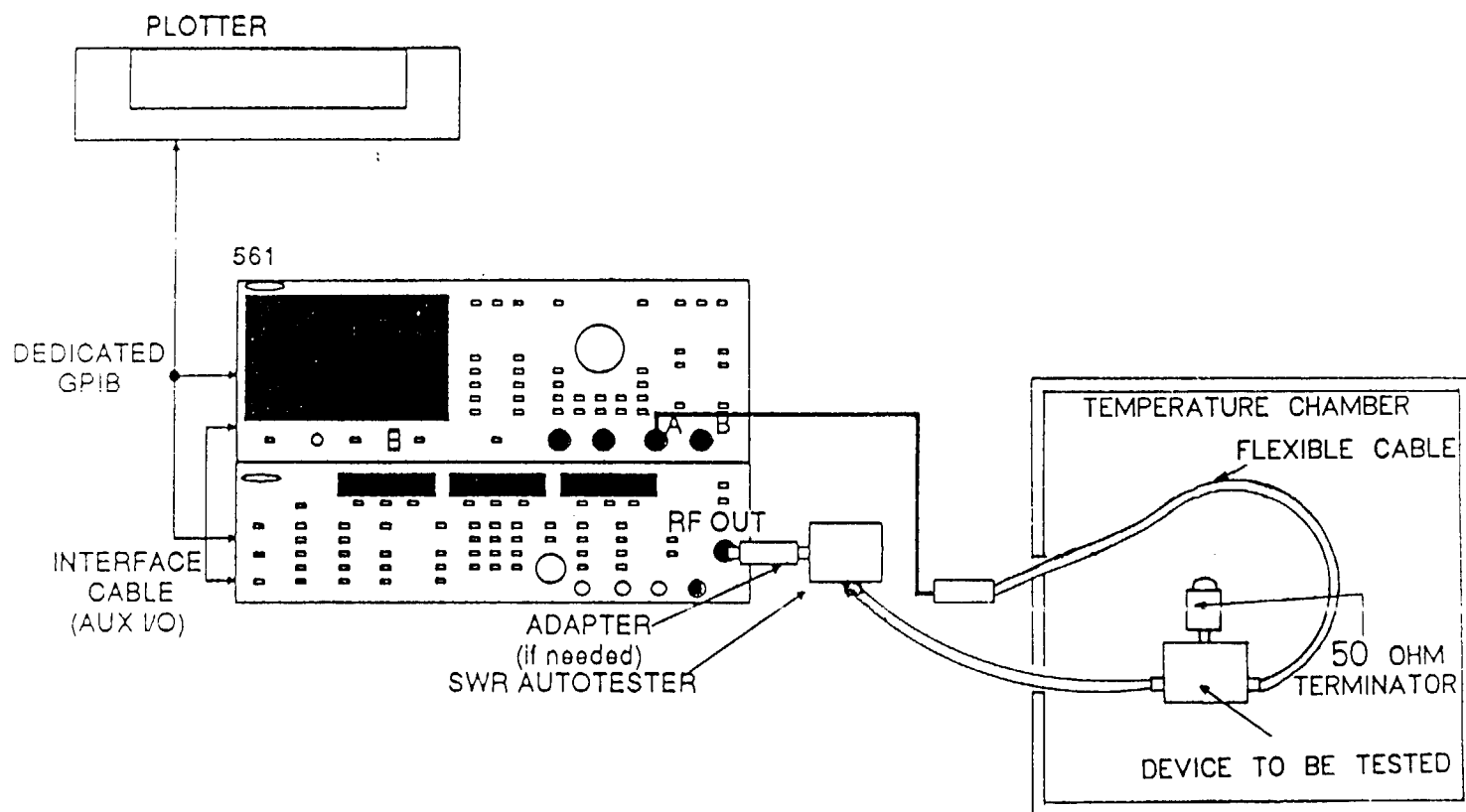


Figure 6.4 Circulator Temperature Testing Setup (Insertion Loss & Isolation Test)

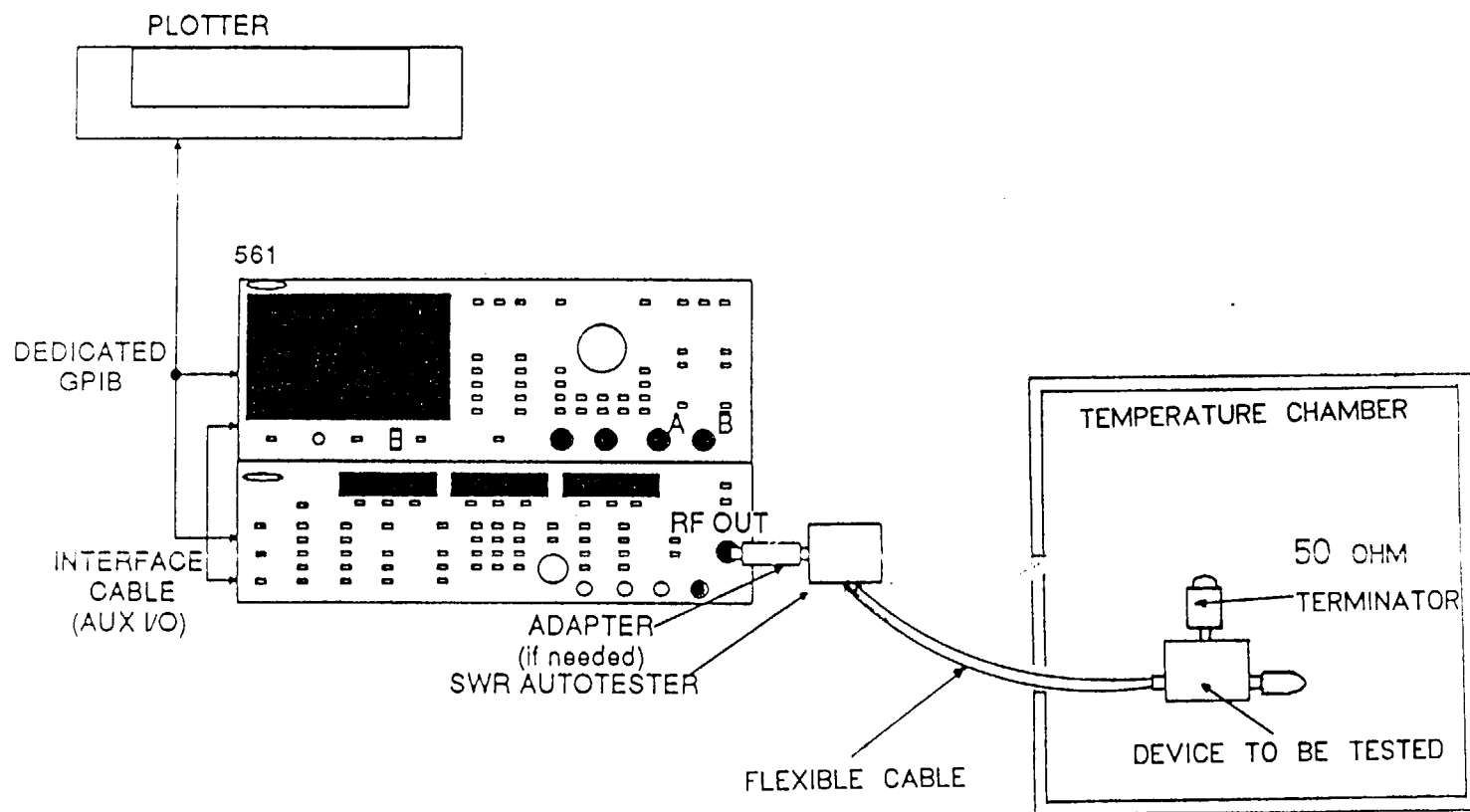


Figure 6.5 Circulator Temperature Testing Setup (Return Loss)

The chamber has precision temperature control in both its heating and refrigeration cycles. Before conducting the temperature cycling test, the thermal characteristics of the coaxial cables used in the test setup were calibrated. The deviation of coaxial cable due to temperature effect is about 0.4 dB, from -20°C to 50°C.

For circulators using the ND-FE-B magnet, a comparison of insertion loss between 30°C and 40°C is shown in Figure 6.6(a) and 6.6(b); the difference in deviation is between 2 dB and 5 dB from 36 GHz to 40 GHz. As the temperature increased, the insertion loss worsened. After one cycle, the temperature was down to 30°C. The value of insertion loss diminished, and there was no significant change in comparison to that of previous 30°C levels. This is due to the temperature effect for the magnet. As the temperature increased, the magnetic field of magnet decayed.

For circulators using the $\text{SM}_2\text{CO}_{17}$ cobalt magnets, circulator performance loss due to temperature effects can be neglected. The insertion loss of circulator at -20°C and 50°C is shown in Figure 6.7(a) and Figure 6.7(b), respectively. In comparison to the results of coaxial cable deviation, the value of intrinsic insertion loss undergoes no significant change due to temperature effect. Figure 6.8(a) and Figure 6.8(b) show the results of circulator return loss, using a $\text{SM}_2\text{CO}_{17}$ cobalt magnets, at -20°C and 50°C, respectively. There was no significant change of the return loss, even when temperature was increased to 90°C.

Identify: 30-40 GHz Test Device: CIRCULATOR Date: 07-24-89
1: TRANSMSSN (A) 1.0 dB/DIV OFFSET +0.0 dB
2: OFF

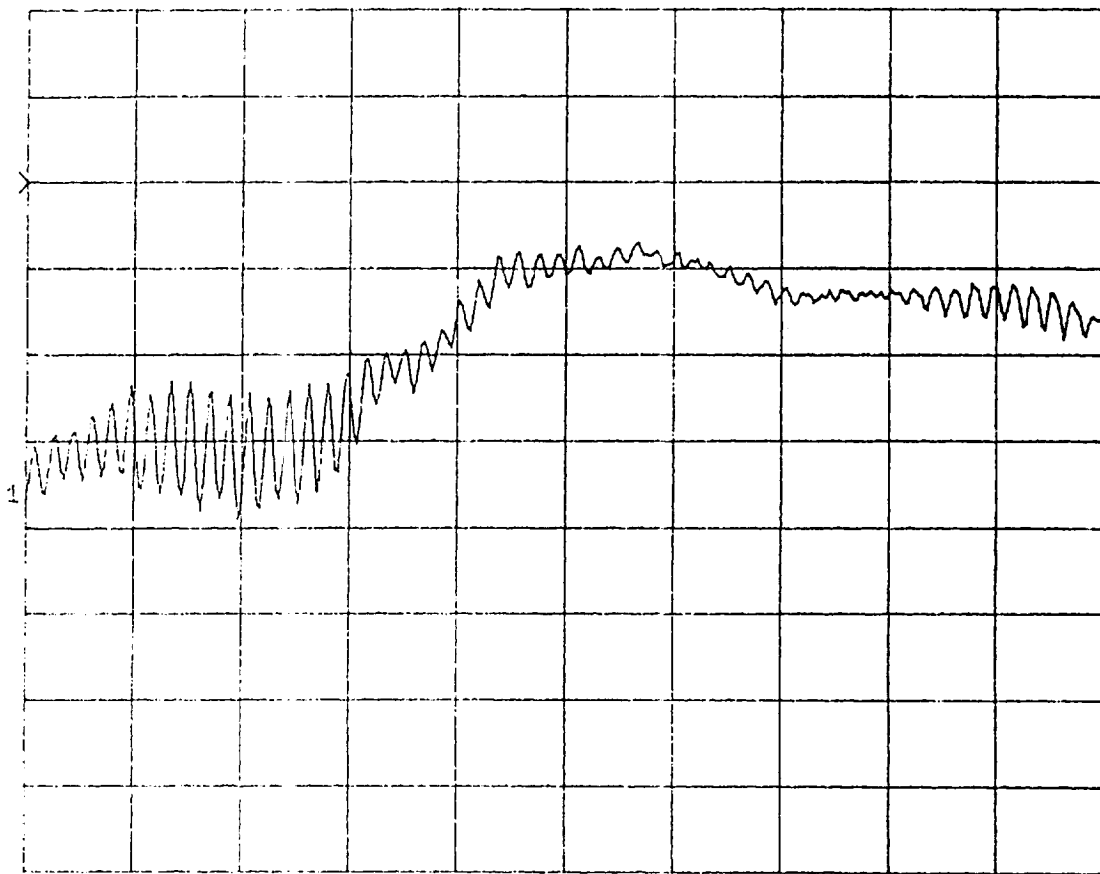
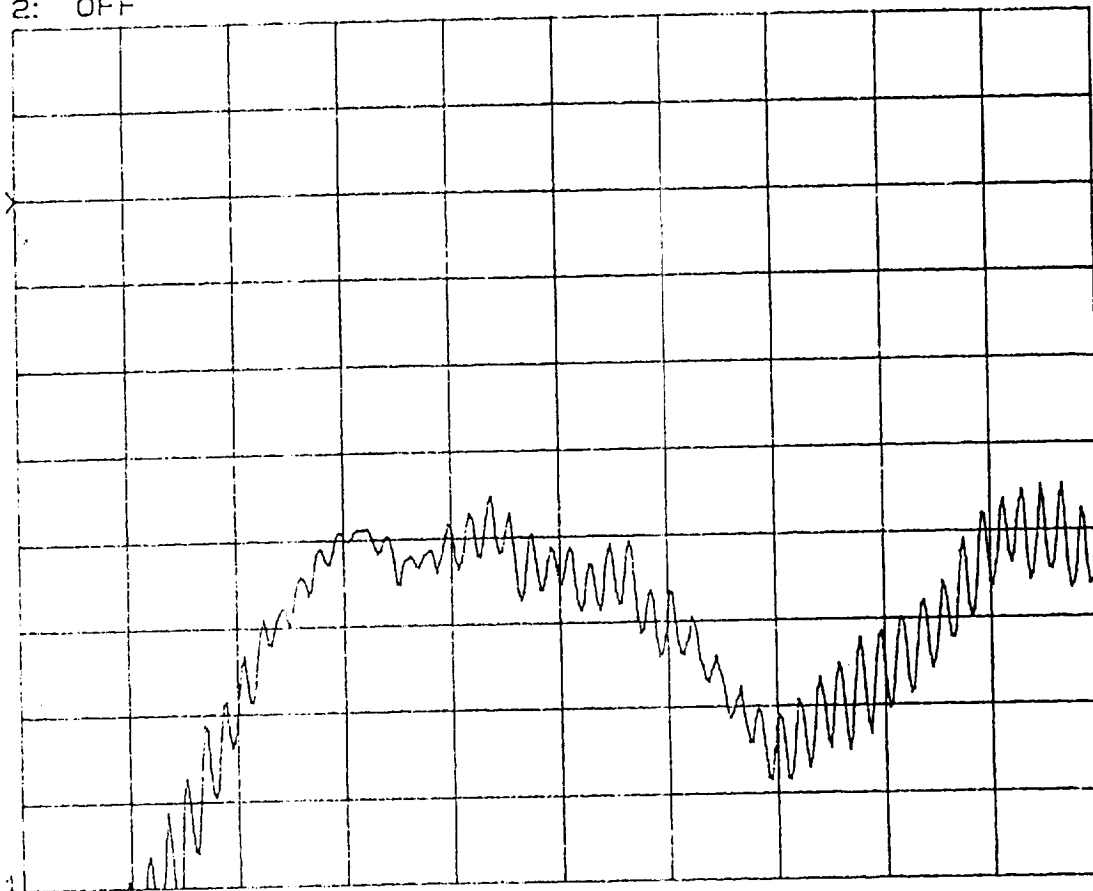


Figure 6.6 (a) Insertion Loss Test of Circulator with ND-FE-B Magnet at 30°c (operation frequency 30-40GHz)

ORIGINAL PAGE IS
OF POOR QUALITY

Identify: 30-40 GHz Test Device: CIRCULATOR Date: 07-24-89
 1: TRANSMSSN (A) 1.0 dB/DIV OFFSET +0.0 dB
 2: OFF



401 points

Figure 6.6 (b) Insertion Loss Test of Circulator with ND-FE-B
 Magnet at 40°C (operation frequency 30-40 GHz)

ORIGINAL PAGE IS
 OF POOR QUALITY

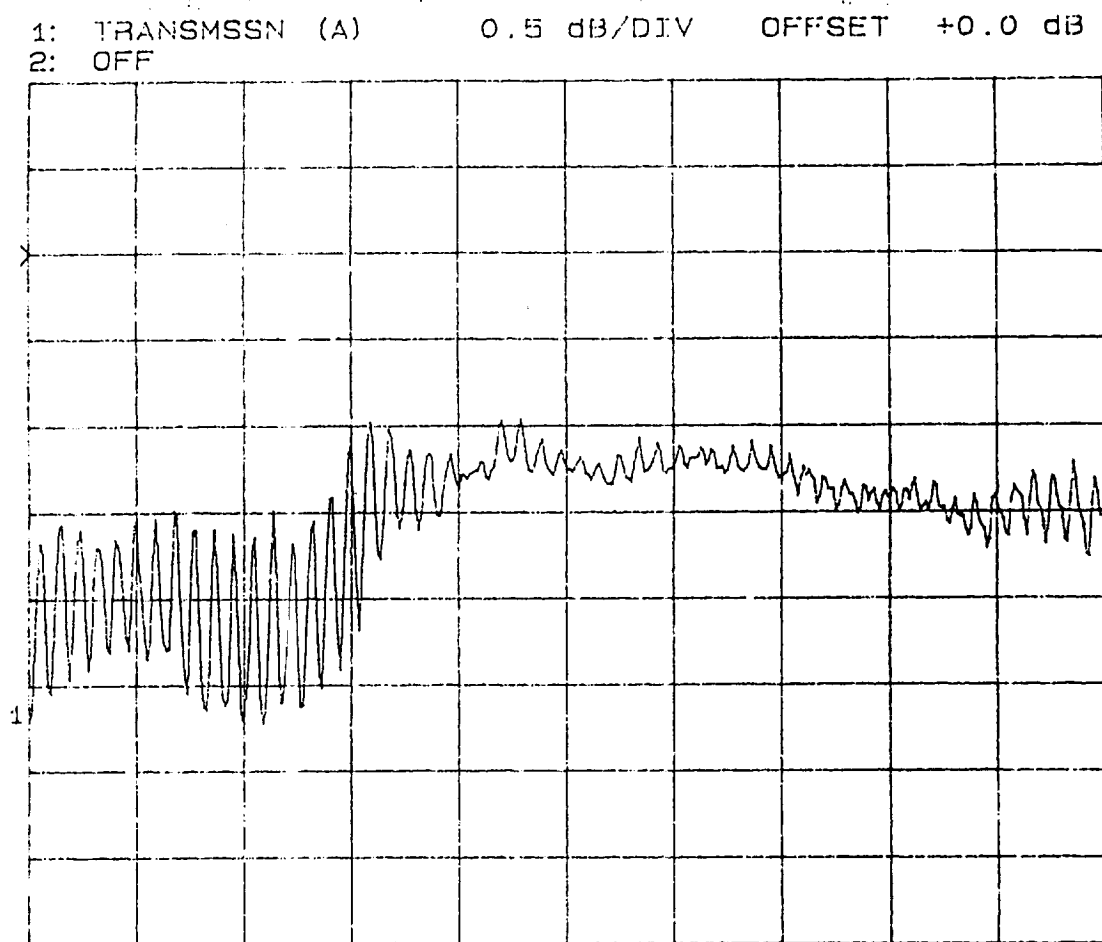
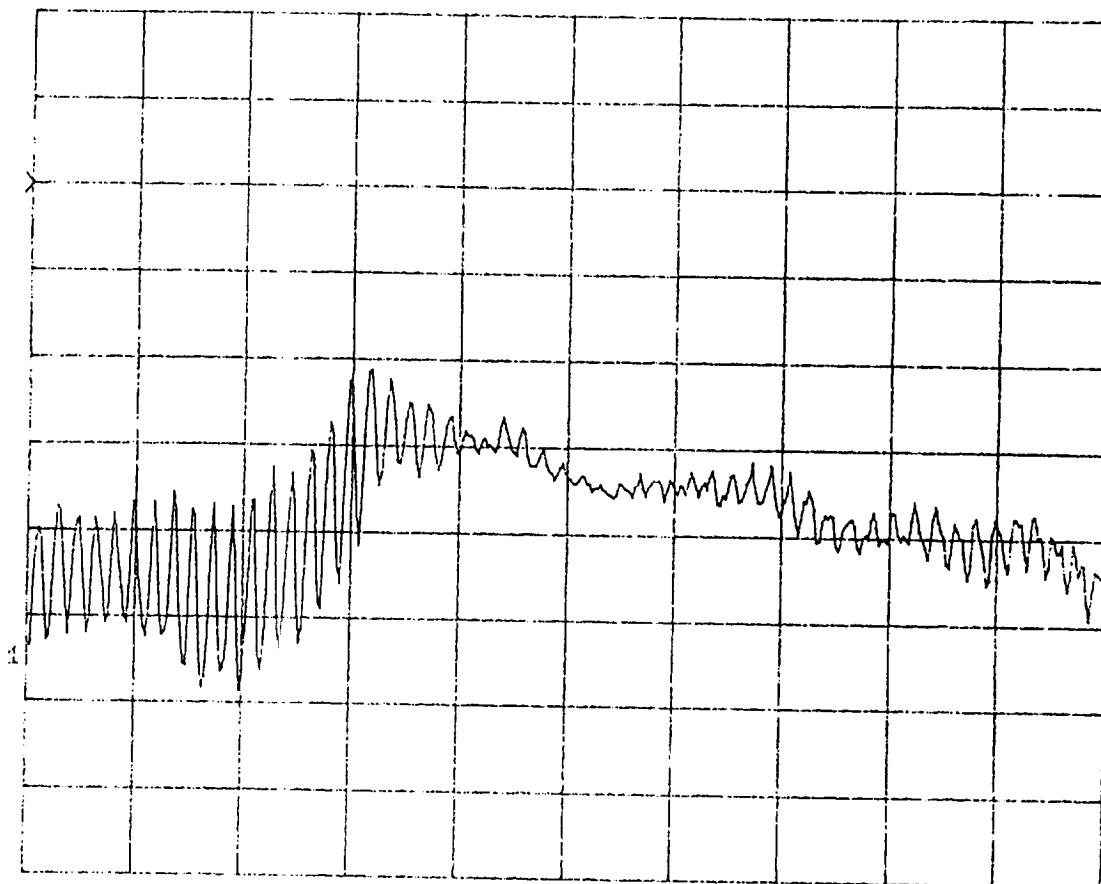


Figure 6.7 (a) Insertion Loss Test of Circulator with $\text{SM}_2\text{CO}_{17}$ Cobalt Magnet at -20°C (Operation Frequency 30-40 GHz)

ORIGINAL PAGE IS
OF POOR QUALITY

1: TRANSMSSN (A) 0.5 dB/DIV OFFSET +0.0 dB
2: OFF

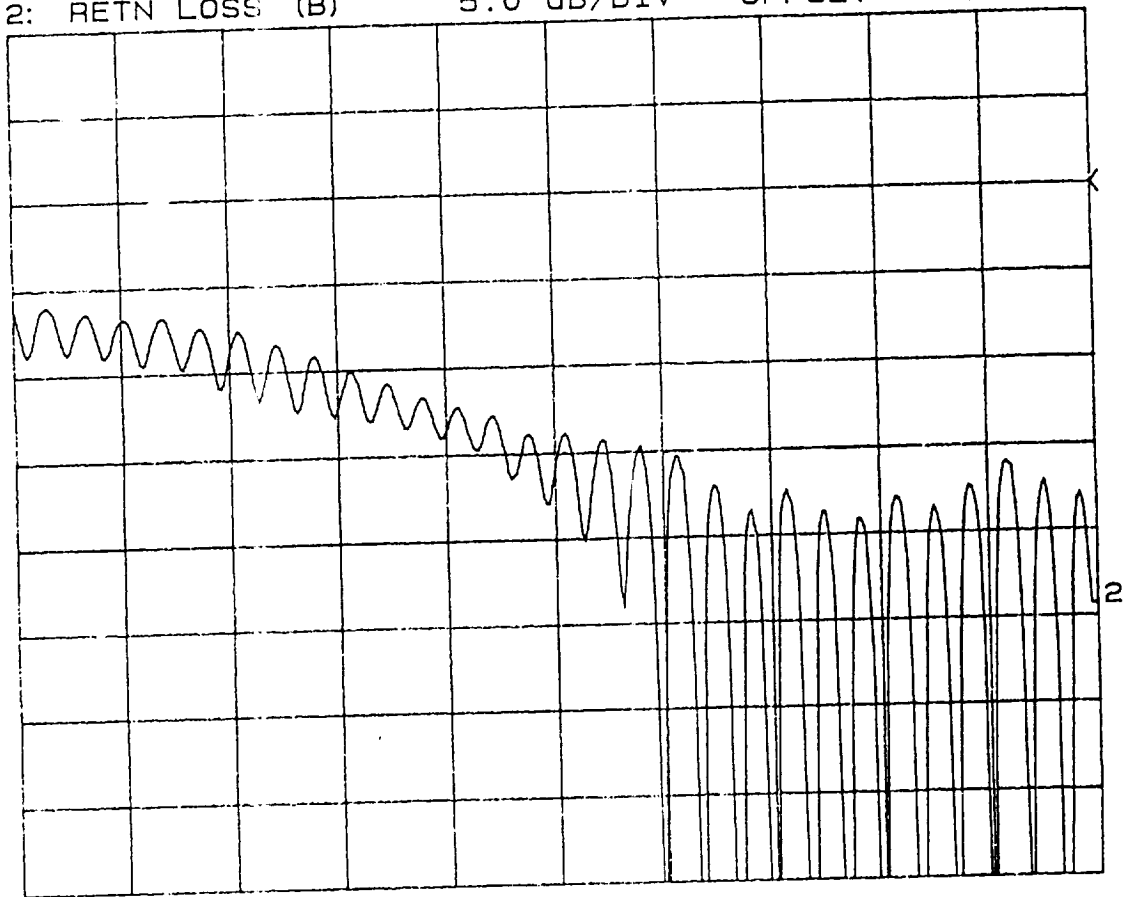


401 points

Figure 6.7 (b) Insertion Loss Test of Circulator with $\text{SM}_2\text{CO}_{17}$ Cobalt Magnet at 50°C (Operation Frequency 30-40 GHz)

ORIGINAL PAGE IS
OF POOR QUALITY

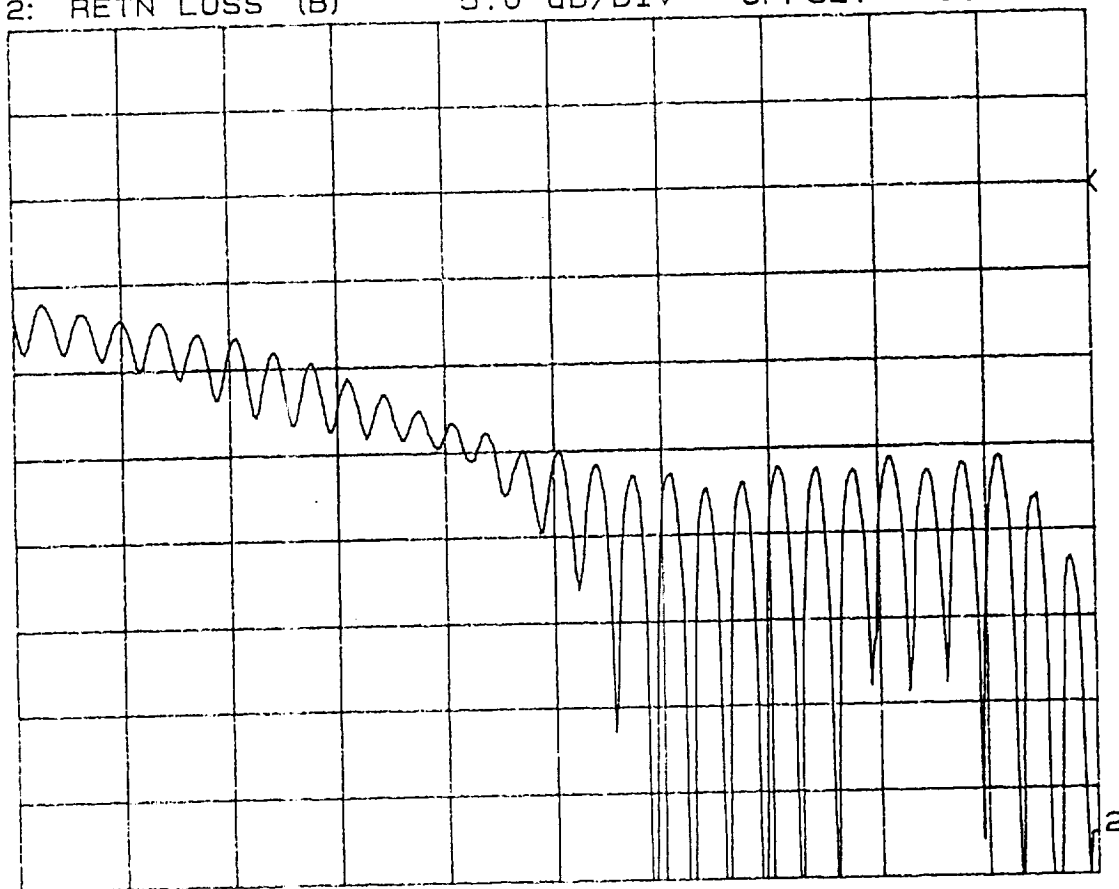
Identify: 30-40 GHz Test Device: CIRCULATOR Date: 08-03-89
 1: OFF
 2: RETN LOSS (B) 5.0 dB/DIV OFFSET +0.0 dB



401 points

Figure 6.8 (a) Return Loss Test of Circulator with $\text{SM}_2\text{CO}_{17}$ Cobalt Magnet at -20°C (operation frequency 30-40 GHz)

Identify: 30-40 GHz Test Device: CIRCULATOR Date: 08-03-89
 1: OFF
 2: RETN LOSS (B) 5.0 dB/DIV OFFSET +0.0 dB



401 points

Figure 6.8 (b) Return Loss /Test of Circulator with $\text{SM}_2\text{CO}_{17}$ Cobalt Magnet at 50°C (operation frequency 30-40 GHz)

7.0 Conclusion and Recommendation

7.1 Summary and Conclusion

- (1) The high performance millimeter-wave circulator is extremely important for many system applications, including reflection amplifier fabrication, impedance matching, isolation diplexing, etc.. It is a key component in microwave and millimeter-wave communications, radar, sensors, and electronic warfare systems.
- (2) Presently, most of the millimeter-wave circulators are available only in waveguide or stripline configuration. E-Tek's proposed microstrip configured circulator is superior in the following respects:
 - Compatibility with microstrip integrated circuit (MIC) or monolithic millimeter-wave integrated circuit (MMIC)
 - Size/weight
 - Wide operational bandwidth
 - Fabrication simplicity
 - Potentially low cost
- (3) Commercially available, low loss millimeter-wave ferrite substrates and temperature stable magnets are available for high performance microstrip circulator fabrication.

- (4) Ka band circulators were designed and optimized, based on computer simulation and laboratory test results.
- (5) A test fixture was designed, fabricated, and evaluated for measuring drop-in circulator performance, the demonstrated repeatability of performance results is acceptable.
- (6) Performance of the Ka band microstrip circulator is considered to be satisfactory. The prototype circulators have isolation and return loss of greater than 16 dB, and insertion loss of less than 0.7 dB. This level of performance meets the design specifications.
- (7) A temperature impact evaluation was done to test the performance of a 36 to 40 GHz microstrip circulator over the temperature range of -20°C to 50°C for 3 continuous cycles. The results show that the circulator package designed and fabricated in Phase II, was adequate for wide temperature operation.
- (8) A wideband stub-tuned configured microstrip circulator with operating frequency from 31 to 37 GHz was designed and fabricated for deep space applications. This circulator has insertion loss less than 0.8dB, and isolation and return loss better than 15dB.

7.2 Recommendations

The following recommendations are made for the continued investigation, following completion of Phase II R&D.

- The Ka band circulator size can be further reduced to 0.10" x 0.10" x 0.005", which will be very useful for MMIC or MIC applications. A test circulator sample with 0.15" x 0.15" x 0.005" dimensions is displayed on a dime coin (Figure 7.1).
- Miniature wideband circulators, using stub-tuned or ring shaped configurations, will have great potential for a variety of applications, together with excellent performance.
- New millimeter-wave ferrite substrate and temperature stable permanent magnets (some attaining an energy product of 40 MGO) will almost surely be available over the next few years, which will make an enhanced performance, microstrip circulator possible.
- Optimize circulator performance and reliability over very wide temperature range (-50°C to +100°C)
- Evaluate circulator performance and survival rate within

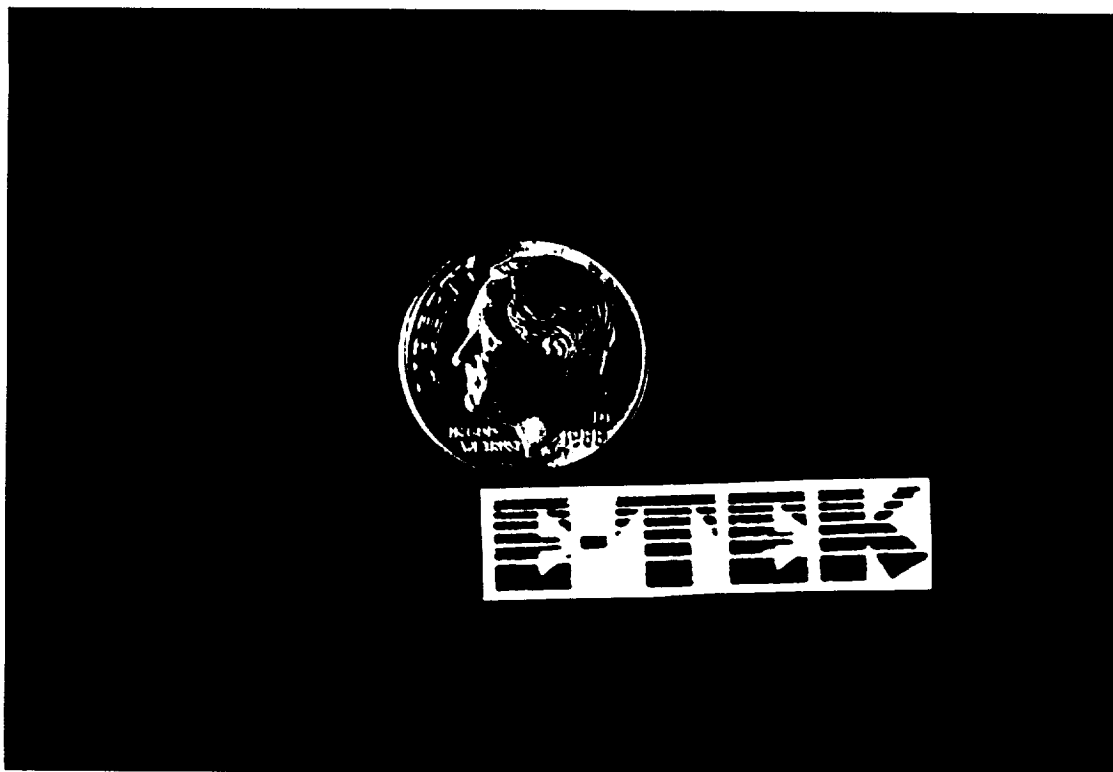


Figure 7.1 A Ka-Band Circulator (Magnet Is Not Shown)

hostile environments such as quick temperature change,
shock, vibration, moisture, timing, etc.

- Improve and simplify production, increase producibility
and optimize fabrication integration with MMIC.
- Minimize cost

Appendix A

Stub Tuned Microstrip Circulator Analysis

In considering the electromagnetic field in the microstrip line, as shown in Figure A1, it is assumed that the distance between the two conducting plates of a microstrip line is much smaller than its width, thus, the fringing fields effect can be neglected.

In that case, the dominant mode is:

$$E_z = A e^{\pm \alpha x} \cdot e^{\pm j \beta y} \quad (1)$$

$$H_x = \pm \sqrt{\frac{\epsilon_o \epsilon_r}{\mu_o \mu}} \cdot A \cdot e^{\pm \alpha x \pm j \beta y} \quad (2)$$

For higher-order modes:

$$E_z = C \cdot \left[\cos(\alpha_m x) - \frac{k}{\mu} \frac{\beta_m}{\alpha_m} \cdot \sin(\alpha_m x) \right] e^{-j \beta_m y} \quad (3)$$

$$H_y = \frac{jC}{\omega \mu_o \mu_{eff}} \left[\alpha_m + \left(\frac{k}{\mu} \right)^2 \cdot \frac{\beta_m^2}{\alpha_m} \right] \cdot \sin(\alpha_m x) e^{-j \beta_m y} \quad (4)$$

$$H_x = \frac{C}{\omega \mu_o \mu_{eff}} \left[-\frac{k}{\mu} \left(\alpha_m + \frac{\beta_m^2}{\alpha_m} \right) \sin(\alpha_m x) + \beta_m \frac{\mu_{eff}}{\mu} \cdot \cos(\alpha_m x) \right] e^{-j \beta_m y} \quad (5)$$

where μ and k are the components of the permeability tensor of the ferrite, ϵ_r is the dielectric constant of the ferrite,

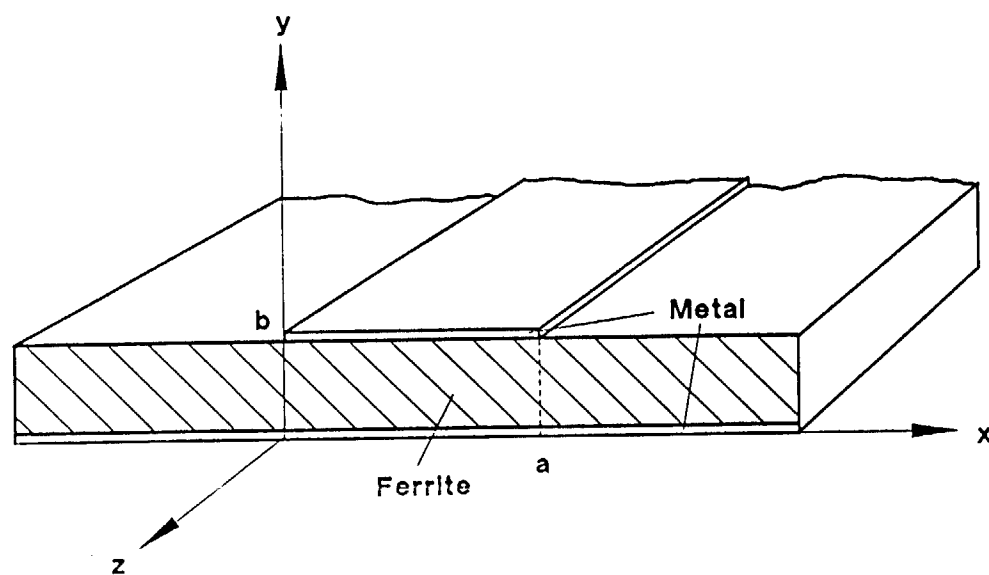


Figure A 1 Microstrip Line

$$\mu_{\text{eff}} = \frac{\mu^2 - k^2}{\mu} \quad \beta = \omega \sqrt{\mu_o \mu \epsilon_o \epsilon_r} \quad \alpha = \beta \frac{k}{\mu} \quad \alpha_m = \frac{m\pi}{W}$$

$$\beta_m = \sqrt{\omega^2 \epsilon_o \epsilon_r \mu_o \mu_{\text{eff}} - \alpha_m^2}, \quad m = 1, 2, 3, \dots$$

$$\mu = 1 + \frac{\omega_o \omega_m}{\omega_o^2 - \omega^2}$$

$$k = \frac{\omega \omega_m}{\omega_o^2 - \omega^2}$$

$$\omega_o = \gamma H_o$$

$$\omega_m = \gamma 4\pi M_s$$

The geometry diagram of a microstrip circulator is shown in Figure A.2. Arms 1, 2 and 3 are the input and output ports of the microstrip circulator, arms 4, 5 and 6 are open ended. W_1 and W_2 are the width of the coupling arm and open ended arm, respectively. ψ_1 and ψ_2 are the half-coupling angles of the coupling arm and the open-ended arm, respectively.

For TE_{10} mode electromagnetic fields in cylindrical coordinates:

$$E_z = \sum_{n=-\infty}^{+\infty} A'_n B s_n(X_e) e^{jn\theta} \quad (6a)$$

$$H_\theta = \frac{-j}{\omega \mu_o \mu_{\text{eff}}} \sum_{n=-\infty}^{+\infty} A'_n \left[K_e B s'_n(X_e) - \frac{nk}{r\mu} B s_n(X_e) \right] e^{jn\theta} \quad (6b)$$

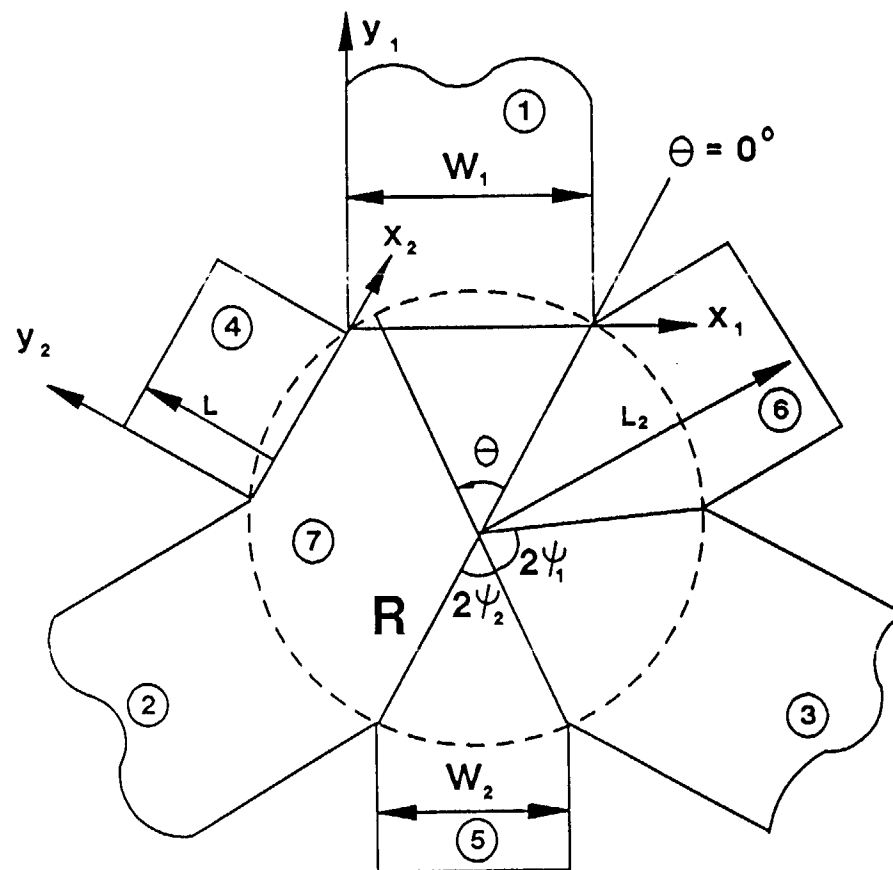


Figure A 2 Configuration of Wideband Stub-tuned Microstrip Circulator

$$H_r = \frac{-1}{\omega \mu_o \mu_{eff}} \sum_{n=-\infty}^{+\infty} A'_n \left[\frac{n}{r} B s_n(X_e) - \frac{k}{\mu} K_e B s'_n(X_e) \right] e^{jn\theta} \quad (6c)$$

where k_e is defined as $K_e = \omega \sqrt{\epsilon_o \epsilon_r \mu_o \mu_{eff}}$

$$X_e = K_e r$$

$$B s_n(X_e) = \begin{cases} B s_n(X_e) & \mu_{eff} \geq 0 \\ I_n(X_e) & \mu_{eff} < 0 \end{cases}$$

The electromagnetic fields in the coupled arms are:

$$E_{z1} = e^{\alpha(x_1 - w_1) + j\beta y_1} + B_1 e^{-\alpha x_1 - j\beta y_1} + \sum_{m=1}^{\infty} C_{m1} \left[\cos(\alpha_{m1} X_1) - \frac{k}{\mu} \frac{\beta_{m1}}{\alpha_{m1}} \sin(\alpha_{m1} X_1) \right] e^{-j\beta_{m1} Y_1} \quad (7a)$$

$$H_{x1} = \sqrt{\frac{\epsilon_o \epsilon_r}{\mu_o \mu}} \left[-A_1 e^{\alpha(x_1 - w_1) + j\beta y_1} + B_1 e^{-\alpha x_1 - j\beta y_1} \right] + \sum_{m=1}^{\infty} \frac{C_{m1}}{\omega \mu_o \mu_{eff}} \left[-\frac{k}{\mu} \left(\alpha_{m1} + \frac{\beta_{m1}^2}{\alpha_{m1}} \right) \sin(\alpha_{m1} X_1) + \beta_{m1} \frac{\mu_{eff}}{\mu} \cos(\alpha_{m1} X_1) \right] e^{-j\beta_{m1} Y_1} \quad (7b)$$

$$H_{y1} = \sum_{m=1}^{\infty} \frac{j C_{m1}}{\omega \mu_o \mu_{eff}} \left[\alpha_{m1} + \left(\frac{k}{\mu} \right)^2 \frac{\beta_{m1}^2}{\alpha_{m1}} \right] \sin(\alpha_{m1} X_1) e^{-j\beta_{m1} Y_1} \quad (7c)$$

In the open-ended arms, the electromagnetic fields are:

$$E_{z_1} = B_1 \left[e^{-\alpha x_1 - j\beta y_1} + e^{\alpha(x_1 - w_2) + j\beta(y_1 - 2L)} \right] \quad (8a)$$

$$\begin{aligned} H_{x_1} = & \sqrt{\frac{\epsilon_o \epsilon_r}{\mu_o \mu}} B_1 \left[e^{-\alpha x_1 - j\beta y_1} - e^{\alpha(x_1 - w_2) + j\beta(y_1 - 2L)} \right] \\ & + \sum_{m=1}^{\infty} \frac{C_{m_1}}{\omega \mu_o \mu_{eff}} \left[-\frac{k}{\mu} \left(\alpha_{m_1} + \frac{\beta_{m_1}^2}{\alpha_{m_1}} \right) \sin(\alpha_{m_1} x_1) \right. \\ & \left. + \beta_{m_1} \frac{\mu_{eff}}{\mu} \cos(\alpha_{m_1} x_1) \right] e^{-j\beta_{m_1} y_1} \end{aligned} \quad (8b)$$

$$H_y = \sum_{m=1}^{\infty} \frac{jC_{m_1}}{\omega \mu_o \mu_{eff}} \left[\alpha_{m_1} + \left(\frac{k}{\mu} \right)^2 \frac{\beta_{m_1}^2}{\alpha_{m_1}} \right] \sin(\alpha_{m_1} x_1) e^{-j\beta_{m_1} y_1} \quad (8c)$$

The field components must be continuous at the boundary $r = R$, which is

$$E_z^{\text{region7}} \Big|_{r=R} = E_z^{\text{region1-6}} \Big|_{r=R} \quad (9)$$

$$H_\theta^{\text{region7}} \Big|_{r=R} = H_\theta^{\text{region1-6}} \Big|_{r=R}$$

The H_θ can be expressed in terms of H_x , H_y as follows:

$$H_Q = \begin{cases} H_y \sin(\psi_1 - \theta) - H_x \cos(\psi_1 - \theta) & \text{coupling arm} \\ H_y \sin(\psi_2 + 2\psi_1 - \theta) - H_x \cos \psi \left(+ \psi_2 + 2\psi_1 - \theta \right) & \text{open-ended arm} \end{cases} \quad (10)$$

From the symmetrical properties of the junction, the eigenvector excitation is selected, and $n = 3q + 1$ ($q = 0, \pm 1, \pm 2, \dots$, $1 = -1, 0, 1$). Substituting Eqs. (6), (7) and (8) into Eq. (9), multiplying $e^{-jn\theta}$ and integrating from 0 to $2\pi/3$, we have:

$$\begin{aligned} A'_n J_n(X_e) = & \frac{3}{2\pi} \int_0^{2\psi_1} \left\{ B_1 e^{-\alpha x_1 - j\beta y_1} + e^{\alpha(x_1 - w_1) + j\beta y_1} \right. \\ & + \sum_{m=1}^{\infty} C_{m_1} \left[\cos(\alpha_{m_1} X_1) - \frac{k}{\mu} \frac{\beta_{m_1}}{\alpha_{m_1}} \right. \\ & \cdot \sin(\alpha_{m_1} X_1) \left. \right] e^{-j\beta_{m_1} y_1} \left. \right\} e^{-jn\theta} d\theta \\ & + \frac{3}{2\pi} \int_{2\psi_1}^{2\pi/3} \left\{ B_2 \left[e^{-\alpha x_2 - j\beta y_2} + e^{\alpha(x_2 - w_2) + j\beta(y_2 - 2L)} \right] \right. \\ & + \sum_{m=1}^{\infty} C_{m_2} \left[\cos(\alpha_{m_2} X_2) - \frac{k}{\mu} \frac{\beta_{m_2}}{\alpha_{m_2}} \sin(\alpha_{m_2} X_2) \right] \\ & \cdot e^{-j\beta_{m_2} X_2} \left. \right\} e^{-jn\theta} d\theta \end{aligned} \quad (11)$$

$$\frac{-jA'_n}{\omega \mu_o \mu_{eff}} \left[k_{en} B S'_n(X_e) - \frac{n}{R} \cdot \frac{k}{\mu} B S_n(X_e) \right]$$

$$\begin{aligned}
&= \frac{3}{2\pi} \int_0^{2\psi_1} \left\{ -\sqrt{\frac{\epsilon_o \epsilon_r}{\mu_o \mu}} \left[B_1 e^{-\alpha x_1 - j\beta y_1} - e^{\alpha(x_1 - w_1) + j\beta y_1} \right] \cos(\psi_1 - \theta) \right. \\
&\quad - \sum_{m=1}^{\infty} \frac{C_{m_1}}{\omega \mu_o \mu_{eff}} \left[-\frac{k}{\mu} \left(\alpha_{m_1} + \frac{\beta_{m_1}^2}{\alpha_{m_1}} \right) \sin(\alpha_{m_1} x_1) + \beta_{m_1} \frac{\mu_{eff}}{\mu} \cos(\alpha_{m_1} x_1) \right] \\
&\quad \cdot \cos(\psi_1 - \theta) e^{-j\beta_{m_1} y_1} \\
&\quad + \sum_{m=1}^{\infty} \frac{jC_{m_1}}{\omega \mu_o \mu_{eff}} \left[\alpha_{m_1} + \left(\frac{k}{\mu} \right)^2 \frac{\beta_{m_1}^2}{\alpha_{m_1}} \right] \sin(\alpha_{m_1} x_1) e^{-j\beta_{m_1} y_1} \\
&\quad \cdot \sin(\psi_1 - \theta) \Big\} e^{-jn\theta} d\theta \\
&+ \frac{3}{2\pi} \int_{2\psi_1}^{2\pi/3} \left\{ -\sqrt{\frac{\epsilon_o \epsilon_r}{\mu_o \mu}} B_2 \left[e^{-\alpha x_2 - j\beta y_2} - e^{(\alpha(x_2 - w_2) + j\beta(y_2 - 2L))} \right] \right. \\
&\quad \cdot \cos(\psi_2 + 2\psi_1 - \theta) \\
&\quad - \sum_{m=1}^{\infty} \frac{C_{m_2}}{\omega \mu_o \mu_{eff}} \left[-\frac{k}{\mu} \left(\alpha_{m_2} + \frac{\beta_{m_2}^2}{\alpha_{m_2}} \right) \sin(\alpha_{m_2} x_2) + \beta_{m_2} \frac{\mu_{eff}}{\mu} \cos(\alpha_{m_2} x_2) \right] \\
&\quad \cdot e^{-j\beta_{m_2} y_2} \cos(\psi_2 + 2\psi_1 - \theta) \\
&\quad + \sum_{m=1}^{\infty} \frac{jC_{m_2}}{\omega \mu_o \mu_{eff}} \left[\alpha_{m_2} + \left(\frac{k}{\mu} \right)^2 \frac{\beta_{m_2}^2}{\alpha_{m_2}} \right] \sin(\alpha_{m_2} x_2) \\
&\quad \cdot \sin(\psi_2 + 2\psi_1 - \theta) e^{-j\beta_{m_2} y_2} \Big\} e^{-jn\theta} d\theta
\end{aligned}$$

(12)

Eliminating the constant A'_n and truncating the high order term in coupled arm and open-ended arm to M and $M-1$ th order respectively, results in

$$a_1(n) \cdot B_1 + a_2(n) B_2 + \sum_{m=1}^M a_{2+m}(n) C_{m_1} + \sum_{m=1}^{M-1} a_{2+M+m}(n) C_{m_2} = b(n) \quad (13)$$

where:

$$a_1(n) = \int_0^{2\psi_1} \left[jD_n - G \cos(\psi_1 - \theta) \right] e^{-\alpha x_1 - j\beta y_1 - jn\theta} d\theta$$

$$a_2(n) = \int_{2\psi_1}^{2\pi/3} \left\{ \left[jD_n - G \cos(\psi_2 + 2\psi_1 - \theta) \right] e^{-\alpha x_2 - j\beta y_2} + e^{-j\beta 2L} \right. \\ \left. \cdot \left[jD_n + G \cos(\psi_2 + 2\psi_1 - \theta) e^{\alpha(x_2 - y_2) + j\beta y_2} \right] e^{-jn\theta} d\theta \right.$$

$$a_m(n) = \int_0^{2\psi_1} \left\{ jD_n \left[\cos(\alpha_{m_1} X_1) - \frac{k}{\mu} \frac{\beta_{m_1}}{\alpha_{m_1}} \sin(\alpha_{m_1} X_1) \right] \right. \\ \left. - \left[-\frac{k}{\mu} \left(\alpha_{m_1} + \frac{\beta_{m_1}^2}{\alpha_{m_1}} \right) \sin(\alpha_{m_1} X_1) + \beta_{m_1} \frac{\mu_{eff}}{\mu} \cos(\alpha_{m_1} X_1) \cos(\psi_1 - \theta) \right] \right. \\ \left. + j \left[\alpha_{m_1} + \left(\frac{k}{\mu} \right)^2 \frac{\beta_{m_1}^2}{\alpha_{m_1}} \right] \sin(\alpha_{m_1} X_1) \sin(\psi_1 - \theta) \right\} e^{-j\beta_{m_1} - jn\theta} d\theta$$

$$3 \leq m \leq M+2$$

$$a_m(n) = \int_{2\psi_1}^{2\pi/3} \left\{ jD_n \left[\cos(\alpha_{m_2} X_2) - \frac{k}{\mu} \frac{\beta_{m_2}}{\alpha_{m_2}} \sin(\alpha_{m_2} X_2) \right] \right.$$

$$\begin{aligned}
& - \left[-\frac{k}{\mu} \left(\alpha_{m_2} + \frac{\beta_{m_2}^2}{\alpha_{m_2}} \sin(\alpha_{m_2} X_2) + \beta_{m_2} \frac{\mu_{eff}}{\mu} \cos(\alpha_{m_2} X_2) \right. \right. \\
& \left. \cos(\psi_2 + 2\psi_1 - \theta) + j \left[\alpha_{m_2} + \left(\frac{k}{\mu} \right)^2 \frac{\beta_{m_2}^2}{\alpha_{m_2}} \right] \sin(\alpha_{m_2} X_2) \right. \\
& \left. \cdot \sin(X_2 + 2\psi_1 - \theta) \right\} e^{-j\beta_{m_2} y_2 - jn\theta} d\theta
\end{aligned}$$

$$M+3 \leq m \leq 2M+1$$

$$b(n) = - \int_0^{2\psi_1} \left[jD_n + G \cos(\psi_1 - \theta) \right] e^{\alpha(X_1 - W_1) + j\beta y_1 - jn\theta} dB$$

$$G = \omega \mu_o \mu_{eff} \sqrt{\frac{E_o E_r}{\mu_o \mu}}, \quad D_n = K_e \frac{Bs'_n(X_e)}{Bs_n(X_e)} - \frac{n}{R} \frac{K}{\mu}, \quad \alpha_{m_1} = \frac{m\pi}{W_1}, \quad \alpha_{m_2} = \frac{W\pi}{W_2}$$

$$W_1 = 2R \cdot \sin\psi_1, \quad W_2 = 2R \cdot \sin\psi_2, \quad \beta_{m_i} = \sqrt{K_e^2 - \alpha_{m_i}^2}, \quad i = 1, 2,$$

The relationship between the coordinators X_i , y_i and R , θ on the circle is:

$$\begin{cases} X_1 = R \cdot [\sin\psi_1 + \sin(\psi_1 - \theta)] \\ Y_1 = R \cdot [\cos(\psi_1 - \theta) - \cos\psi_1] \end{cases}$$

and

$$\begin{cases} X_2 = R \cdot [\sin\psi_2 + \sin(2\psi_1 + \psi_2 - \theta)] \\ Y_2 = R \cdot [\cos(2\psi_1 + \psi_2 - \theta) - \cos\psi_2] \end{cases}$$

From Eq. (13), there are $2M+1$ unknowns. In order to make the number of equations equal to the number of unknowns, $q = -M, -M+1, \dots, M-1, M$ is chosen. Now we have the number of n equals $2M+1$ for a fixed value of I :

$$n = -3M + I, \quad -3(M-1) + I, \dots, 3(M-1) + I, \quad 3M + I$$

A matrix equation can be set up:

$$A \cdot X = B \quad (14)$$

where:

$$A = \begin{bmatrix} a_1(n_1) & a_2(n_1) & \dots & a_{2M+1}(n_1) \\ a_1(n_2) & a_2(n_2) & \dots & a_{2M+1}(n_2) \\ \vdots & \vdots & \ddots & \vdots \\ a_1(n_{2M+1}) & a_2(n_{2M+1}) & \dots & a_{2M+1}(n_{2M+1}) \end{bmatrix}$$

$$B = \begin{bmatrix} b(n_1) \\ b(n_2) \\ \vdots \\ b(n_{2M+1}) \end{bmatrix}, \quad X = \begin{bmatrix} B_1 \\ B_2 \\ \vdots \\ C^{m_1} \\ \vdots \\ C^{m_2} \end{bmatrix}$$

Putting $I = -1, 0, +1$, the solutions B_i in the matrix equation (14) are the eigenvalues S_{-1} , S_0 , and S_+ , respectively.

The scattering parameters of the stub tuned junction and the external characteristics are:

$$S_{11} = \frac{1}{3}(S_o + S_- + S_+)$$

$$S_{12} = \frac{1}{3}(S_o + S_+ e^{j2\pi/3} + S_- e^{-j2\pi/3}) \quad (15)$$

$$S_{13} = \frac{1}{3}(S_o + S_+ e^{-j2\pi/3} + S_- e^{j2\pi/3})$$

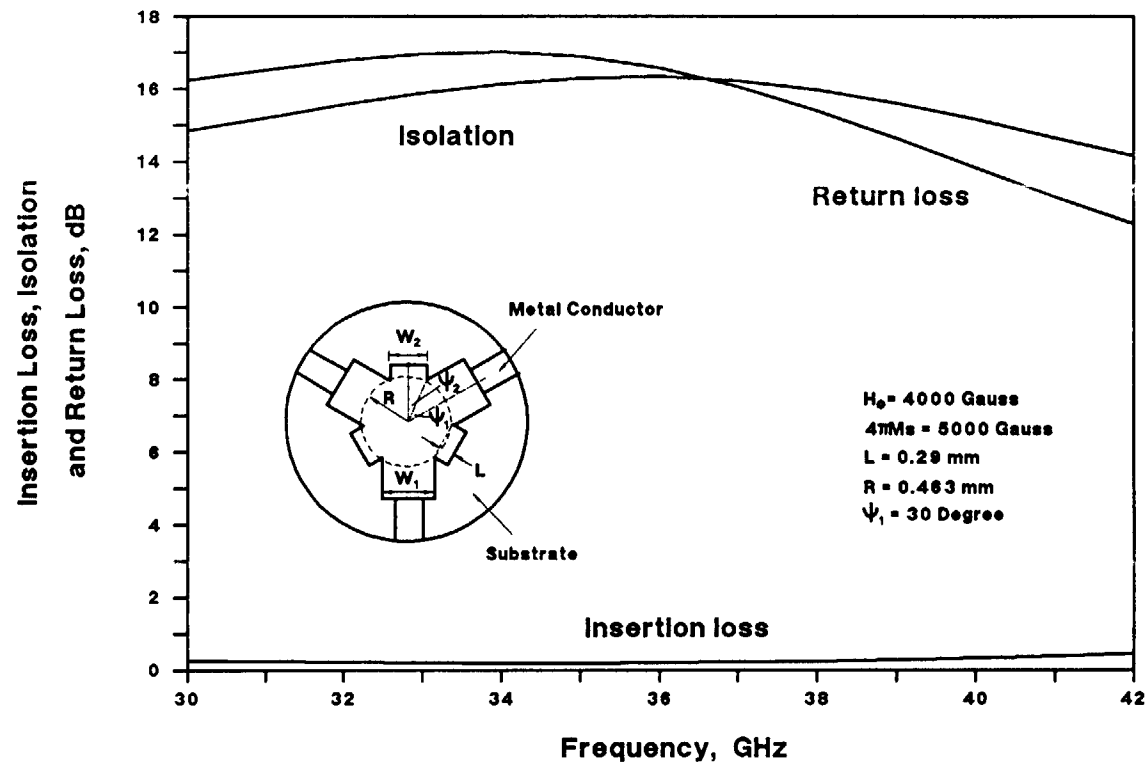
and

$$\text{Isolation} = 20 \log |S_{13}| \text{ dB}$$

$$\text{Insertion Loss} = 20 \log |S_{12}| \text{ dB} \quad (16)$$

$$\text{Reflection Loss} = 20 \log |S_{11}| \text{ dB}$$

A computer program is developed according to the formulas derived in Appendix A. The simulated results are illustrated in Figure A3, A4,, which indicate that the stud-tuned microstrip circulator has the property of wide operation bandwidth.



31-26-19-c15

Figure A 3 Insertion Loss, Isolation and Return Loss of Wideband Stub Tuned Microstrip Circulator

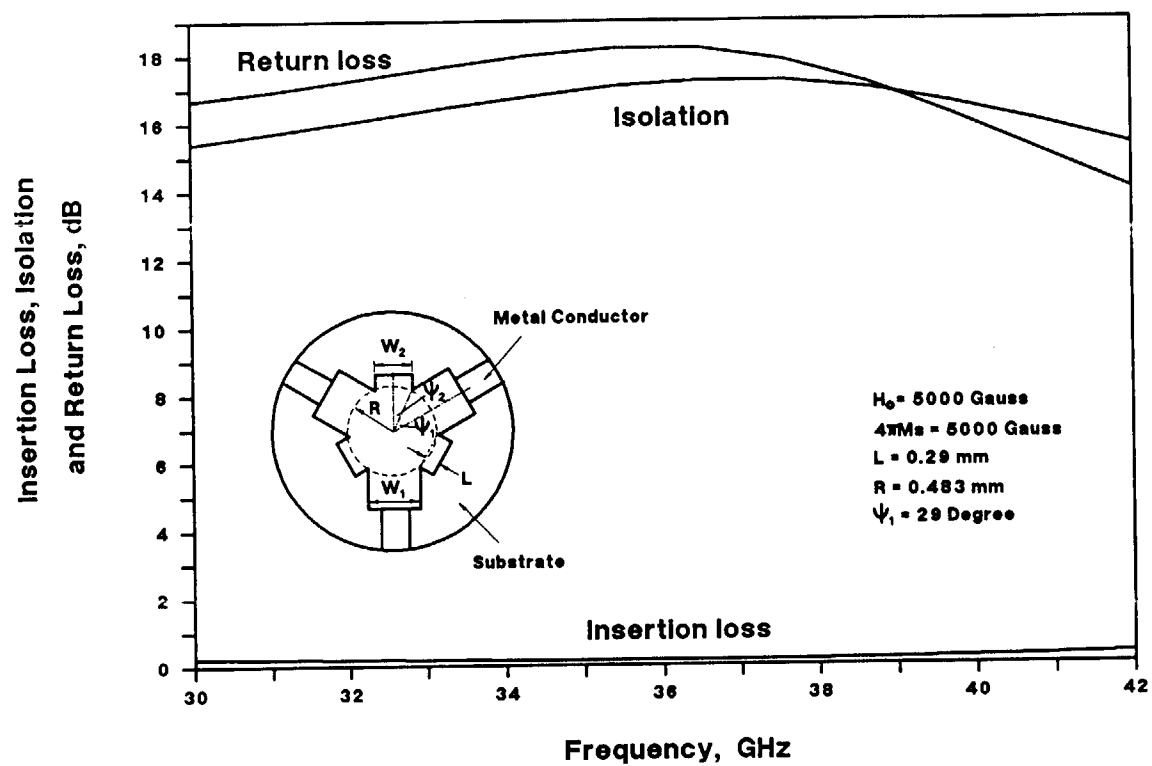


Figure A 4 Insertion Loss, Isolation and Return Loss of Wideband Stub Tuned Microstrip Circulator

Appendix B

B.0 Active Circulator

GaAs based microwave monolithic integrated circuits (MMIC) provide the advantages of mass producibility, cost-effectiveness of production, ruggedness, miniature size, and good reliability. The MMIC requires both circulator and isolator to perform various circuit functions and to improve operations. The conventional microwave circulator is a passive device and uses ferrite and magnet. The compatibility of the passive circulator with MMIC is not impressive at the present moment.

A novel approach is realized with an active circulator in the form of GaAs MMICs, without using any ferrite material or external magnets. The active circulator possesses all of the advantages of the MMIV, however, it also has some minor deficiencies, including:

- Bias and power supply required
- Additional thermal noise generated

B.1 Active Circulator Configuration and Operation Principle

Four different active circulator configurations using MESFETs and HEMTs are feasible and were investigated. The four configurations are:

- 3- to 6-Port active circulator

- Delta connection with a through element
- Circulating MESFETs
- 4-port circulator using one magic-T and a coupler

B.1.1 3- to 6-Port Active Circulator

The 3- to 6-port active circulator, as depicted in Figure B.1, consists of three active isolators and three directional couplers. An active isolator is a two-port non-reciprocal network which must have sufficient gain to compensate for the dissipation and coupling loss in the directional couplers. The bandwidth of the active circulator is determined by the bandwidths of both directional couplers and active isolator. Normally, the MESFET amplifiers have excellent return isolation and can serve as the active isolators.

Either a Wilkinson divider or a Lange interdigital directional coupler can provide wide bandwidth operation. An active circulator with an operational frequency 3-8.5 GHz has been fabricated and demonstrated by I. Bahl. The insertion gain varies from 0.1 to 0.6 dB with a minimum return loss of 15 dB and a minimum isolation of 16 dB. The three active isolators consume 180 mW of dc power.

B.1.2 Delta Connection with a Through Element

The structure of a delta connection circulator is illustrated in Figure B.2. The two-port "Thru" components provide a

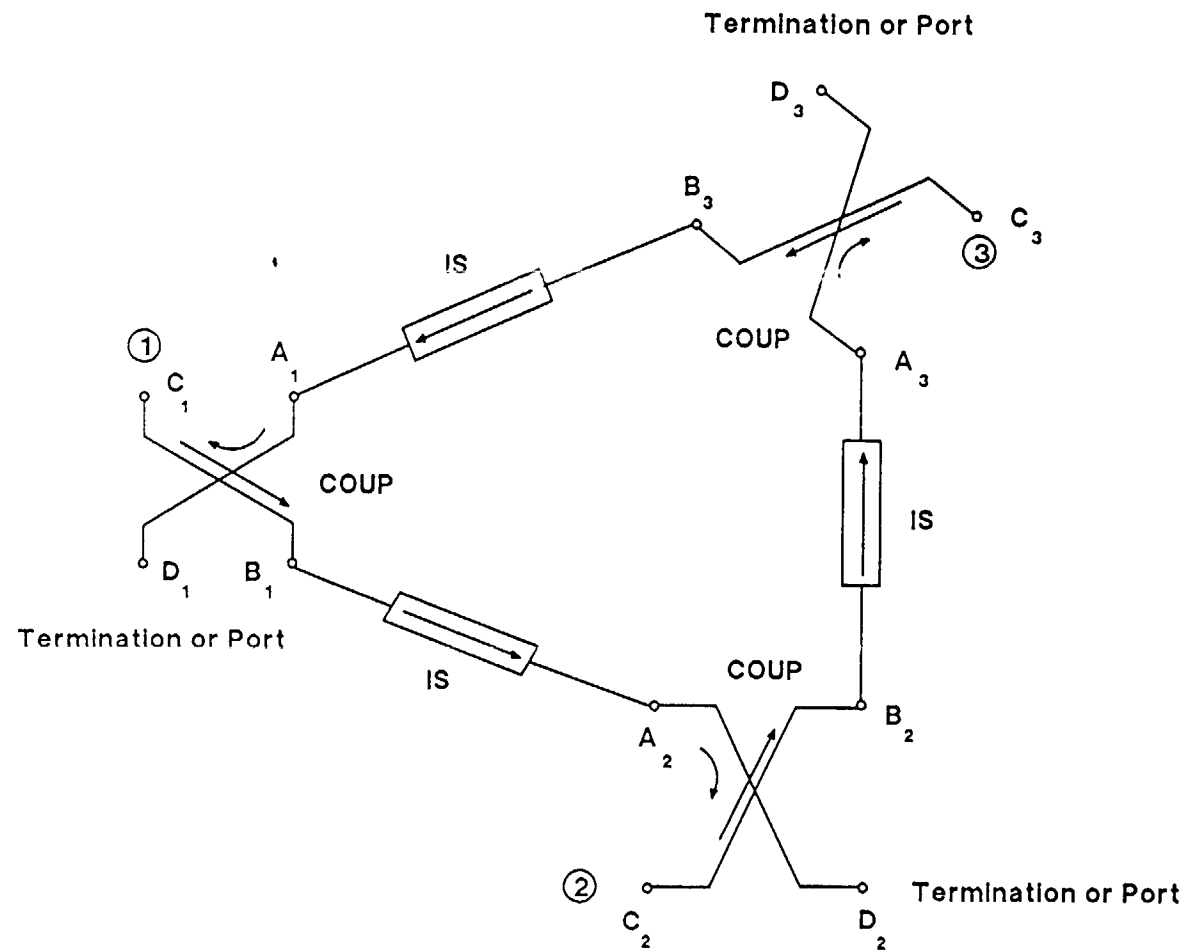


Figure B.1 3 to 6 Ports Active Coupler (After I. Bahl)

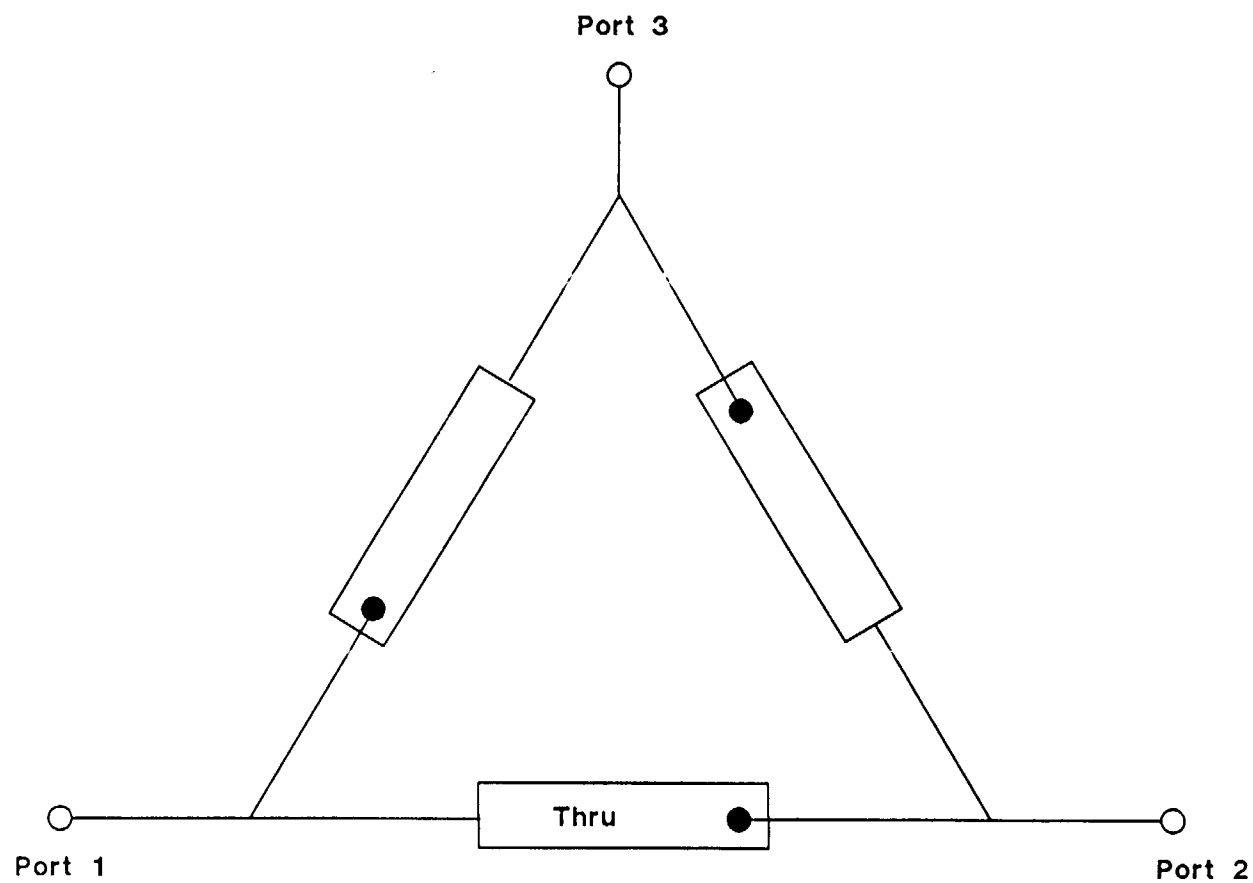


Figure B.2 3-Port Junction Active Circulator Formed by a Delta Connection of Thru Elements (After Y. Ayasli)

non-reciprocal phase shifter with minimum loss. The ideal performance for these "Thru" elements are a 120° phase shift in the circulation direction and a 60° phase shift in the reverse, with zero forward or reverse insertion loss. Under these ideal conditions, the signals are in-phase for the coupled port, and completely cancel each other at the isolated port. This delta configuration can act as a perfect circulator with ferrite isolation and return loss.

The non-reciprocal phase shifter can be constructed using MESFET or HEMT with a transmission. This delta connection is feasible for narrow band operation.

B.1.3 Circulating MESFETs Circulator

Circulating MESFETs circulators, as illustrated in Figure B.3, have been demonstrated by both Texas Instruments (TI) and Motorola in MMIC forms. This active circulator utilizes three active devices. The sources of the three GaAs MESFET's are tied together, and a common source resistor allows interaction between the devices. Another feedback mechanism is introduced by the shunt feedback resistor between the drain and the gate of each transistor. By properly adjusting the values of the resistors, and the sizes of the MESFETs in the circuit, the ports match and a null is obtained simultaneously in the reverse transmission characteristic.

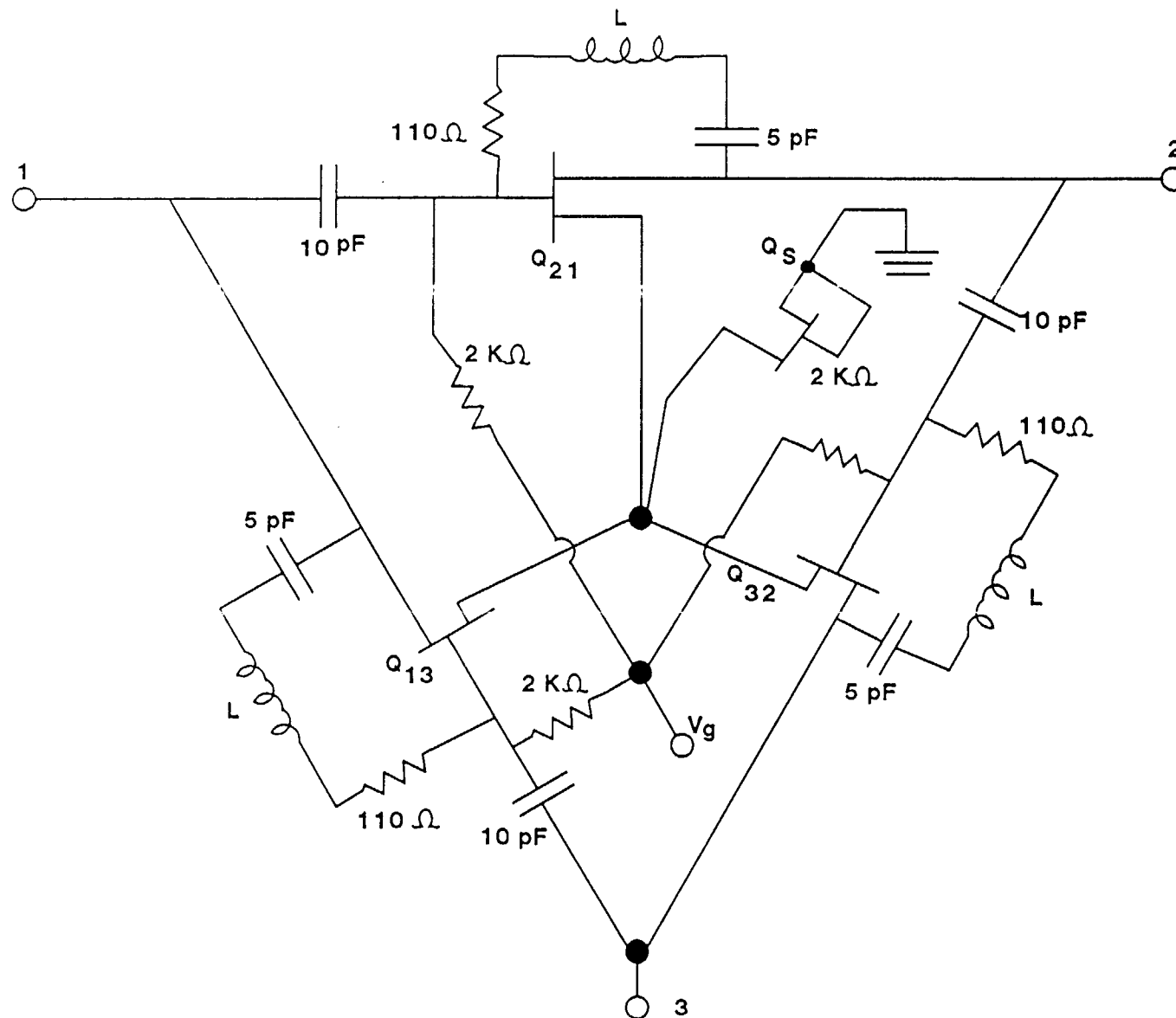


Figure B.3 Active Circulator Using Three MESFETs (After R. Dougherty)

A circulator chip of 1.1 x 1.0 mm was fabricated by TI with an operating frequency of 0.1 to 2.1 GHz. The device has insertion gain of -6 dB, return loss larger than 15 dB, and isolation loss larger than 20 dB.

B.1.4 4-Port Circulator Using a Magic-Tee

A four-port circulator based on a non-reciprocal phase shifter was proposed by Y. Ayosli, as depicted in Figure B.4. The four-port circulator requires a magic-tee. The magic-tee implemented in the MMIC form was demonstrated by T. Hirota, et al¹, using both Coplanar waveguide and Coplanar waveguide and slotline.

B.2 Power Handling Capability, DC Power Requirements and Noise Contribution of Active Circulators

The power handling capability of active circulators depends on the selection of GaAs MESFETs or GaAlAs HEMTs. For high power handling, a high power active device should be selected. With present technology, a 6-18 GHz active circulator from 1 to 1.5 Watts can be constructed. However, the high power active circulator suffers from the following shortcomings:

1. T. Hirota, H. Ogama, Y. Tarurawa, K. Owade, "Planar MMIC Hybrid Circuit and Frequency Converter", IEEE 1986 Microwave and Millimeter-Wave Monolithic Circuits Symposium Digest, pp. 103-105, Baltimore, MD, June 1986.

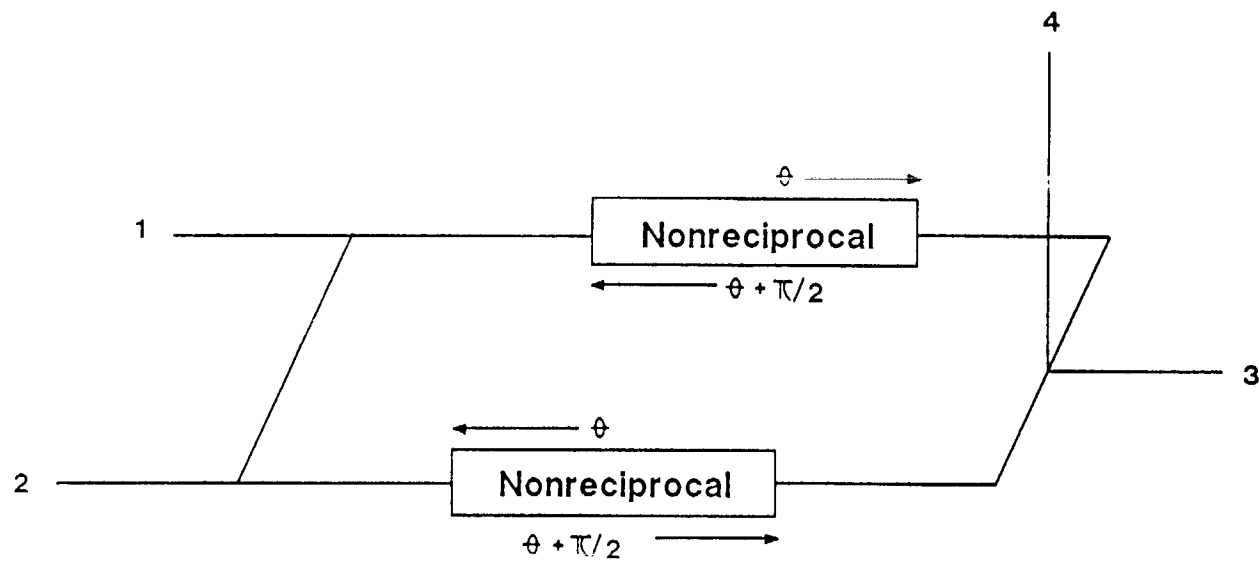


Figure B.4 4-Port Circulator Using One Active Magic-T and One Coupler
(After Y. Ayasli)

- Low efficiency and high DC power consumption
- High noise temperature
- Large physical size
- Thermal dissipation problems
- Relatively low production yield
- Narrow operation bandwidth (due to wideband impedance matching difficulty)
- Degradation of circulator performance parameters (due to the characteristics of high power MESFETs)

Low power active circulators (less than 100 mW RF signal) typically require 1.5 mm of gate periphery and 500 mW of DC supply power. Medium power active circulators (1 Watt RF signal) have narrow operational bandwidths (10% to 15% bandwidth) and need about 5 mm of periphery, with 2 to 2.5 Watts DC power. For wideband (20% - 40%) medium power circulator design, a DC power of 4-5 Watts is needed.

Although an active circulator with gain can be designed the MESFETs used in the circulator tend to raise the noise temperature higher than ambient due to their active bias. The noise figure or noise temperature of the active circulator is determined by:

- Device selection
- Impedance matching and operation bandwidth
- Bias condition

Using commercially available MESFETs, the estimated noise

level of a 100 mW 6-18 GHz active circulator is in the range of 4 to 7 dB.

B.3 Comparison of Active Circulator and Passive Circulator

The performance of microwave active and passive circulators is compared and presented in Table B.1.

B.4 Comments on Active Circulator for Ka band Phased Arrays

The active circulator provides excellent compatibility for phased-array antennas which use MMIC's. However, the wide band Ka band active circulator may increase the complexity of some systems or impose additional burdens, including:

- Large size (due to bias and stabilization circuit)
- High excess noise
- Power handling capability
- Additional DC power consumption

Table B.1

Comparison of Active and Passive Circulator

<u>Performance Parameter</u>	<u>Active Circulator</u>	<u>Passive Circulator</u>
● Excess Noise	Yes	None
● Bias Requirements	Yes	No
● Total Size/Weight	Medium	Medium, Small
● Ferrite/Magnet Needs	No	Yes
● Power Handling	0.1 - 2 W	0.5 - 10 W
● Overall Cost	Medium	Medium Low
● Ruggedness	Yes	Yes
● Radiation Resistance	Limited	High
● Compatibility with MMIC	Excellent	Good
● Narrow Band Performance	Excellent	Excellent
● Wideband Performance	Fair Good	Good



Report Documentation Page

1. Report No.	2. Government Accession No.	3. Recipient's Catalog No.	
4. Title and Subtitle High Performance Millimeter-Wave Microstrip Circulators and Isolators		5. Report Date February, 1990	
		6. Performing Organization Code	
7. Author(s) Ming Shih and J.J. Pan		8. Performing Organization Report No. 19-F001	
		10. Work Unit No.	
9. Performing Organization Name and Address E-Tek Dynamics, Inc. 1885 Lundy Avenue San Jose, California 95131		11. Contract or Grant No.	
		13. Type of Report and Period Covered Final Report June 1988 - January 1990	
12. Sponsoring Agency Name and Address NASA Resident Office - JPL 4800 Oak Grove Drive Pasadena, California 91109		14. Sponsoring Agency Code	
15. Supplementary Notes			
16. Abstract <ul style="list-style-type: none">Developed stub-tuned microstrip circulator configuration utilizing the eletromagnetic fields perturbation techniqueDesigned and optimized Ka band microstrip circulators based on the material test data and computer simulation resultsImproved the adhesion of microstrip metallization on the new, highly polished ferrite substrateEnhanced the performance of drop-in circulators and test fixture to meet the design specificationDesigned, fabricated, and improved the ruggedized circulator package over temperatures of -20° c to +50° c.			
17. Key Words (Suggested by Author(s)) Millimeter-Wave, High Performance Microstrip, Circulators, Isolators		18. Distribution Statement	
19. Security Classif. (of this report)	20. Security Classif. (of this page)	21. No. of pages	22. Price